
ETD Archive

2013

Computational Fluid Dynamics Modeling of a Gravity Settler for Algae Dewatering

Scott A. Hug
Cleveland State University

Follow this and additional works at: <https://engagedscholarship.csuohio.edu/etdarchive>

 Part of the [Biomedical Engineering and Bioengineering Commons](#)

How does access to this work benefit you? Let us know!

Recommended Citation

Hug, Scott A., "Computational Fluid Dynamics Modeling of a Gravity Settler for Algae Dewatering" (2013). *ETD Archive*. 813.
<https://engagedscholarship.csuohio.edu/etdarchive/813>

This Thesis is brought to you for free and open access by EngagedScholarship@CSU. It has been accepted for inclusion in ETD Archive by an authorized administrator of EngagedScholarship@CSU. For more information, please contact library.es@csuohio.edu.

COMPUTATIONAL FLUID DYNAMICS MODELING OF A
GRAVITY SETTLER FOR ALGAE DEWATERING

SCOTT A. HUG

Bachelor of Chemical Engineering

Cleveland State University

August 2011

Submitted in partial fulfillment of the requirements for the degree

MASTER OF SCIENCE IN CHEMICAL ENGINEERING

at the

Cleveland State University

August 2013

© COPYRIGHT BY SCOTT A. HUG 2013

This thesis has been approved
for the Department of CHEMICAL AND BIOMEDICAL ENGINEERING
and the College of Graduate Studies by

Thesis Committee Chairperson, Jorge E. Gatica, Ph.D
Department of Chemical & Biomedical Engineering
Cleveland State University

Department & Date

Joanne M. Belovich, Ph.D
Department of Chemical & Biomedical Engineering
Cleveland State University

Department & Date

Chandra Kothapalli, Ph.D.
Department of Chemical & Biomedical Engineering
Cleveland State University

Department & Date

Dhananjai B. Shah, Ph.D.
Department of Chemical & Biomedical Engineering
Cleveland State University

Department & Date

ACKNOWLEDGEMENTS

First, I would like to acknowledge the Choose Ohio First Scholarship Program, the Department of Chemical and Biomedical Engineering at Cleveland State University, Fenn College of Engineering, and Research Experiences for Undergraduates at Cleveland State University, for providing funding for this research project.

I would like to acknowledge my academic advisor, Dr. Jorge E. Gatica, the chairperson of my Thesis Committee. In addition to these roles, Dr. Gatica explained the fundamental application of SolidWorks[®] and COMSOL Multiphysics[™], two programs that were used extensively in this project. In addition, I would like to acknowledge the other members of my Thesis Committee: Dr. Joanne M. Belovich, Dr. Chandra Kothapalli, and Dr. Dhananjai B. Shah.

I would like to acknowledge the “Algae team,” a group of chemical and biomedical engineering students at Cleveland State University under the direction of Dr. Joanne Belovich. This group of students contributed to the design and experimentation on the gravity settler model used in the simulations in this experiment. Three students whose contributions are especially important to this experiment are Zhaowei Wang, Jing Hou, and Dustin Bowden.

Last, I would like to extend gratitude to my family and friends who have supported me during my time as both an undergraduate and graduate student at Cleveland State University. I would especially like to acknowledge my parents, Doris and Jeffrey Hug, and my brother Daniel Hug, whose support is a very important reason that I have been able to complete this project.

COMPUTATIONAL FLUID DYNAMICS MODELING OF A GRAVITY SETTLER
FOR ALGAE DEWATERING

SCOTT A. HUG

ABSTRACT

Algae are the future of lipid sources for biodiesel production. Algae can produce more biodiesel than soybean and canola oil and can be grown in more diverse locations. Algae concentrations are naturally around 0.1% by weight. Enough water must be removed for the algae level to reach 5%, the minimum concentration in which lipids can be used in the transesterification process for biofuel production is 5%. Current dewatering methods involve the use of settling tanks and centrifugation. The costs of centrifugation limit the commercial viability of algae based biodiesel.

A novel inclined gravity settler design at Cleveland State University is analyzed in this project. A major difference between this and a traditional gravity settler is that the inlet of this gravity settler is at the top, whereas traditional gravity settlers have inlets at the bottom. A computational fluid dynamics model for the system has been developed to allow the simulations of fluid flow and particle trajectories over time. These simulations determine the optimal conditions for algae dewatering.

Results show that the concentration increase of algae is largely dependent on the settler's angle of inclination, inlet flow rate, and the split ratio of water between the overflow (predominantly water) and underflow (concentrated algae) outlets. A 50-fold concentration increase requires multiple settlers set up in series. A two- or three-settler design is sufficient to increase algae concentration to the desired level.

TABLE OF CONTENTS

	Page
ABSTRACT.....	v
LIST OF TABLES.....	viii
LIST OF FIGURES.....	ix
CHAPTER	
I. INTRODUCTION.....	1
1.1. Background.....	1
1.2. Literature Survey.....	9
II. MATERIALS AND METHODS.....	17
2.1. The Gravity Settler.....	17
2.2. The Algae.....	20
2.3. Design and Simulation.....	20
III. MODELING.....	27
3.1. Overview of Fluid Flow and Particle Tracing Modules.....	27
3.2. 2-Dimensional Model.....	28
3.2.1. Force Distribution.....	28
3.2.2. Settling Velocity.....	34
3.2.3. Velocity Profile.....	39
3.2.4. Particles Near the Bottom of the Settler.....	43
3.3. 3-Dimensional Model.....	45
3.4. Particle Size Distribution.....	48
3.4.1. Size Distribution Found in Literature.....	48
3.4.2. Comparison of Algae Strains.....	51

3.4.3. Particle Mass Distribution.....	55
3.5. Flow Distribution.....	57
3.6. Simulation Algorithm.....	60
IV. RESULTS AND DISCUSSION.....	65
4.1. Base Case.....	65
4.2. Residence Time vs. Settling Time.....	67
4.3. Effect of the Outlet Flow Rate Ratio on Settler Performance.....	72
4.4. Multi-Stage Experiment.....	74
4.5. Effect of the Angle of Inclination on Settler Performance.....	78
4.6. Effect of the Inlet Flow Rate on Settler Performance.....	80
4.7. Effect of the Length of the Gravity Settler on its Performance..	82
4.8. Number of Stages.....	84
4.9. Summary of Optimal Conditions.....	85
V. COMPARISON OF RESULTS TO SIMILAR EXPERIMENTS.....	86
VI. CONCLUSIONS AND RECOMMENDATIONS.....	95
6.1. Concluding Remarks.....	95
6.2. Recommendations and Further Research.....	96
REFERENCES.....	99
APPENDIX.....	104
Tables and Charts.....	105
Sample Calculation.....	115
MATLAB [®] Script for First Settler.....	118
MATLAB [®] Script for Second Settler.....	127

LIST OF TABLES

Table	Page
I. Summary of Concentrations and Flow rates for a Two-Stage System.....	84
II. Optimal Conditions for Algae/Water Separation.....	85
III. Particle Sizes, Masses, and Settling Properties.....	105
IV. Comparing Outlet Flow Rate Ratio.....	113
V. Comparing Angle of Inclination.....	113
VI. Determining Optimal Angle of Inclination.....	114
VII. Comparing Inlet Flow Rate.....	114
VIII. Comparing Settler Length.....	115

LIST OF FIGURES

Figure		Page
1.	Side View of Gravity Settler.....	6
2.	Gravity Settler Design on SolidWorks.....	7
3.	Model of Gravity Settler at 45 Degree Angle of Inclination.....	18
4.	Gravity Settler, Top and Side Views.....	19
5.	Graphical Overview of the Model.....	21
6.	3D Velocity Profile of Settling Region.....	22
7.	2D Velocity Profile of Settling Region.....	23
8.	3D and 2D particle Trajectories.....	25
9.	2D Representation of Gravity Settler.....	29
10.	Visual Depiction of Particle Diameter Measured from its Mid-Section....	33
11.	2D Velocity Profile of the Fluid in the Gravity Settler.....	40
12.	Streamline Plots of Velocity Profile.....	41
13.	Streamline Plot of Velocity Profile Near Outlet Split.....	42
14.	Critical Reynolds Number as a Function of Archimedes Number.....	43
15.	Critical Reynolds Number Compared to Particle Reynolds Number.....	44
16.	Velocity Profile as a function of y	46
17.	Cross-Sectional Velocity Profile for 3D settler.....	48
18.	Particle Size Distribution of <i>D. Tertiolecta</i> from Literature.....	50
19.	Distribution of <i>S. Dimorphus</i> Cells.....	52
20.	Predicted Particle Size Distribution of <i>S. Dimorphus</i>	53
21.	Mass Distribution of <i>S. Dimorphus</i>	56

22.	Flow Distribution near the Inlet for a 2D Gravity Settler Model.....	59
23.	Comparison of Particle Movement between MATLAB Model and COMSOL Simulations.....	66
24.	Residence Time as a Function of Settling Time and Inlet Flow Rate.....	69
25.	Residence Time as a Function of Settling Time and Angle of Inclination.	70
26.	Residence Time and Settling Time as a Function of Particle Diameter.....	71
27.	Enrichment Factor and Recovery as Functions of Outlet Flow Rate Ratio	73
28.	Schematic of 2-Stage Gravity Settler System.....	75
29.	Velocity profile for gravity settlers 9.6 cm and 0.96 cm in width.....	76
30.	Enrichment Factor and Recovery as Functions of Angle of Inclination.....	78
31.	Velocity of a 20 μm Particle at $z=0.02$ cm as a Function of Inclination....	79
32.	Optimal Angle of Inclination.....	80
33.	Enrichment Factor and Recovery Rate as Functions of Inlet Flow Rate....	81
34.	Enrichment factor vs. inlet flow rate for a two-stage system.....	82
35.	Enrichment Factor and Recovery Rate as Functions of Length.....	83
36.	Comparison of this Project to Research by Salem et al. (2011).....	88
37.	Comparison of Calculated Settling Velocity to Values in Literature.....	89
38.	Comparison of Calculated Settling Velocity to Calculations by Pitt and Clark (2007).....	90
39.	Comparison of Results to Data Recorded by Wang et al. (2013).....	91
40.	Comparison of Results to Data Recorded by Wang et al. (2013).....	92
41.	Comparison of Increasing Settler Length for Scale-Up to Increasing Settler Width for Scale-Up.....	97

CHAPTER I

INTRODUCTION

1.1. Background

Future world energy needs necessitate the search for alternative and sustainable energy sources. Biodiesel is one such source that has many upsides, but current production methods are flawed. Currently, sources such as soybeans, canola oil, and palm oil are being cultivated in biofuel production. Over the past few decades, research has been conducted on the use of algae as a source for biofuel. These studies have shown that algae are a very viable option for biofuel production.

The consumption of oil and natural gas has declined over recent years, but their production has declined at a higher rate (Suali 2012). There are several advantages to using algae over other fuel sources. First, algae have high lipid content. For some strains, the lipid content can be up to 70% on a dry weight basis (Suali 2012). Lipids, specifically triglycerides, are important in biofuel production. The lipids extracted from algae have qualities, such as a higher amount of polyunsaturated fatty acids with several

double bonds than those extracted from vegetable oils, resulting in a higher fuel quality (Mutanda 2011).

Second, algae can be grown anywhere, including ponds, fresh water, and salt water (Campbell 2008), and wastewater (U.S. Department of Energy 2008); on land in many climates ranging from arctic climates to deserts (U.S. Department of Energy 2008); and inside photobioreactors (Campbell 2008). Because algae can be grown in unconventional locations, algae do not compete with food crops for space on traditional farmlands in a way that soybeans, canola, and other biofuel source crops do.

Third, algae can produce biofuel at a much higher rate than other sources. One acre of algae can produce 5,000 to 10,000 gallons of biofuel per year (Subharda 2010). In contrast, soybeans can only produce 48 gallons of biofuel per acre per year (Addison 2007) and canola oil can only produce 247 (Anderson 2008). Even the most effective oil-producing crop, palm oil, can only produce 635 gallons of biofuel per acre per year (Addison 2007), approximately ten percent of the biofuel production from algae.

Fourth, the portions of the algae not used in biofuel production can be recycled for other uses. Compounds can be isolated from algae for medical uses, such as treatments for coughs and asthma among other diseases (Kandale 2011). They can also be used as traditional cosmetics and for the reduction of headaches (Kandale 2011). Some algae, in particular seaweeds that grow near the shore, can also be used as a food source. These seaweeds are rich in iodine and calcium, and are a source of protein, vitamin C, vitamin B₁₂ (Kandale 2011), omega-3 compounds, and other nutritional supplements. Recently, algae have also been used as animal feed. Algae are a valuable alternative to more conventional protein sources and have been used primarily to feed

poultry and aquatic animals (Becker 2007).

Algae may also be used to capture CO₂ emissions from power plants. Algae's photosynthetic efficiency is considerably higher than that of terrestrial plants (Suali 2012). The algae can convert this CO₂ emission into green energy (Suali 2012). Furthermore, algae can be used for wastewater treatment. Algae can reduce the chemical and biochemical oxygen demands in wastewater. The wastewater in turn contributes to algae growth by supplying high amounts of several amino acids that algae require in order to grow (Suali 2012).

There are, however, a few disadvantages of using algae as a source for biofuel. Before any cultivation takes place, the algae cells must be de-watered. Typical biomass associated with autotrophic pond growth accounts for just 0.05%-0.1% of the total mass of the system, with the balance being water (Smith 2013). A 50-100 fold increase is needed to increase the mass percentage of algae to 5%, the percentage typically found after microbial fermentations (Smith 2013). This process can be both expensive and time consuming. The algae dewatering process is responsible for up to 30% of the total cost of the manufacture of crude oil from algae (Molina Grima 2003). Dewatering methods that are presently being used include the use of settling ponds or tanks, centrifugation, flocculation, flotation, and filtration (Milledge 2012).

A settling pond or settling tank retains the mixture and algae long enough to allow the algae particles within the water to settle. Settling ponds do not require high capital or maintenance costs (Suali 2012). Settling is also useful for wastewater treatment (Park 2011). The biggest shortcoming to using settling ponds is the amount of time needed for

separation. Some ponds can take several hours or as much as 1-2 days (Park 2011) in order to achieve any separation. Conical settling ponds increase the amount of algae harvested while decreasing the residence time to around three hours (Park 2011), however the amount of separation of algae from water is still low.

Settling ponds have many limitations in addition to large amount of settling time needed. Open ponds leave algae susceptible to contaminants and other organisms that may affect the settling rate (Suali 2012). Insufficient stirring systems may result in a slower increase in algae concentration (Suali 2012). Open ponds require large amounts of land and the settling of algae may be limited by factors such as temperature and the amount of time the pond is exposed to sunlight (Suali 2012).

Chemical flocculation uses a chemical (the flocculent) to stick to the algae particles, forcing them to move together in large clumps. The cost of flocculation is largely driven by the type of flocculent used. Organic flocculants can be obtained naturally or synthetically (Suali 2012). Synthetic organic flocculants, as well as some inorganic flocculants, have a high separation rate, but these flocculants can be more expensive (Suali 2012). Flocculation is used in combination with another separation method, such as filtration, centrifugation, flotation, or sedimentation, as well as a drying process (Suali 2012). These processes increase the cost of separation. Furthermore, the removal of the flocculent from the separated algae can be very difficult (Milledge 2012).

Filtration uses a membrane that would stop the algae particles but allow the liquid water to pass through. Filtration is only suited for large algae cells, as smaller cells would flow through the membrane. Clogging can also become an issue (Milledge 2012).

Ultrafiltration can be used for small algae cells, but the cost is prohibitive (Milledge 2012). Flootation is a process in which air bubbles are introduced into the water in order to bring algae particles to the surface. While this process can be done quickly, it is specific to the algae and has high capital and operational costs (Milledge 2012).

Another dewatering method that can be used is centrifugation. Centrifugation is a preferred method for harvesting microalgae because it can be completed quickly without the use of chemicals (Suali 2012). While centrifugation is efficient in small-scale operations, such as laboratory use, the cost becomes very high when the operation is pushed up to large-scale industrial use (Molina Grima 2003). The biggest disadvantage of centrifugation is the high cost associated with the process. These costs include purchase and installation of the large machinery, labor costs, and operating costs such as the use of significantly more electrical energy than other separation methods (Suali 2012).

This project analyzes an alternative method for dewatering algae: Settling with an inclined gravity settler design. Settling is a process in which particles move toward the bottom of a liquid in the direction of a force, such as gravity (Del Coz Díaz 2011). In the recent past, inclined gravity settlers have been used for removal of solid waste from wastewater, with some algae dewatering applications. A 1996 experiment by Nurdogan and Oswald showed the gravity settler produced a four-fold increase in the amount of the microalgae *Micractinium* over conical settling tanks when the same volumetric flow rate to surface area ratio was used.

The inclined gravity settler studied in this project is different than the design of

traditional inclined gravity settlers in that the inlet to the settler is at the top, rather than the bottom. An advantage of placing the Inlet at the top of the settler is that the water and the settled cells would move in the same direction. When the flow moves upward from the bottom of the settler, the settled particles would move downward, against the flow of the fluid, which creates a greater fluid resistance to the flow of the algae particles. Two prototypes have been tested in previous experiments and these experiments indicate that the technique is effective at dewatering algae. The gravity settler design is shown in Figures 1 and 2.

The model formulation is based on the mixed model. The mixed model considers a system where there is a dispersed phase of either solids or liquid droplets or bubbles in a continuous liquid phase. The geometrical model has been developed based on the simplified geometry of the gravity settler shown in Figures 1 and 2. After validation experiments were completed and results with simplified relations for settling velocities

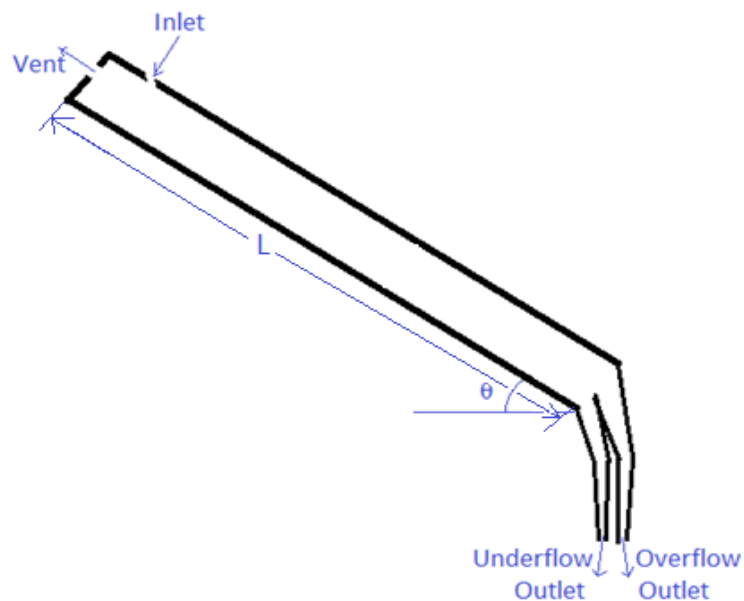


Figure 1: Side-view of gravity settler

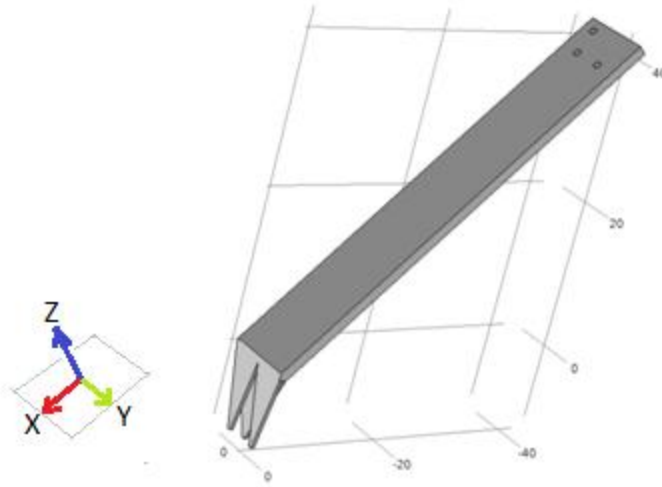


Figure 2: gravity settler design on SolidWorks®

were evaluated, the simulation environment was updated to the more advanced geometry geometry of the prototypes by means of Solidworks® and COMSOL™ LiveLink™ for Solidworks®. This LiveLink™ enables the user to import complex geometries into COMSOL™ as well as formulation of parametric studies where the computer aided design software is used to interactively modify geometric parameters that may show relevance in the performance of the settler. Solidworks® parameters can also be used in COMSOL™ to perform parametric sweeps.

Using this LiveLink™ functionality, parametric sweeps were demonstrated as tools to optimize the settler's design and operation by analyzing several parameters on the model. Geometric parameters, such as the settler length (noted by L on Figure 1) and the angle of inclination (noted by θ on Figure 1) were analyzed, as well as operating variables such as inlet and outlet fluid flow rates and velocities. The optimized design was physically prototyped and experimented on to validate the computational fluid dynamics modeling.

It was hypothesized that the greatest separation would be attained at low inlet velocities and low angles of inclination. The inlet velocity refers to the velocity of the fluid. This hypothesis is supported by the model. A lower velocity allows for a higher residence time. The algae particles would have more time to settle on the bottom of the gravity settler, and a greater amount of algae would leave through the bottom exit region. This also allows for an increase in algae recovery, meaning a higher percent of algae that entered the settler would exit through the lower “underflow” outlet stream with concentrated algae.

At lower angles of inclination, the direction of flow has less influence from gravity, so the velocity of the flow would not increase as quickly through the settler. Again, this would allow for a higher residence time. However, the model showed that there is an optimal angle of inclination somewhere between 15 degrees and 45 degrees from the horizontal. At very low angles when the flow region is almost horizontal, more particles will settle to the bottom of the gravity settler, but the particles will be more likely to stick to the bottom and not move than if the angle of inclination were higher. This is because the component of gravity in the direction of flow, and as a result, the acceleration of the particle in the direction of the flow, decreases as the angle of inclination decreases.

The objective of this project was to determine the operating parameters that produce the most optimal conditions for algae dewatering for this particular gravity settler design. These optimal conditions would result in a high percentage of fluid being removed from the system, but a low percentage of algae being removed from the system. In addition, the optimal settler would allow for the settling process to be completed

without particles sticking to the bottom of the settler and building up. This objective was accomplished by designing a model of the settler using SolidWorks[®], modeling the fluid flow through the settler using COMSOL Multiphysics[™], and formulating an interface on MATLAB[®] to measure the particle trajectories based on the fluid flow and fluid-particle interactions.

The significance of this project lies in the opportunity to dewater algae on a large scale while avoiding the natural limitations of settling ponds and the high costs of centrifugation. This project models the fluid flow and generates particle trajectories to determine optimal settling conditions in the gravity settler at the laboratory scale. These calculations are necessary for the anticipated scale-up of the equipment for industrial use, as the optimal conditions would allow biofuel to be produced more quickly than other conditions would.

1.2 Literature Survey

The use of gravity to separate suspended particles from fluid dates back to the 1800s. Settling tanks were originally used to separate sewage from water. The water/sewage mixture entered at the top of the tank, and a stirrer agitated the flow. The mixture is sent to the settling region in which most of the heavy sewage particles would settle toward the bottom of the region and into an underflow outlet. This “heavy phase” is a sludge that consists of a much higher concentration of sewage than the inlet. The overflow outlet would consist primarily of water and has a much lower sewage concentration than the feed to the settler (Berman 2003).

A lamella clarifier is a type of settler in the suspended particles within the fluid flocculate on a series of inclined plates within the settler. The flocculated particles will

then simply sink to the underflow of the settler, while much of the fluid and only the smallest, lightest particles will exit through the settler's overflow. This type of settler was also used to separate sewage from water (Schaffner 2011). The inflow to these settlers is distributed between several lamellas, or small channels, at a specified angle above the horizontal plane. Water rises through these channels, but the denser particles sink and stick to the inclined planes (Schaffner 2011).

Sarkar, Kamilya, and Mal (2007) examined an inclined plate gravity settler for wastewater treatment. They determined that the separation efficiency was dependent on the Reynolds number (Re), a function of velocity, cross-sectional flow area, and the viscosity and density of the water. The efficiency was highest at low Re . Between 600 and 1000, the efficiency rapidly decreased as Re increased, until it would level off around $Re = 900$. Sarkar, Kamilya, and Mal also determined that separation efficiency was dependent on the angle of inclination of the plates within the settler. At low angles of inclination from the horizontal, the settling efficiency increased as the angle increased, until a peak was reached between 40 and 45 degrees. The separation efficiency then decreased as the angle increased for angles greater than 45 degrees.

Del Coz Díaz et al (2011) studied the separation of particles from fluid in an "urban sustainable gravity settler." This settler is a large rectangular prism with an inlet near the top of one face, and the outlet near the top of the opposite face. Near the inlet, the fluid hits a deflector, which forces all of the fluid near the bottom of the settler. The fluid is then pulled up from suction through the outlet. As the fluid is being pulled up, the force of gravity keeps the particles from being pulled upward as quickly and it pulls some of the larger particles down. The separation was most efficient for large deflector

sizes (i.e. the space between the floor of the settler and the bottom of the deflector was smallest). A smaller space between the floor and the deflector implies that the fluid and particles would have to travel upward a greater distance to the outlet, meaning a greater drag force on the particle is needed to overcome the force of gravity in order for particles to leave the settler through the fluid outlet.

Bikiri, Chebli, and Nacef (2012) studied a clarifier that treats wastewater by separating sewage particles from the water. They determined the outlet concentration of sewage particles in the underflow of the settler increased exponentially as the depth of the settler increased, but at after a certain depth, the concentration would remain constant. This is likely because at larger depths, the particles have more time to settle, a characteristic that transfers to inclined gravity settlers. Eventually, almost all of the particles would settle, meaning any further increase in settler depth, and as a result, an increase in residence time, would not affect the concentration of the sewage stream in the underflow.

Sharrer et al. (2010) compared the cost and effectiveness of gravity thickening settlers (GTS), similar in appearance and function to a lamella clarifier, to two other means of separating suspended particles from fluid: Inclined belt filters (IBF) and geotextile bag filters (GBF). While the authors maintained that the IBF had the highest separation efficiency of the three machines, it was not cost-effective. Its capital costs were more than twice that of the GTS. The GTS also had relatively inexpensive operating costs, especially compared to GBS which requires routine maintenance constant replacement of parts. While the treatment in the GTS is not as complete as the other two machines, it still can separate a very high percentage of solid particles from

water at a considerably lower cost than the other separation methods examined.

Inclined gravity settlers, such as the one examined in this experiment, are based on the concept of lamella clarifiers. These settlers are much smaller, as there is only one channel, rather than a large tank, and have been shown to be more effective at separating particles from fluid (Nurdogan 1996). Studies on this type of inclined gravity settler have also been conducted in the past.

Nasr-El-Din, Masliyah, and Nandakumar (1990) examined the separation of light suspended polystyrene and heavy polychloride beads in a salt solution at varying feed flow rates, solids concentrations, angles of inclination, and split fractions of fluid to the overflow and underflow streams. The feed entered the center of the inclined settler, which was designed to send the light particles up toward an overflow stream and the heavy particles down toward an underflow stream. Nasr-El-Din et al. explain that an inclined settler is more effective at separating the particles than a vertical settler. The concentration of light particles in the overflow increases as a higher percentage of the fluid feed goes away the overflow and toward the underflow, while the concentration of heavy particles in the underflow increases as a higher percentage of the fluid feed goes away the underflow and toward the overflow. A more complete separation between heavy and light particles was observed at a lower fluid flow rate.

As described earlier, Nurdogan and Oswald (1996) examined the separation of water and algae using both inclined gravity settlers and less modern conical settling tanks. They determined that inclined settlers could remove algae seven to eight times more efficiently than settling tanks could. Nurdogan and Oswald also demonstrated that the overflow rates (OFRs) in traditional clarifiers are too low to remove algae efficiently.

OFRs could be increased four to five times using the inclined settler.

Davis and Gecol (1996) studied the settling of multiple species of particles within a single inclined gravity settler, with each particle type having a different density. Davis and Gecol found that the settler was capable of separating the particle types based on the differences in particle density. The heaviest particles quickly settled to the underflow outlet while the drag force from the fluid velocity could overcome the light particles' settling velocity, allowing the light particles to reach the overflow outlet. The researchers argue that at a carefully chosen inlet flow rate, an inclined settler can be extremely effective at separating heavy particles from lighter particles.

Nelson, Liu, and Galvin (1997) used an inclined counterflow settler to separate particles of two species with different densities that were suspended in a fluid. The feed entered the settler as slurry. The fluid travelled upward through the inclined settler while the particles of the heavier feed species would eventually flow downward to an underflow outlet at the same end of the settler as the inlet. The fluid and the lighter feed particles would flow upward toward the outlet at the other end of the settler. Nelson et al. show that at correct feed rates, separation efficiencies of over 90% can be achieved with an inclined settler.

Laskovski et. al (2006) examined the separation of suspended particles in suspended fluidized beds, similar in nature to the gravity settler used in this experiment. Their system consisted of several inclined channels above a vertical mixing zone. Particles with diameters between 50 and 250 μm were separated using the settler. The light particles that did not settle eventually went up to the overflow, while heavier particles sunk to the underflow. Although there was a small range of particle sizes in

which some particles would go in each exit, particles of a given size would either almost all rise to the overflow or sink to the underflow. They also found that a greater number of particles sunk to the underflow of the settler in systems with higher angles of inclination from the horizontal plane.

Salem, Okoth, and Thoming (2011) studied the separation of solid particles in water using a settler similar to the settler used in this project, except having inclined plates set up throughout the middle of its body to agitate the flow. The results of their experiment show that as the inlet flow rate increases, the separation efficiency will decrease. Salem, Okoth, and Thoming also determined that the configuration of the inlet has a small effect on the separation efficiency, in which flow from a nozzle distributor has slightly greater separation efficiency than flow entering from a pipe.

Smith and Davis (2013) used an inclined settler with multiple levels in a process to achieve particle concentration using inclined sedimentation via sludge accumulation and removal. This design combines the concepts of inclined settlers and lamella clarifiers, but is similar in appearance to inclined plate settlers used in other experiments. Their experiment shows that a greater inlet fluid velocity results in a greater amount of particles in the overflow and a less concentrated underflow. However, at low velocities below a critical velocity, all particles would settle and exit via the underflow. This critical velocity is a function of angle of inclination and the densities of the fluid and particles. The critical velocity is extremely low because the residence time of the fluid in the settler must be long enough for even the smallest of particles to settle.

Smith and Davis (2013) found a “90%-retention velocity,” which is the maximum fluid velocity that allows for 90% of the particles to settle to the bottom of the settler.

Smith and Davis also predicted sludge build-up within the settler as a function of residence time (effectively a function of inlet velocity) but did not find sludge build-up to be a significant factor except at extremely low velocities (those below 1 cm/h, which is less than the expected velocity in this experiment), as the continuous dilute inlet flow can keep the sludge build-up moving to a certain extent.

Smith and Davis (2013) also propose their settler design as a method to dewater algae effectively and at a low cost. In experiments involving algae, Smith and Davis found similar behavior patterns between the settling of algae particles and those observed in their sludge experiments. The degree of separation between algae and water is a function of the inlet velocity and settling velocity of the algae particles.

Research has been conducted on inclined gravity settlers for approximately the past twenty years. This research has primarily focused on the separation of light and heavy particles and the removal of sludge and other waste products from wastewater. The results produced by these experiments show that an inclined gravity settler may be a viable option for the dewatering of algae. While there are some differences between the gravity settler examined in this experiment and the settlers used in the experiments in literature, it is expected that the results from this experiment will have the same trends as previous studies.

While previous studies have primarily focused on using a gravity settler to separate sludge from wastewater, this project examines the gravity settler as a means to remove algae from a fluid. While the applications are similar, the specific particles are different, which may lead to different optimal operating conditions. Also, this project differs from all the project designs from literature in that the entrance to the settler is at

the top, rather than the bottom of the settler. This results in a concurrent flow between the fluid and the particles, rather than a countercurrent flow. Using a concurrent flow reduces the flow resistance between the fluid and the particle, because the settling velocity of the particle is in a direction similar to the flow of the fluid. While there are some differences between this project and projects conducted previously, the results and conclusions drawn from previous studies can be used as a basis for this project.

CHAPTER II

MATERIALS AND METHODS

2.1. The Gravity Settler

The main piece of equipment examined in this experiment is an inclined plate gravity settler design. The gravity settler is constructed with polycarbonate sheets on the top, bottom, and all sides. The sheets on the top and bottom of the settler are $\frac{3}{8}$ of an inch thick, while the side walls are $\frac{1}{4}$ of an inch thick (Team Plastic, Inc. Cleveland). The settler is divided into two regions, the settling and outlet regions.

The settling region is a rectangular prism 59 cm long, 9.6 cm wide, and 1 cm high. These dimensions are not fixed, and the different lengths of the settler will be examined to find the optimal settling conditions. The outlet region of the settler is divided into an upper section for the overflow stream (water), and a lower section for the underflow stream (concentrated algae). Each section measures 0.4 cm in height and the sections were divided by a polycarbonate sheet $\frac{1}{16}$ inch thick. The outlet region is 18 cm long. The overflow outlet is two channels each measuring 4.75 cm wide and narrowing to 0.5 cm at a constant rate throughout the region. The underflow outlet is a single channel 9.5 cm wide that narrows to 0.5 cm evenly throughout the region. All of the

polycarbonate sheets were manufactured using Max Bond epoxy (Polymer Composites, Los Angeles) and autoclaved at 121°C.

Flexible silicone tubing (Cole-Parmer, size 13) is connected to the outlet ports and the inlet ports of the settler. The settler is held at a specific angle of inclination above the horizontal by a support apparatus. The inlet ports are located on the top of the settler 5 cm from its back edge. A port located on the back wall of the settler is used as an air vent, however the vent is closed for this experiment. The flow rates of the outlet streams are controlled by peristaltic pumps. Figure 3 is a model of the gravity settler, designed on SolidWorks®. Figure 4 shows the top and side views of the settler.

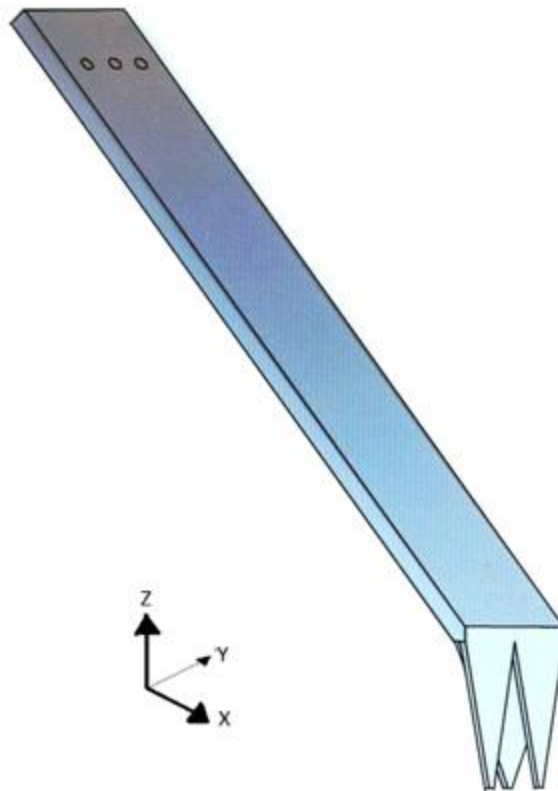
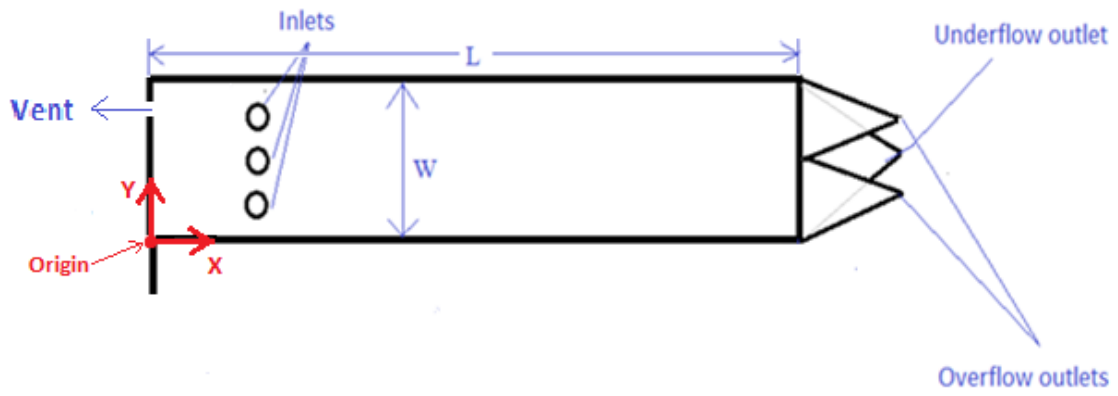
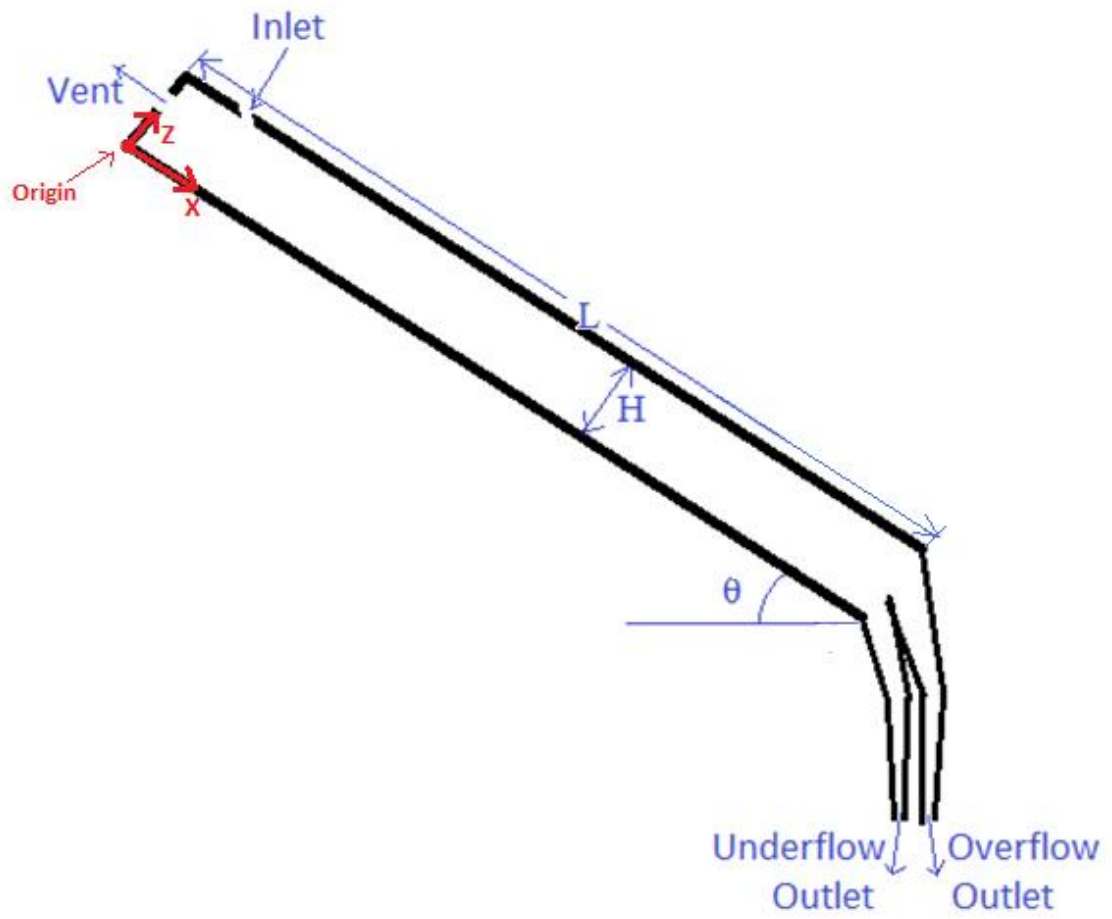


Figure 3: Model of gravity settler, designed on SolidWorks®, at a 45-degree angle of inclination. The three holes near the top of the settler are the fluid inlet ports. The triangles at the bottom are the outlet region, with fluid leaving the settler through holes on the bottom of the triangles.



(a) Top View



(b) Side View

Figure 4: Gravity settler, (a) top view and (b) side view

2.2. The Algae

This experiment examines the removal of water from the microalgae *Scenedesmus dimorphus*. *S. Dimorphus* cells are used because they have a high lipid content of up to 32% on a dry weight basis (Shen 2009), which is greater than most other strands of algae (Balat 2010). *S. Dimorphus* cells also have a high specific growth rate of 1.6 day^{-1} (Yang 2003). These cells typically have a length of 5-20 μm and often colonize in pairs and groups of three or four cells (Shen 2009). Grouping algal cells together increases the size of a particle and allows them to settle more quickly.

2.3. Design and Simulation

First, the design of the gravity settler is modeled on SolidWorks®. It is modeled using the Cartesian coordinate system so that the positive x-direction is the direction of flow; gravity occurs at an angle between the positive x- and negative z-directions, and the y-direction measures the width of the settler. The settler is modeled in such a way that the angle of inclination and length of the settling region can be easily adjusted on the program. This design is then imported into COMSOL Multiphysics™ using COMSOL™'s LiveLink™ for SolidWorks® application. The gravity settler is modeled for both 3-dimensional (3D) and 2-dimensional (2D) cases, with the 2D case ignoring the y-direction.

Figure 5 shows a graphical overview of the model. The algae/water mixture enters the settler through the inlet and travels in the positive x-direction. While traveling in the positive x-direction, the algae particles will settle in the negative z-direction, at a velocity determined from several equations as described in Section 3.1. The two outlets are referred to as the “overflow outlet,” which consists of a high percentage of the water

and the small algae particles that do not have enough time to settle; and the “underflow outlet,” which consists of a small fraction of the water and the large algae particles that have enough time to settle toward the bottom of the settler before reaching the outlet region.

This project makes use of COMSOL™’s laminar flow and particle tracing modules. The laminar flow application allows for the laminar flow of water to be simulated throughout the gravity settler and for a velocity profile to be made. This module applies the non-slip boundary condition that makes the velocity of the fluid at any wall equal to the velocity of the wall (zero in this case). The velocity of the fluid at the inlet and outlet ports of the settler is given. Figure 6 shows the velocity profile for 3D gravity settler model and Figure 7 shows the velocity profile for a 2D model. Figures 5 and 6 measure only the fluid velocity profile and do not consider fluid-particle interaction.

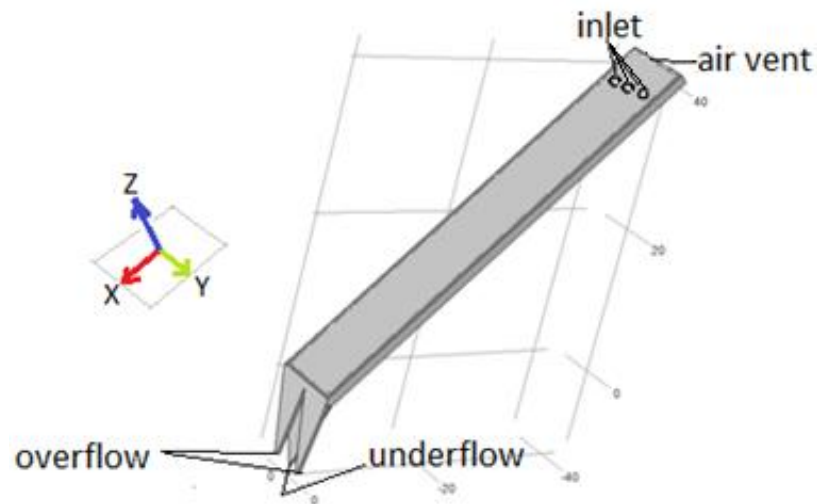


Figure 5: Graphical overview of the model

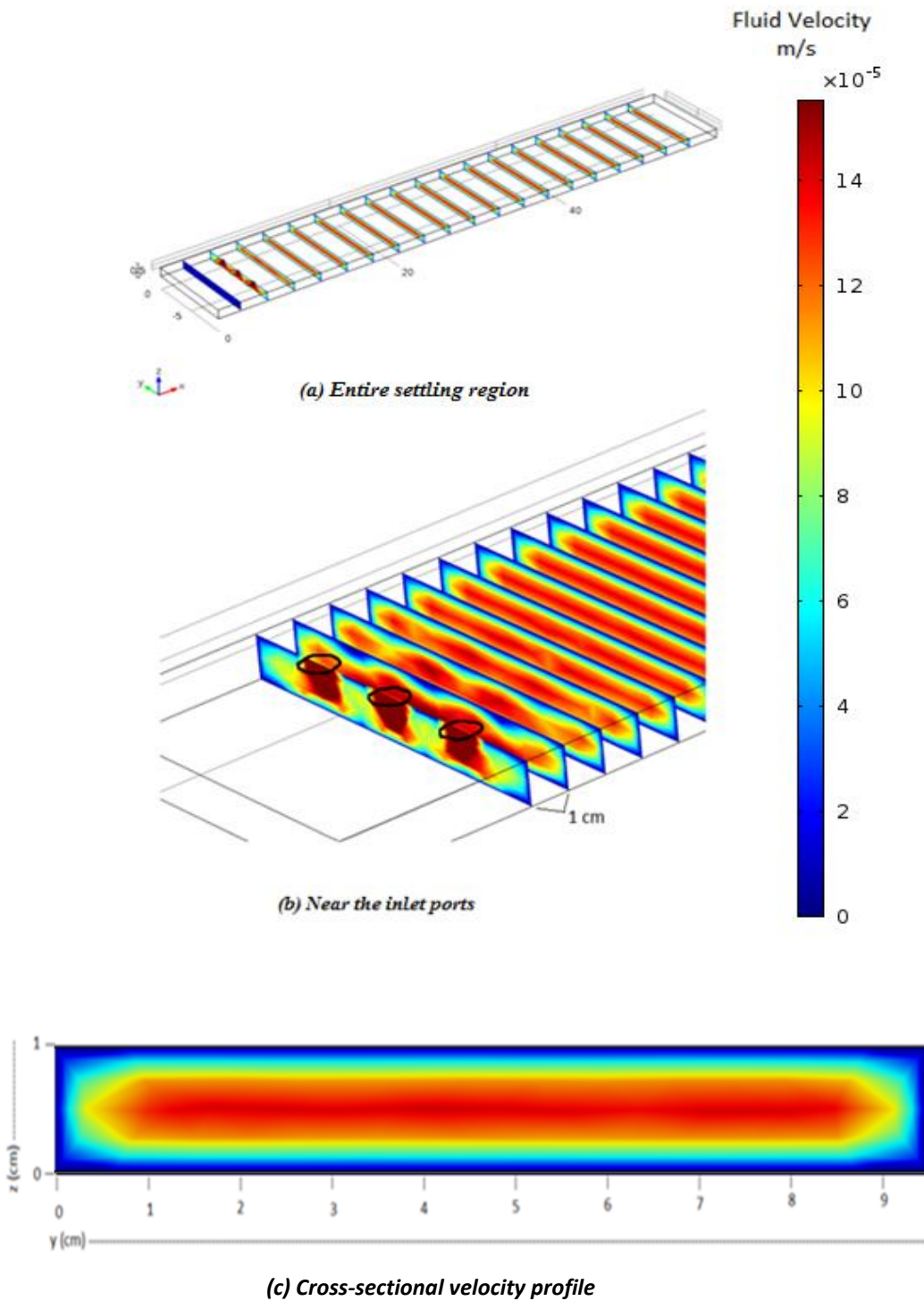
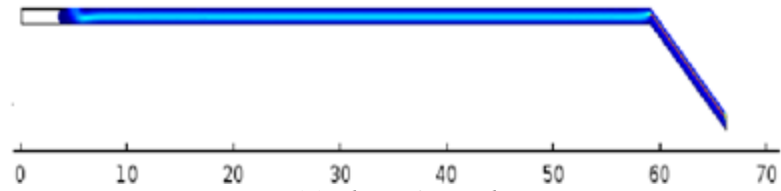
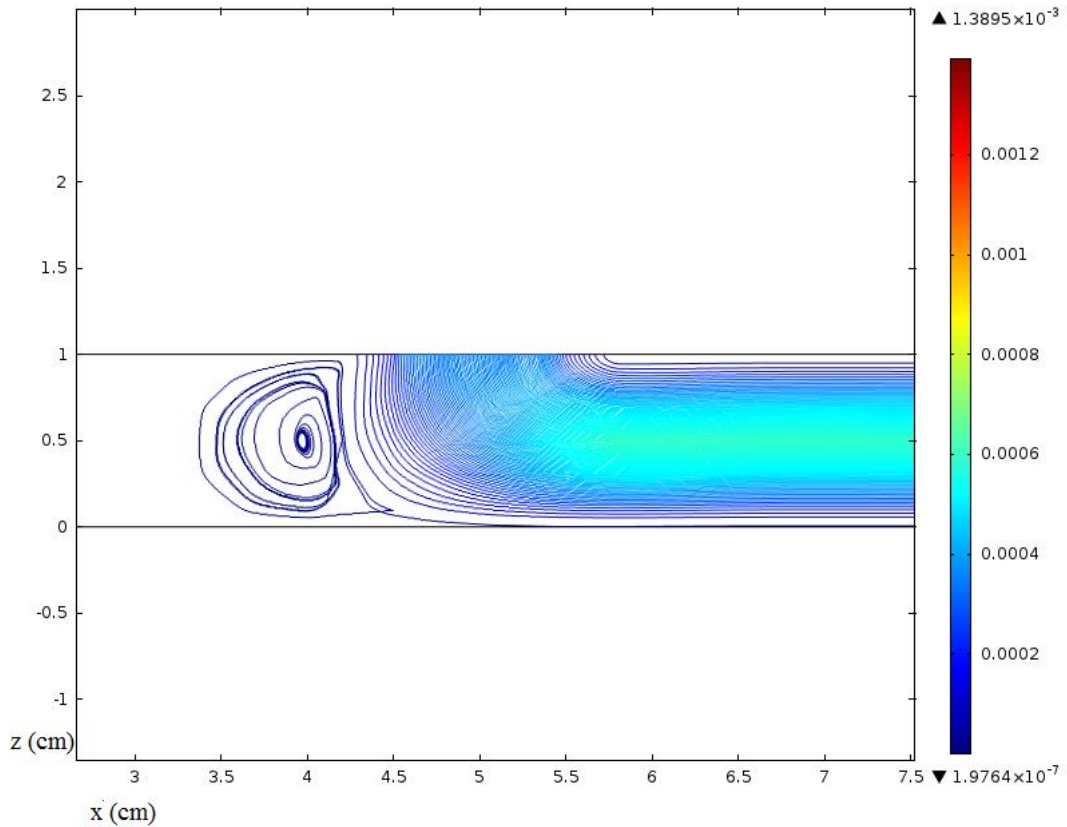


Figure 6: 3D velocity profile for the settling region: (a) the entire settling region; (b) the region near the inlet ports, (c) a cross section of fully developed flow. The angle of inclination is 45 degrees and the inlet flow rate is 20 mL/min.



(a) *The entire settler*



(b) *Near the inlet port*

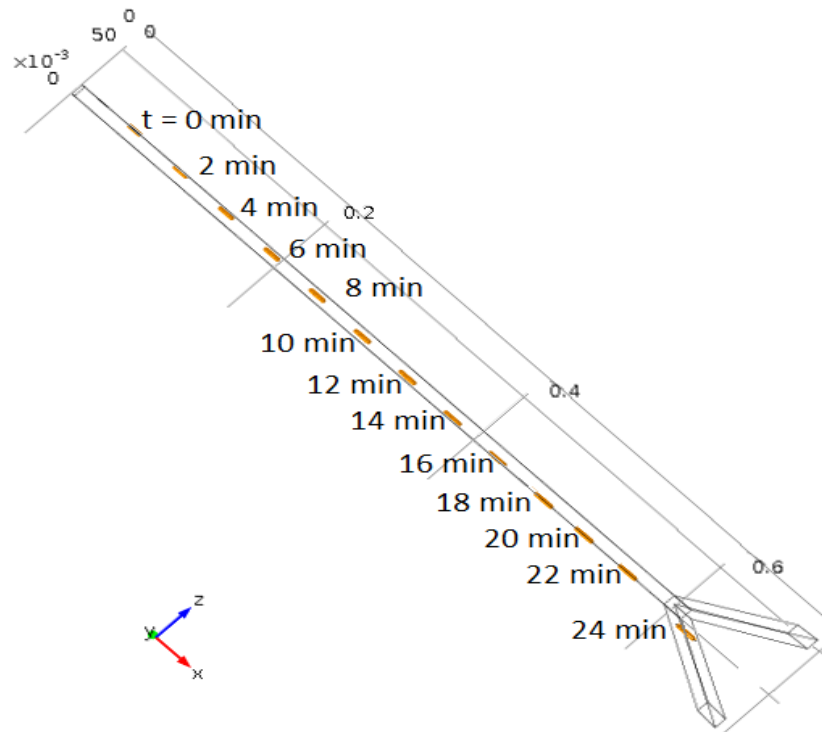
Figure 7: 2D velocity profile for the settling region on a streamline plot: (a) the entire settler; (b) the region near the inlet port. The angle of inclination is 45 degrees and the inlet flow rate is 20 mL/min.

The particle tracing module measures the trajectory of the particles throughout the gravity settler. The algae particles move as a result of the drag force from the water and the force of gravity (Zhang 1998). A particle's settling velocity is the speed in which it "settles" toward the bottom of the settler. This velocity is in the direction of gravity and is a function of the particle diameter, particle and fluid density, and fluid viscosity (Kondrat'ev 2003). The density of both the algae and water remain constant, and the

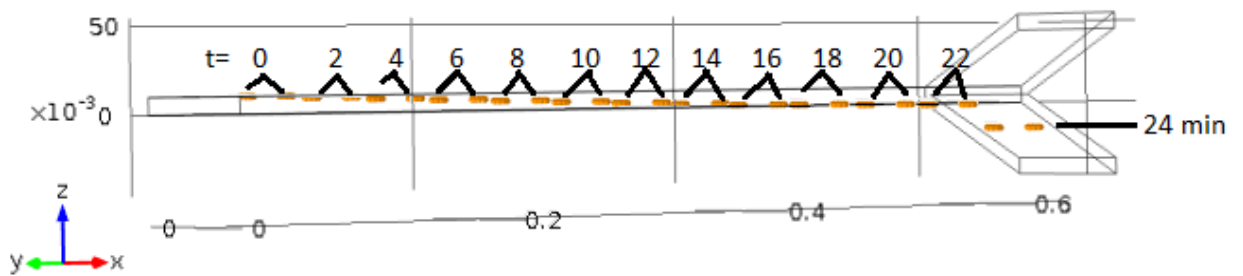
viscosity of the water also remains constant. Therefore, for this project, settling velocity is only a function of the particle diameter. It is estimated using the equations found in Section 3.1.

The particle tracing module evaluates the settling velocity for particles of a given size and calculates the particle velocity in both the x-and z-directions. Since the flow is laminar, particle velocity in the y-direction is negligible (Geankoplis 2003). All cells in these simulations are assumed to be spherical, although actual algae cells are generally oblong (Shen 2009). The particle trajectories for several different particle sizes, ranging from 0.5 μm to 200 μm are examined. As will be further explained in Section 3.3, particles smaller than 0.5 μm and larger than 200 μm have an insignificant contribution to the total mass of the algae in the system.

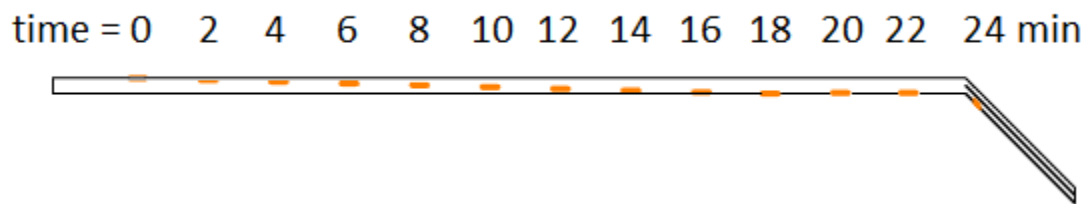
Like the laminar flow module, the particle tracing module was applied to both the 2D and 3D models of the gravity settler. Figure 8 shows the trajectory for a particle of 20 μm diameter using (a, b) a 3D gravity settler model and (c) a 2D model. The trajectories for the particles in the 2D model match those for the 3D model, except at the side walls of the settler, when the fluid velocity is reduced because of the non-slip condition. This is demonstrated in the fluid velocity profile shown in Figure 6(c). For both the laminar flow and the particle tracing modules, a panoramic sweep was used to simulate flow at different angles of inclination. This function of COMSOLTM's LiveLinkTM for SolidWorks[®] application allows for simultaneous simulations while changing one of the variables on the settler and allows for comparison of the results.



(a) 3D model, side view



(b) 3D model, isometric orientation



(c) 2D model

Figure 8: (a,b)3D and (c) 2D particle trajectories for $10\ \mu\text{m}$ diameter particles, a 45-degree angle of inclination, and an initial flow rate of $20\ \text{mL/min}$ falling from the top of the settler. Around $t = 18\ \text{min}$, the particles settle to the bottom of the settler. Per Patankar (2001), the particles will be forced along the bottom of the settler after that point by gravity and the slow fluid flow near the bottom of the settler. Figures 8 (a) and (b) do not account for particles near the sides of the settler whose velocity would be decreased due to the non-slip condition of the walls.

The biggest disadvantage of simulating the model on COMSOLTM is that only one size of particle can be simulated per particle tracing module. Multiple particle tracing modules may be established on the same simulation, but this would increase the time it takes to set up a simulation, and greatly increase the time it takes to simulate the particle and fluid flow. This project makes use of 319 particle size ranges, with each size range accounting for a different percentage of the total mass of algae. This would make COMSOLTM's particle tracing module an extremely time-consuming option for finding the trajectory of all particles in the system.

The most critical assumption made while modeling is the assumption that all particles travel independently of each other and that particle-particle interactions do not take place. According to Liu (2006), when two particles collide with each other, the center of gravity of the system can cause the spheres to experience repulsive motion and the particles can travel across streamlines and in any direction. This assumption can be made because the fluid is extremely dilute as algae naturally accounts for less than 0.1% of the total mass of an algae/water system (Smith 2013). Also, all algae particles are traveling from the inlet of the settler toward the exit region, so the x-component of velocity is positive for all particles. Likewise, the z-component is negative for all particles because they are traveling from the top to the bottom of the settler. The flow is laminar, so the y-component of a particle's velocity is zero. With particles traveling in approximately the same direction, the chance for particle-particle interactions or collisions is significantly reduced from a case in which the flow of particles is random. Neglecting particle-particle interactions also allows for Stokes' Law to be applied (Kraipech 2005).

CHAPTER III

MODELING

3.1. Overview of Fluid Flow and Particle Tracing Modules

The COMSOL Multiphysics™ simulations model fluid flow based on the equations of continuity and motion. The equation of continuity is defined as:

$$\nabla \cdot (\rho_f u_f) = 0 \quad (3.1)$$

in which ρ_f and u_f are the density and velocity of the fluid. ρ_f is the fluid density and This equation implies that the sum of the mass that enters the settler is equal to the sum of the mass that leaves the settler. $\nabla \cdot (\rho u)$ refers to the combined inlet and outlet mass flow rates in the x, y, and z directions (or just the x- and z-directions for 2D flow). The symbol ∇ refers to the mathematical operator, such that

$$\nabla \rho = \vec{i} \frac{\partial \rho}{\partial x} + \vec{j} \frac{\partial \rho}{\partial y} + \vec{k} \frac{\partial \rho}{\partial z} \quad (3.2)$$

in which i, j, and k are unit vectors in the x-, y-, and z-directions, respectively.

Equation 3.2 is the equation used by COMSOL™ to simulate fluid flow. This equation is based on the Navier Stokes equations (Hesketh 2008).

$$\rho(u_f \nabla)u = \nabla \cdot \left[-pl + \mu_f \left(\nabla u_f + (\nabla u_f)^T \right) - \frac{2}{3} (\nabla \cdot u)l \right] + F_G \quad (3.3)$$

In which μ_f is the viscosity of the fluid, p is the pressure, l is the length vector, and “T” refers to the transpose of the ∇u matrix. This equation assumes a fluid constant density and viscosity within the settler. The equation states that the accumulation of momentum per unit volume is equal to the shear stress, minus the rate of momentum, minus the forces related to pressure, plus the forces related to gravity (Hasketh 2008).

COMSOL™’s particle tracing module is based on a momentum balance of the particle, as shown in Equation 3.4.

$$\frac{d(m_p u_p)}{dt} = F_t \quad (3.4)$$

in which the total force, F_t , is equal to the change in momentum over time. m_p refers to the mass of a particle and u_p refers to the particle’s velocity. The next several sections expand upon these equations for fluid flow and particle tracing to generate the model that is used for this experiment.

3.2. 2-Dimensional Model

3.2.1. Force Distribution

A 2-dimensional (2D) model was developed to simulate the motion of the water and the algae particles. The y-direction (the width of the settler) is not considered in this model, as the velocity of the fluid is essentially constant at all y values except near the edges of the settler. This model considers the x- and z-directions. Flow occurs in the positive x-direction. Gravity occurs at an angle between the positive x-direction and the

negative z-direction. This angle is the angle of inclination and is varied to determine the optimal result. This model is shown in Figure 9.

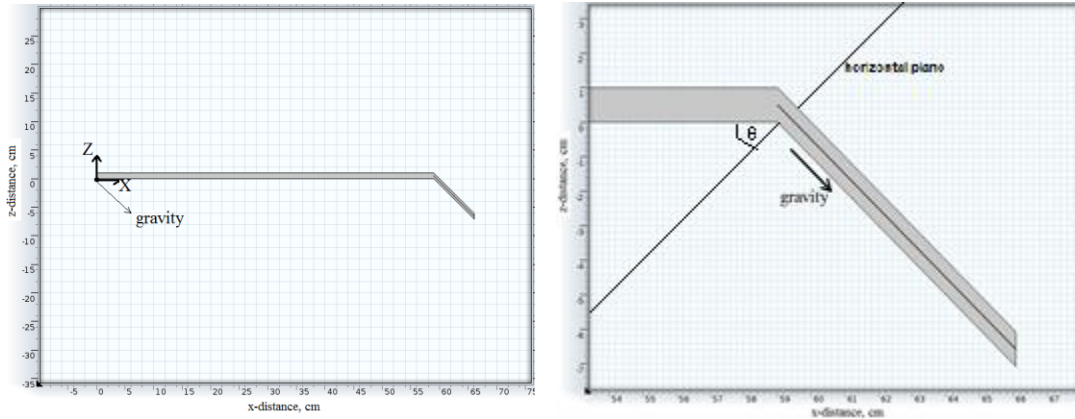


Figure 9: 2D representation of the gravity settler at a 45-degree angle of inclination. (a) Entire settler (b) close-up view of the outlet region. The horizontal axis is in the x-direction and the vertical axis is in the z-direction

This experiment models the flow of algae particles in a fluid. The fluid is a mixture of water and several types of salt. It is assumed to have the same physical properties as water. The three forces on a particle in a fluid are gravity pulling the particle downward; the buoyant force, exerted in the opposite direction of the gravity, that pushes the particle upward; and the drag force exerted by the fluid that pushes the particle in the direction of the fluid. The drag force occurs when relative motion between the particle and the fluid exist (Zhang 1998). The force of gravity, as shown in Equation 3.5, is the product of the particle's mass and its acceleration due to gravity.

$$F_g = -g * m_p \quad (3.5)$$

in which g is the gravitational constant, 9.8065 m/s^2 and m_p is the mass of the particle.

This project uses the directional convention in upward forces are considered positive and

downward forces are considered negative. As the acceleration due to gravity is downward, the g term is negative for this equation.

The buoyant force is calculated by Archimedes' law. It is the mass of the fluid displaced by the particle, multiplied by the gravitational acceleration. The mass of the fluid displaced by the particle, m_f , is:

$$m_f = m_p \frac{\rho_f}{\rho_p} \quad (3.6)$$

where ρ_p and ρ_f are the densities of the particle and fluid, respectively. The density of algae ranges between 1,050 and 1,080 kg/m³ (Cerff 2012, Smith 2012). The fluid in this system is assumed to have the density of water, which is 1,000 kg/m³. The equation for buoyant force becomes:

$$F_b = g * m_f \quad (3.7)$$

In this case, since the buoyant force is acting upward, the gravitational acceleration is considered positive.

The drag force on a particle is calculated from the drag coefficient, which is a function of the Reynolds number. The Reynolds number is:

$$Re = \frac{D_p u_f \rho_f}{\mu_f} \quad (3.8)$$

in which D_p is the diameter of the particle, u_f is the velocity of the fluid, and μ_f is the dynamic viscosity of the fluid. For particles of any Reynolds number, the equation:

$$C_d = \frac{24}{Re}(1 + 0.27Re)^{0.43} + 0.47[1 - \exp(-0.04Re^{0.38})] \quad (3.9)$$

can be used to determine the drag coefficient (Cheng 2009). The particle Reynolds number can be used to categorize the flow of the particle within a fluid into three groups. Particles with a Reynolds number below 1.0 have relative laminar movement relative to the fluid (Terfous 2013). In this region, the first term in Equation 3.5 is responsible for almost the entire drag coefficient (Kondrat'ev 2003). A transitional region, in which properties of laminar and turbulent flow exist for the particle relative to the fluid, is present for Reynolds numbers between 1.0 and 1,000 (Terfous 2013). Lastly, a turbulent flow regime is developed around the particle for Reynolds numbers greater than 1,000 (Terfous 2013). At these values, the drag coefficient becomes essentially constant at 0.47 (Cheng 2009).

Equation 3.10 shows that the flow of algae particles in water for this experiment is in laminar for all cases. The density of water is 10^3 kg/m^3 , its viscosity is a function of temperature. The experiment is being run at room temperature (25°C), in which water has a viscosity of $0.8937 * 10^{-3} \text{ kg/(m/s)}$ (Geankoplis 2003). Velocity of the water is on the order of 10^{-3} to 10^{-4} m/s , and the diameter of algae particles ranges from approximately $2 * 10^{-4}$ to 10^{-6} m (Reynolds 2010). Combining these values into Equation 3.10 produces an approximate maximum Reynolds number that is well below 1.0.

$$Re = \frac{(2 * 10^{-4}m) * (10^{-3} \text{ m/s}) * (10^3 \text{ kg/m}^3)}{(0.8937 * 10^{-3} \text{ kg/ms})} = 0.22 \quad (3.10)$$

The drag force can then be calculated using Equation 3.11:

$$F_d = 3\pi\mu_f u_f D_p + \frac{53\pi D_p^2 \rho_f u_f^2}{8(Re + 32)} + 0.05\pi D_p^2 \rho_f u_f^2 \quad (3.11)$$

(Kondrat'ev 2003). For Reynolds numbers on the order being considered in this project, the first term of Equation 3.5, $24/Re*(1+0.27Re)^{0.43}$, is responsible for the vast majority of the drag coefficient, while the remaining term only makes up about 1% of the drag coefficient (Kondrat'ev 2003). The first term in Equation 3.11 is the Stokes formula used to calculate drag force of particles with Reynolds numbers below 1.0, written as $F_{d,s}$. (Kondrat'ev 2003, Zhang 1998). The Stokes formula is written in Equation 3.12:

$$F_{d,s} = 3\pi\mu_f u_f D_p \quad (3.12)$$

Two thirds of the Stokes drag force is due to friction on the surface of the particle and the other third is a result of different pressures acting on the sphere (Kondrat'ev 2003).

Therefore, Equation 3.12 can be rewritten as:

$$F_{d,s} = \pi\mu_f u_f (2D_s + D_m) \quad (3.13)$$

D_s is the particle's equivalent diameter as determined by measuring the particle's surface area S_s (Kondrat'ev 2003), as shown in Equation 3.14. D_m is the diameter of a particle measured from the mid-section of the particle based on its length (Kondrat'ev 2003). A measurement of D_m is illustrated in Figure 10.

$$D_s = \sqrt{\frac{S_s}{\pi}} \quad (3.14)$$

The gravity, buoyant force, and drag force can all be calculated in both the x- and z- directions. The x-component of each force is equal to the total force multiplied by the

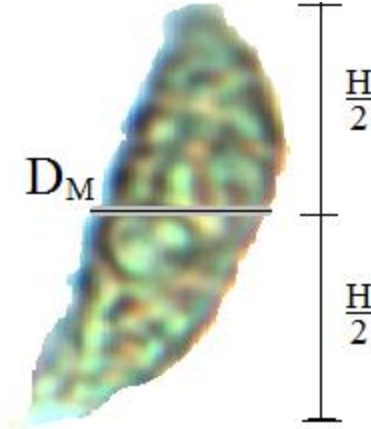


Figure 10: Visual depiction of D_M , the diameter of the particle measured from its mid-section. Image adapted from *S. dimorphus* cell examined at the University of Colorado.

sine of the angle of inclination from the horizontal plane, while the z-component of each force is equal to the total force multiplied by the cosine of this angle. The x- and z-components of each force can be written as:

$$F_{g,x} = F_g * \sin(\theta) \quad (3.15)$$

$$F_{g,z} = F_g * \cos(\theta) \quad (3.16)$$

$$F_{b,x} = F_b * \sin(\theta) \quad (3.17)$$

$$F_{b,z} = F_b * \cos(\theta) \quad (3.18)$$

$$F_{d,x} = F_d * \sin(\theta) \quad (3.19)$$

$$F_{d,z} = F_d * \cos(\theta) \quad (3.20)$$

The three forces can be added together to determine the total force on the particle. Force, according to Newton's Second Law of Motion, is equal to mass times acceleration (Milton 2007). Therefore, with a constant particle mass, the acceleration of the particles can be calculated using Equations 3.21 and 3.22 below.

$$m_p \frac{du_x}{dt} = F_{g,x} + F_{b,x} + F_{d,x} \quad (3.21)$$

$$m_p \frac{du_z}{dt} = F_{g,z} + F_{b,z} + F_{d,z} \quad (3.22)$$

where m_p is the mass of the particle, u_x and u_z are the velocity of the particle relative to the fluid in the x and z directions, respectively, $F_{g,x}$ and $F_{g,z}$ are gravity in the x and z directions, $F_{b,x}$ and $F_{b,z}$ are the buoyant force in the x and z directions, and $F_{d,x}$ and $F_{d,z}$ are the drag force in the x and z directions (Zhang 1998). Note that in Equations 3.21 and 3.22 the gravity and buoyant force are added to each other. This is because the force of gravity is defined in Equation 3.5 as having a negative value and the buoyant force is defined as having a positive value in Equation 3.7.

Equations 3.21 and 3.22 can be combined with Equations 3.5 through 3.7, 3.13, and 3.15 through 3.20 to form Equations 3.23 and 3.24, which define the force on a particle as a function of the particle mass, gravitational acceleration, particle and fluid density, and the velocity and dynamic viscosity of the fluid::

$$F_x = m_p g_x \frac{\rho_p - \rho_f}{\rho_p} + \pi \mu_f u_{f,x} (2D_s + D_m) \quad (3.23)$$

$$F_z = m_p g_z \frac{\rho_p - \rho_f}{\rho_p} + \pi \mu_f u_{f,z} (2D_s + D_m) \quad (3.24)$$

3.2.2. *Settling Velocity*

Within the gravity settler, the solid particles settle in the direction of gravity as the fluid flows toward the outlet. The rate at which these particles settle is the settling velocity, u_s (Kondrat'ev 2003). According to Kondrat'ev (2003), the drag force can be balanced with the variation between gravity and the buoyant force. This relationship is shown in Equation 3.25:

$$F_d = F_g + F_b = \frac{\pi(\rho_p - \rho_f)gD_v^3}{6} \quad (3.25)$$

Per Equations 3.5 and 3.7, the gravity force is based on negative acceleration due to gravity and the buoyant force is based on positive gravitational acceleration. The term D_v in Equation 3.25 refers to the diameter of a particle in relation to its volume. This diameter can be determined using Equation 3.26 (Kondrat'ev 2003):

$$D_v = \left(\frac{6V_p}{\pi}\right)^{\frac{1}{3}} \quad (3.26)$$

in which V_p is the volume of the particle. By associating the result of Equation 3.11 with Equation 3.25, a cubic equation for particle settling velocity, Equation 3.27, can be obtained.

$$\begin{aligned} u_s^3 + \left(\frac{\nu_f}{D_m}\right) \left(20 \frac{2D_s + D_m}{D_m} + 493.5 \frac{D_m}{2D_s + D_m}\right) u_s^2 \\ + \left(\frac{\nu_f}{D_m}\right)^2 \left(1920 - \frac{10Ar}{3}\right) u_s \\ - 320 \left(\frac{\nu_f}{D_m}\right)^3 \left(\frac{D_m Ar}{2D_s + D_m}\right) = 0 \end{aligned} \quad (3.27)$$

The value u_s is the settling velocity, ν_f is the kinematic viscosity of the fluid. The kinematic viscosity of the fluid for this experiment is assumed to be equal to the kinematic viscosity of water, $10^{-6} \text{ m}^2/\text{s}$. Ar is the Archimedes number, defined by Equation 3.28 (Kondrat'ev 2003, Mostoufi 1999):

$$Ar = \frac{(\rho_p - \rho_f)\rho_f g D_v^3}{\mu_f^2} \quad (3.28)$$

An iterative process is required to solve for the settling velocity, u_s . In order to solve for the settling velocity, the settling velocity is estimated. The initial estimation of settling velocity is referred to as $u_{s,0}$, which can be solved for using Equation 3.29:

$$u_{s,0}^2 + 20 \left(\frac{v_l}{D_m} \right) \left(\frac{2D_s + D_m}{D_m} \right) u_{s,0} - 10 \left(\frac{v_l}{D_m} \right)^2 \frac{Ar}{3} = 0 \quad (3.29)$$

Equation 3.29 may be re-written as Equation 3.30.

$$u_{s,0} = 10 \left(\frac{v_l}{D_m} \right) \left(\frac{2D_s + D_m}{D_m} \right) \left\{ \left[1 + \left(\frac{D_m}{2D_s + D_m} \right)^2 \frac{Ar}{30} \right]^{\frac{1}{2}} - 1 \right\} \quad (3.30)$$

After solving for $u_{s,0}$, the actual value of u_s can be solved for iteratively from the recurrence formula (Kondrat'ev 2003). $u_{s,0}$ would be used as the first $u_{s,i}$, which is used to solve for $u_{s,1}$. $u_{s,1}$ will in turn be placed into the recurrence formula to solve for $u_{s,2}$. This process is continued until $u_{s,i+1}$ is approximately equal to $u_{s,i}$. Equation 3.31 displays the recurrence formula.

$$u_{s,i+1} = \frac{2u_{s,i}^3 + au_{s,i}^2 - c}{3u_{s,i}^2 + 2u_{s,i} + b} \quad (3.31)$$

in which a, b, and c are the coefficients of u_s^2 , u_s , and 1, respectively, as shown in Equations 3.32-3.34 (Kondrat'ev 2003):

$$a = \left(\frac{v_f}{D_m} \right) \left(20 \frac{2D_s + D_m}{D_m} + 493.5 \frac{D_m}{2D_s + D_m} \right) \quad (3.32)$$

$$b = \left(\frac{v_f}{D_m} \right)^2 \left(1920 - \frac{10Ar}{3} \right) \quad (3.33)$$

$$c = -320 \left(\frac{v_f}{D_m} \right)^3 \left(\frac{D_m Ar}{2D_s + D_m} \right) \quad (3.34)$$

Equation 3.31 is repeated until $u_{s,i+1}$ is close to $u_{s,i}$. The settling velocity used in combination with the fluid velocity to form a model of particle settling. The overall velocity of a particle in the gravity settler is simply the settling velocity plus the drag velocity. Drag velocity is defined as the velocity of a particle in the direction of fluid

flow that is influenced by the fluid flow. This project assumes the drag velocity to be equal to the velocity profile of the fluid; however the drag velocity may also be influenced by the forces of gravity and buoyancy.

The inlet velocity of the fluid is proportional to the inlet fluid flow rate, which is controlled as part of the experiment. The fluid enters the settler through inlet ports on the top, resulting in an initial velocity in the negative z -direction. Eventually, the fluid is pulled in the positive x -direction by the pumps on the outlets. This model can be used for spherical or oblong particles. Oblong particles rely on diameters calculated from a measured surface area, mid-section area, and volume, respectively, while in a spherical particle, $D_s = D_m = D_v = D$, the actual diameter of the sphere. Equations 3.27-3.34 can be simplified for spherical particles using this relation.

Settling velocity has two components: an x -component and a z -component. The two components are calculated using the angle of inclination from the horizontal plane, θ , by using Equations 3.35 and 3.36:

$$u_{s,x} = u_s \sin(\theta) \quad (3.35)$$

$$u_{s,z} = u_s \cos(\theta) \quad (3.36)$$

The x - and z -components of the total velocity of the particle, u_p , are the respective sums of the velocity from settling and its velocity as a result of drag force. These components can be calculated using Equations 3.37 and 3.38:

$$u_{p,x} = u_{s,x} + u_{d,x} \quad (3.37)$$

$$u_{p,z} = u_{s,z} + u_{d,z} \quad (3.38)$$

in which $u_{d,x}$ and $u_{d,z}$ are the drag velocity in the x- and z-direction, respectively. Since the fluid flow is laminar, it can be assumed that the fluid velocity only occurs in the direction of flow, the x-direction (Geankoplis 2003). This assumption is made after the velocity profile is fully developed, as Figure 7(b) shows an initial flow in the negative z-direction. Therefore, the $u_{f,z}$ term can be removed from Equation 3.38 after the velocity profile becomes fully developed. The particle velocity in the z-direction will be equal to the settling velocity in the z-direction.

Next, the residence time and settling time of the particle are calculated. A particle's residence time is a function of its velocity in the x-direction as well as the length of the gravity settler. It is shown using Equation 3.39:

$$\tau_p = \frac{L}{u_{p,x}} \quad (3.39)$$

in which L is the length of the settler. Likewise, the settling time $t_{s,p}$, is calculated as the amount of time required for a particle to settle from the top to the bottom of the settler. It is a function of the particle's settling velocity and settler height, as shown in Equation 3.40:

$$t_{s,p} = \frac{H}{u_{p,z}} \quad (3.40)$$

where H is the height of the settler. Since the residence and settling times depend on the particle's velocity in the x- and z-directions, they are also dependent upon the settler's angle of inclination, inlet flow rate, length, width, and height.

The distance that a particle travels in the z-direction, dz, is calculated by multiplying the settling velocity by the residence time. Should the calculated dz value be

greater than the height of the settler, then it is expected that the particle would travel in the direction of flow near the bottom of the settler (Patankar 2001). Therefore, dz cannot be greater than the height of the settler:

$$dz = \max(u_{p,z} * \tau_p, H) \quad (3.41)$$

3.2.3. Velocity Profile

Next, the percent of the settler's height that the particle must travel in order to exit the settler through the underflow must be calculated. This is done by taking the integral of the velocity profile. The velocity profile follows the non-slip condition in which fluid velocity at the wall of the settler is equal to the velocity of the wall itself (Geankoplis 2003), which is zero for this experiment. The velocity profile was calculated as a function of the maximum velocity, $u_{f,max}$ from a simulation using COMSOL MultiphysicsTM. The velocity u_f is zero at the top and bottom walls, but it increases to approximately half of $u_{f,max}$ just 0.005 cm from the walls. After which, the fluid velocity increases linearly at the slope of about 1.25 cm^{-1} until the velocity ratio reaches 1. This increase in velocity is seen near both the top and bottom of the gravity settler. Equation 3.42 and Figure 11 illustrate the fully developed velocity profile. Velocity in the x-direction is written as a function of z . For Equation 3.38, z refers to the position on the z axis, given in centimeters.

$$\frac{u_{f,x}}{u_{f,x,max}} = -3.8503z^2 + 3.8481z + 0.0112 \quad (3.42)$$

This velocity profile is shown on Figure 11. The fluid velocity is equal to at least half of the maximum velocity for approximately 70% of the height of the settler. The average velocity can be calculated by taking the integral of the velocity profile equation

between $z = 0$ cm and 1 cm, shown using Equation 3.35, in which h is the height of the settler. Using Equation 3.43, the average velocity was found to be 0.65 times the maximum velocity.

$$\frac{u_{f,av}}{u_{f,max}} = \frac{\int_0^1 \frac{u_f}{u_{f,max}}(z) dz}{h} \quad (3.43)$$

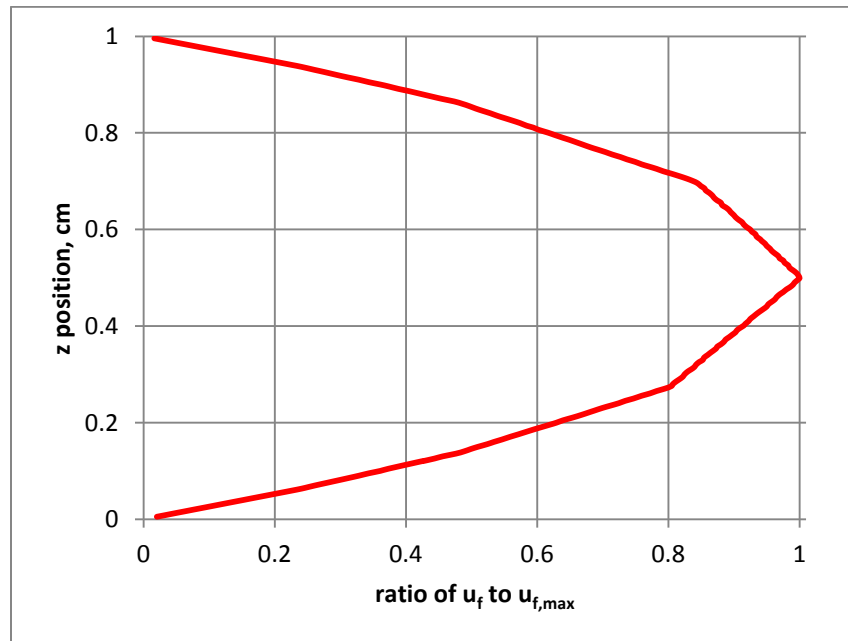


Figure 11: 2D Velocity profile of the fluid in the gravity settler.

Figure 12 shows that the velocity profile throughout settling region of the gravity settler is constant until about 1 cm before the flow separates into the upper and lower outlet regions for various flow separations between the two outlets. Figure 12 shows that in the last centimeter before the settling region splits into the two outlet regions, a fluid velocity in the z direction is introduced. This velocity is the result of different amounts of water leaving each exit region. Note that in Figure 12(d), no fluid velocity in the z -direction occurs because the same amount of water leaves the gravity settler through both

exit regions. Figure 12(a) has the highest discrepancy, where 90% of water leaves the gravity settler through the overflow outlet. In Figure 12(a), the fluid that was in approximately the top 90% of the settling region left the settler through the overflow outlet, while only the fluid in the bottom 10% of the settling region left the settler.

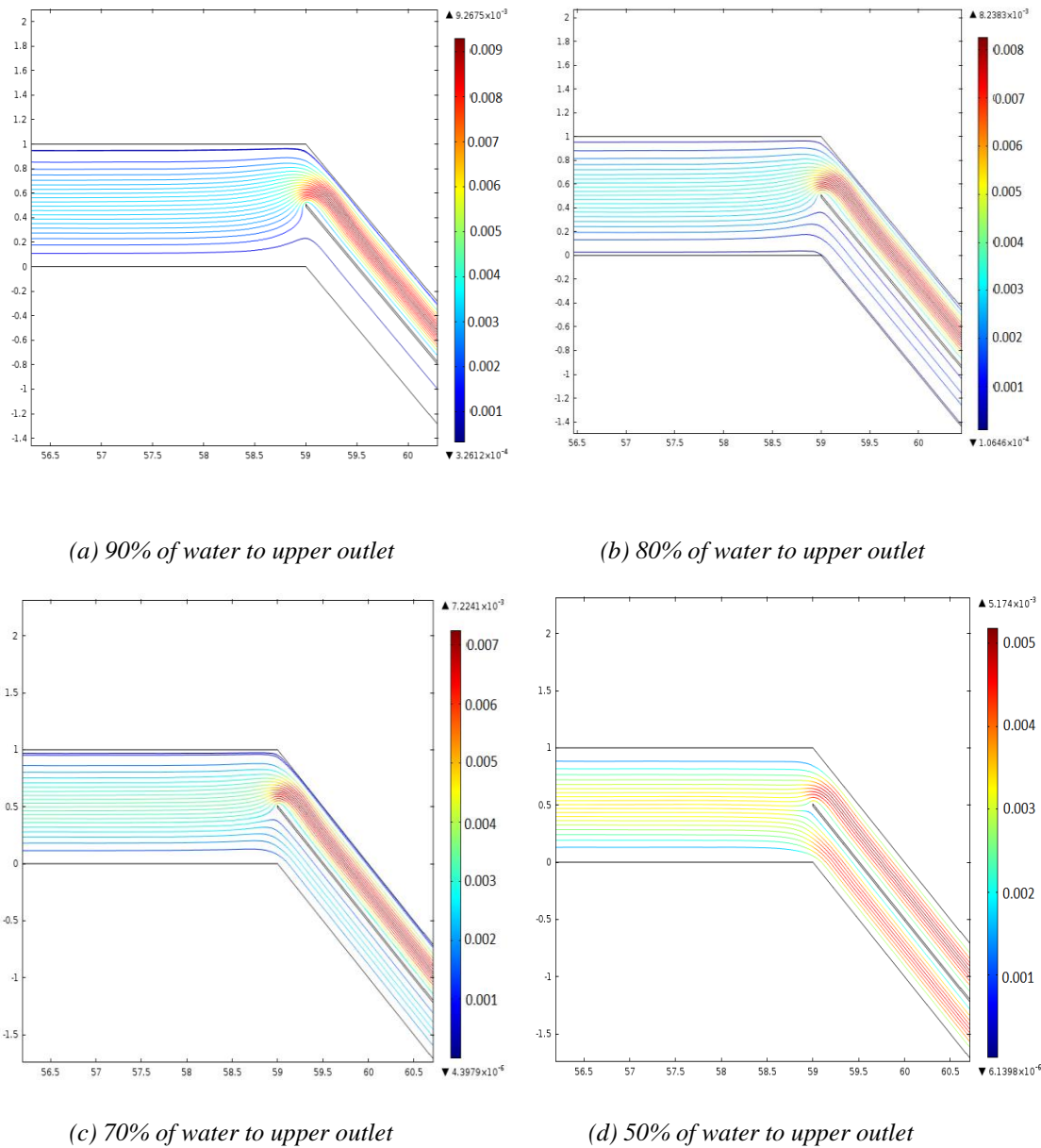


Figure 12: Streamline plot of velocity profile of the fluid through the gravity settler near the split between the settling region and the two outlet region for (a) 90%, (b) 80%, (c) 70%, and (d) 50% of the fluid exiting via the upper outlet.

In order to leave the settler through the underflow outlet, a particle must settle to a z -value such that the fluid at that z -value will also exit through the underflow outlet. This does not correspond to the percent of fluid exiting through the underflow outlet, but is instead related to the velocity profile. For example, Figure 13 shows that if 90% of the fluid exits the settler through the overflow, the bottom 10% of the fluid will exit through the underflow. Figure 13 shows that fluid (and particles) between the bottom of the settler and $z = 0.16$ will exit the settler through the underflow, while fluid (and particles) above this point will exit through the overflow region. Equation 3.44 can be used to calculate the z -value in which fluid above this point will exit through the overflow outlet and fluid below this point will exit through the overflow.

$$\int_0^{z_{split}} u_f(z) dz = PCTF_{underflow} * \int_0^1 u_f(z) dz \quad (3.44)$$

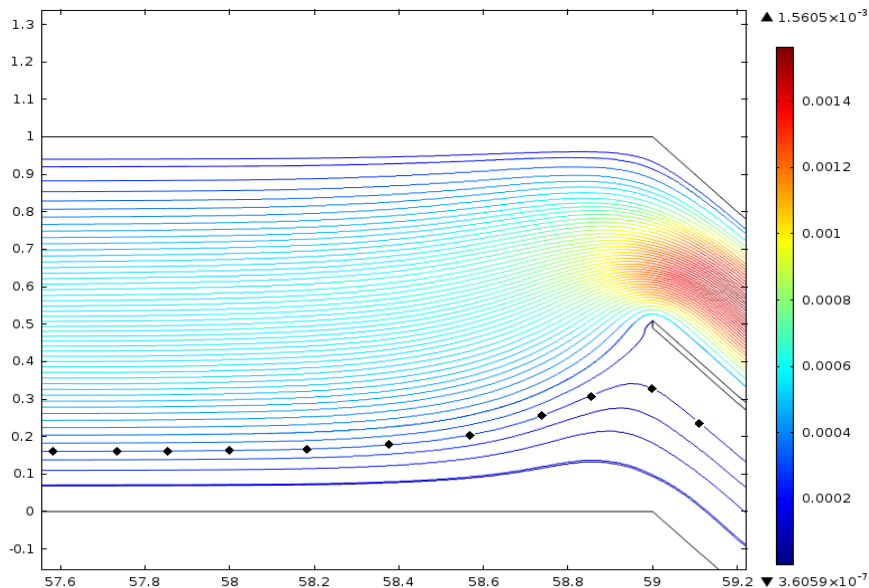


Figure 13: Streamline plot of velocity profile of the fluid through the gravity settler near the split between the settling region and the two outlet region for 90% of the water exiting via the upper outlet. The streamline with the black diamonds on it represents the highest streamline that will exit through the overflow. This streamline is at a value of $z = 0.16$ cm for the fully developed fluid flow prior to $x = 58$ cm.

3.2.4. Particles near the Bottom of the Settler

After the particles reach the bottom of the settler, they will settle on the bottom wall and slowly travel to the underflow outlet. For particles heavier than the fluid, such as algae particles in water, the particles will be forced in the direction of flow on the bottom of the settler by a “plane Poiseuille flow” (Patankar 2001). However, if the particle Reynolds number exceeds a critical Reynolds number, as defined by Patankar (2001), the particle will experience lift (Patankar 2001).

Patankar (2001) defines the critical Reynolds number as a function of the Archimedes number, which is obtained from Equation 3.28. Figure 14 shows a comparison of the Archimedes number to the critical Reynolds number, based on plots in Patankar’s research. Equation 3.45 is derived from Figure 3.6 to relate the Archimedes number to the critical Reynolds number:

$$\log_{10}(Re_{critical}) = 0.5842 * \log_{10}(Ar) + 0.7771 \quad (3.45)$$

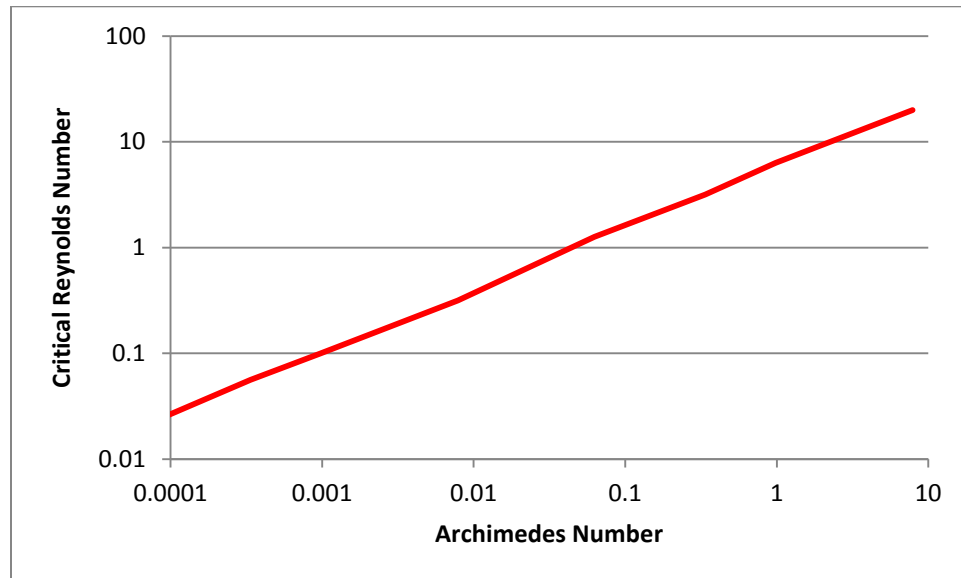


Figure 14: Critical Reynolds number as a function of Archimedes number, adapted from Patankar (2001).

in which $Re_{critical}$ is the critical Reynolds number. Larger diameters result in higher values of Ar . An increase in Ar results in an increase in the Critical Reynolds number, making it less likely for the particles to lift off the bottom of the settler (Patankar 2001).

Figure 15 shows that the particle Reynolds numbers are less than the critical Reynolds numbers for all particle sizes. In the case of large particles which are more likely to settle on the bottom of the gravity settler, the difference is multiple orders of magnitude. With the actual Reynolds number considerably lower than the critical Reynolds number, it is very unlikely that any particles would be lifted from the bottom of the settler and into the middle of the fluid flow (Patankar 2001). The particles that settle to the bottom of the gravity settler will be forced toward the underflow outlet of the settler by the drag force applied by the fluid and the gravitational force.

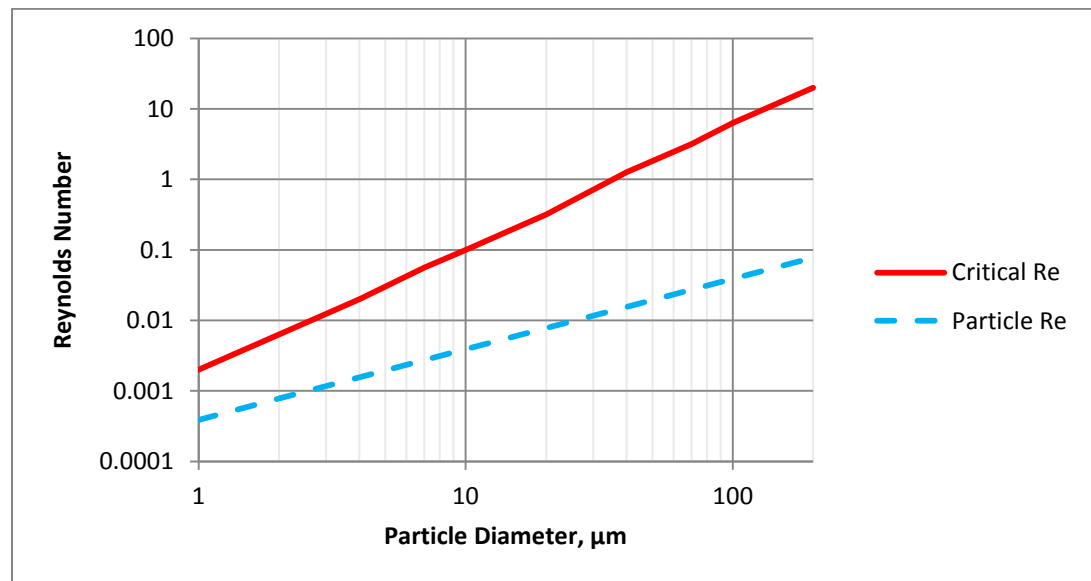


Figure 15: Critical Reynolds numbers compared to actual particle Reynolds numbers for an inlet flow of 10 mL/min

3.3. 3-Dimensional Model

The 2D model was then quickly transformed into a 3-dimensional (3D) model by re-inserting the y-dimension. As was the case in the 2D model, fluid flow occurs in the positive x-direction. Since the flow is laminar, flow will only occur in the x-direction and no fluid flow in the y- or z-direction will take place except near the inlet and outlet of the settler. Gravity occurs at an angle between the positive x-direction and the negative z-direction, as was the case for the 2D model. There is no gravity in the y-direction. Therefore, Equations 3.5-3.34 would be the same for both the 2D and 3D models.

The biggest difference between the two models is the velocity profile of the fluid. In a 3D model, the velocity profile would be calculated as a function of both y and z. The non-slip condition exists for the back wall ($y=0$ cm), front wall ($y=9.5$ cm), bottom ($z=0$ cm), and top ($z=1$ cm). Fluid velocity at these four walls is equal to the velocity of the walls themselves (Geankoplis 2003), which is zero for this experiment. The velocity profile was calculated as a ratio of velocity to the maximum velocity, $u_{f,max}$ from a simulation using COMSOL Multiphysics™.

The velocity profile in the z-direction is constant for y values between about 0.4 cm and 9.1 cm, or any distance at least 0.4 cm from the edges. Likewise, the velocity profile in the y-direction is constant for all z-values between 0.39 and 0.58 cm, and the entire velocity profile decreases near the edges of the settler. The z values in which the velocity of the fluid begins to decrease are the same values in which velocity decreased in the 2D model. The velocity profile of the 3D model can be summarized using Equations 3.42 and 3.46. The velocity profile in the y-direction is shown in Figure 16. The velocity

is approximately equal to the maximum velocity when $0.39 \text{ cm} < z < 0.58 \text{ cm}$ and $0.32 \text{ cm} < y < 9.18 \text{ cm}$, which covers 17.7% of the flow region of the settler.

$$\begin{aligned} \frac{u_f}{u_{f,max}}(y) &= 3.70y^2 + 67.3y - 305 && \text{For } y \leq 0.5 \text{ cm} \\ \frac{u_f}{u_{f,max}}(y) &\approx 1 && \text{For } 0.5 \text{ cm} < y \leq 9.1 \text{ cm} \\ \frac{u_f}{u_{f,max}}(y) &= -3.64y^2 + 3.68y + 0.0052 && \text{For } y > 9.1 \text{ cm} \end{aligned} \quad (3.46)$$

The velocity profile as a function of y and z will be approximated as the minimum value of the velocity profile as a function of y and that of z , as shown in Equation 3.47. The average velocity can be calculated by dividing the double integral of the velocity profile equation between $y = 0 \text{ cm}$ and $y = 9.5 \text{ cm}$ and between $z = 0 \text{ cm}$ and 1 cm by the cross-sectional area of the settler, as shown in Equation 3.48, where y and z are the fluid's respective positions on the y - and z -axes and A is the cross-sectional area of the settler.

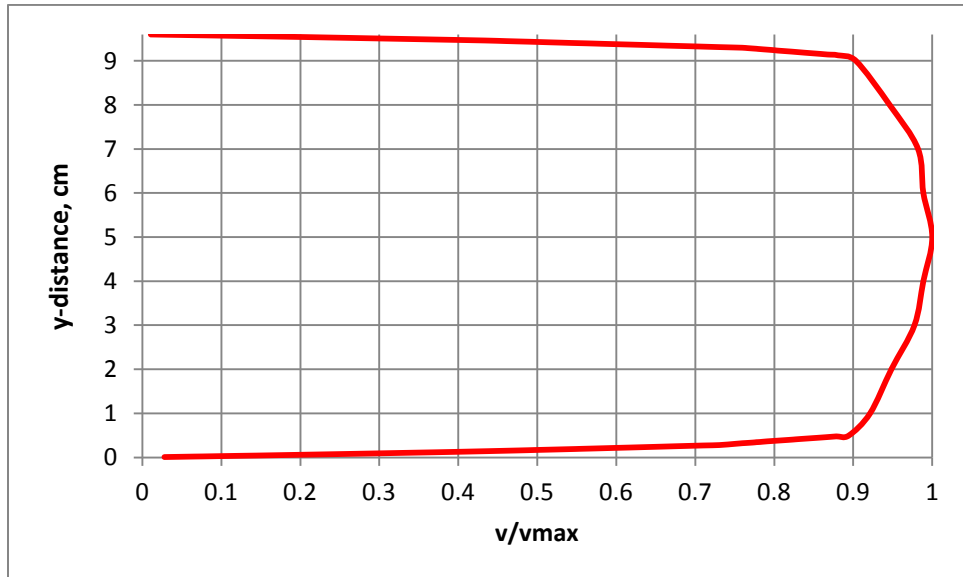


Figure 16: Velocity profile as a function of y at $z = 0.5 \text{ cm}$

$$\frac{u_f}{u_{f,max}}(y, z) \approx \min\left(\frac{u_f}{u_{f,max}}(y), \frac{u_f}{u_{f,max}}(z)\right) \quad (3.47)$$

$$\frac{u_{f,av}}{u_{f,max}} = \frac{\int_0^1 \int_0^5 \frac{u_f}{u_{f,max}}(y, z) dy dz}{A} \quad (3.48)$$

The 3D velocity profile is shown on Figure 17. Figure 17 shows that the fluid velocity is equal to over half of the maximum velocity throughout the entire gravity settler, except at the edges. The velocity increases quickly away from the edges of the settler, as a move of just 0.05 cm increases the fluid velocity to about half of the maximum velocity. The fluid velocity is essentially equal to the maximum velocity when there is no wall within about 0.4 cm in any direction of a given point. The average velocity calculated from this profile using Equation 3.48 is 0.60 times the maximum velocity, an 8% decrease from the average velocity using the 2D model. This small difference is the result of considering the side walls of the 3D model. These walls do not exist in a 2D model. As the width of the settler increases, the disparity between the average velocity in 2D and 3D models will decrease. An infinitely wide 3D settler would have the same velocity profile as a 2D settler. The same can be said for the height of the settler in both a 2D and 3D model. A taller settler will have a higher average velocity because the top and bottom will be further apart and the percentage of the cross-sectional area with maximum velocity will be higher. However, the disadvantage of a taller settler is that it would take more time for the particles to settle, resulting in fewer algae in the underflow and a less concentrated product stream.

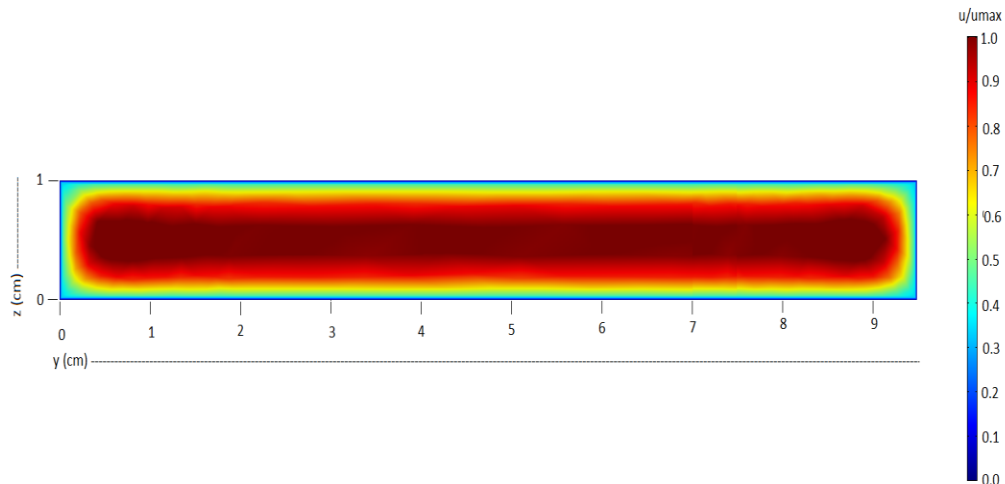


Figure 17: *Cross-sectional velocity profile for flow in a 3D gravity settler model*

Since the difference between average velocities for a 2D and 3D model is less than 10%, the 2D approximations can be used to estimate the separation of algae from the fluid. This difference would cause the algae concentration in the underflow stream to be slightly lower than it actually would be. Furthermore, a settler with a width of 9.6 cm is more suited for laboratory use, whereas a gravity settler in industry would be much larger in order to allow for large amounts of algae to be harvested. A wider settler would result in a lower percentage of fluid having its velocity reduced by being near the edge.

3.4. Particle Size Distribution

3.4.1. Size Distribution found in Literature

Size is a very important factor in determining the motion of algae particles. Larger particles are much more likely to sink further within the fluid than smaller particles are. For this reason, it is important to determine the approximate distribution of particle sizes. Reynolds, Stramski, Wright, and Wozniak (2010) define particle size

distribution as “the average number of particles within a given size class of width ΔD for a unit of suspension:

$$N(D) = N'(D)\Delta D \quad (3.49)$$

in which $N(D)$ is the number of particles per unit volume in a given size interval. There are 319 size intervals used in this project, ranging from 0.5 μm to 200 μm . For this project, particle size is measured as its diameter. $N'(D)$ represents the differential of the distribution of unit size, found by:

$$N'(D) = k \left(\frac{D}{D_0} \right)^{-\gamma} \quad (3.50)$$

where D_0 is a reference diameter, k is measured number of particles at diameter D_0 within a given volume, and $-\gamma$ is the slope of this distribution (Reynolds 2010), with values typically between -3.5 and -4 for underwater species (Jonasz 2007).

Equation 3.50 shows that particle size distribution is not a function of concentration. The number of particles of diameter D [$N'(D)$] is related to the ratio of D to D_0 raised to an exponent. The exponent, $-\gamma$, is the slope on log-log plots of particle distribution vs. diameter. The only changes in $-\gamma$ are the result of a change in diameter and do not have to do with concentration of algae (Reynolds 2010).

Reynolds et al. (2010) determined experimentally that the particle distribution for *Dunaliella tertiolecta*, an algae strain similar to *S. dimorphus*, follows Figure 18. The particles were counted using three distinct methods: a Coulter-counter, which is an electrical impedance particle sizer; the LISST-100X, which is a laser diffractometer; and a flowCAM, which is a particle imaging system (Reynolds 2010). The particle size

distribution was approximately the same with each method, except for the particles of the smallest diameters (Reynolds 2010).

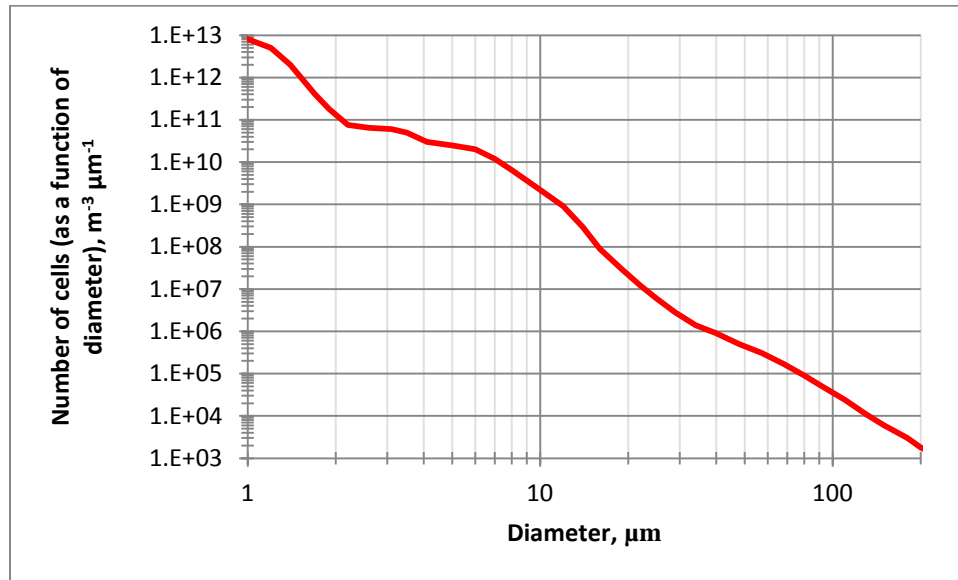


Figure 18: Log-log plot of particle size distribution for *D. tertiolecta* cultures measured using the LISST-100X laser diffractometer (adapted from data acquired by Reynolds, Stramski, Wright, and Wozniak (2010)).

Figure 18 measures the number of cells at a given size using the units of cells per meter cubed per micrometer. The number of cells at a certain size range is calculated as the integral of the data in Figure 18 between a specified minimum and maximum point. The units of this integral are the product of the units of the y-axis (cells/[m³μm]) and the units of the x-axis (μm). The product of these units is cells per cubic meter.

Figure 18 shows that particles with diameters in the order of 1 μm (10⁻⁶ m) are far more numerous than particles in the order of 10 or 100 μm (10⁻⁵ or 10⁻⁴ m). However, a larger particle would have a much greater volume. Equation 3.51 shows that a particle with a diameter of 1 μm has a volume of 0.52 μm³, while Equation 3.52 a particle with a diameter of 100 μm has a volume of 520,000 μm³, a difference of six orders of

magnitude. Particle mass is directly proportional to particle volume, provided that the density of the particles is the same.

$$V_{D=1\mu\text{m}} = \frac{4}{3}\pi\left(\frac{D}{2}\right)^3 = \frac{4}{3}\pi\left(\frac{1\mu\text{m}}{2}\right)^3 = 0.52\ \mu\text{m}^3 \quad (3.51)$$

$$V_{D=100\mu\text{m}} = \frac{4}{3}\pi\left(\frac{D}{2}\right)^3 = \frac{4}{3}\pi\left(\frac{100\mu\text{m}}{2}\right)^3 = 520,000\ \mu\text{m}^3 \quad (3.52)$$

According to Figure 18, there are about 10^{12} particles with a diameter between 1 and 2 μm per cubic meter of fluid and about 10^4 particles with a diameter between 101 and 102 μm per cubic meter, a difference of eight orders of magnitude. When the mass of the algae, rather than the amount of particles, is considered, the difference becomes just two and a half orders of magnitude, meaning there are about 500 kg of algae from particles with a 1 μm diameter for every kilogram of algae from particles with a 100 μm diameter. Particles of diameters between 0.1 μm and 1 mm will be examined. Particles smaller than 0.1 μm have a negligible mass. As the diameter exceeds 1 mm, even though the mass of the particles continues to increase, the amount of particles will become very small in relation to the amount of particles of smaller diameters. Reynolds' data, summarized in Figure 18, will be extrapolated for particles with diameters less than 1 μm and greater than 300 μm .

3.4.2. Comparison of Algae Strains

Like *S. dimorphus* cells, *D. tertiolecta* cells have high oil yields and CO_2 sequestration rates (Reynolds 2010, Tang 2011). Both strains can be grown in non-conventional locations and tolerate high amounts of CO_2 (Jiang 2013, Tang 2011). Cells of both strains are typically between 5 and 11 μm long (Hall 1998, Reynolds 2010, Shen

2009, Tang 2011). The biggest difference between these two strains of algae is that *S. Dimorphus* cells clump together regularly to form small colonies, while *D. tertiolecta* cells do not clump (Hall 1998). According to Wang (2013), *S. Dimorphus* exist in single cells as well as colonies of two, three, and four cells.

Wang et al. (2013) measured the distribution of colonies of each size using a hemocytometer. Figure 19 shows that single cells constitute 10% of the *S. Dimorphus* particles, two-cell colonies make up 14%, three-cell colonies make up 5%, and four-cell colonies make up the balance, 71%. The weighted average colony size is 3.4 cells. In order to measure *S. Dimorphus* particle trajectories using Reynolds' (2010) data found on Figure 18, the cell volume must be multiplied by 3.4. In order to do this, the cell diameter must be multiplied by the third root of 3.4, as shown in Equation 3.53:

$$D_{S.Dim} = D_{D.Ter} * \sqrt[3]{3.4} \quad (3.53)$$

in which $D_{S.Dim}$ and $D_{D.Ter}$ are the diameters of a *S. Dimorphus* colony and a *D. Tertiolecta* cell, respectively. The third root is used because the volume is a function of the cube of the diameter.

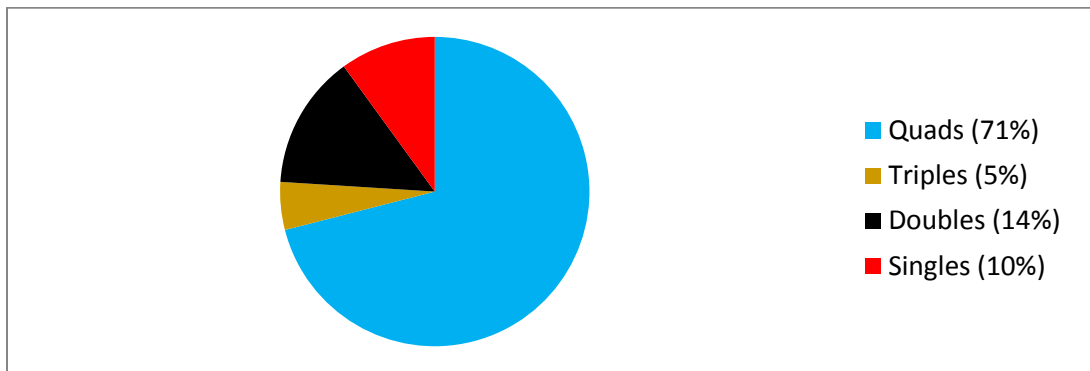
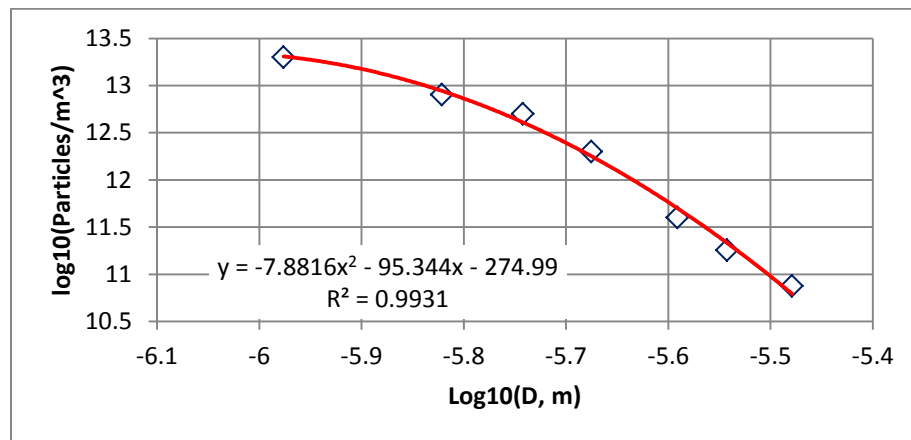


Figure 19: Distribution of *S. Dimorphus* particles between single cells and groups of two, three, or four cells. Adapted from Wang et al. (2013)

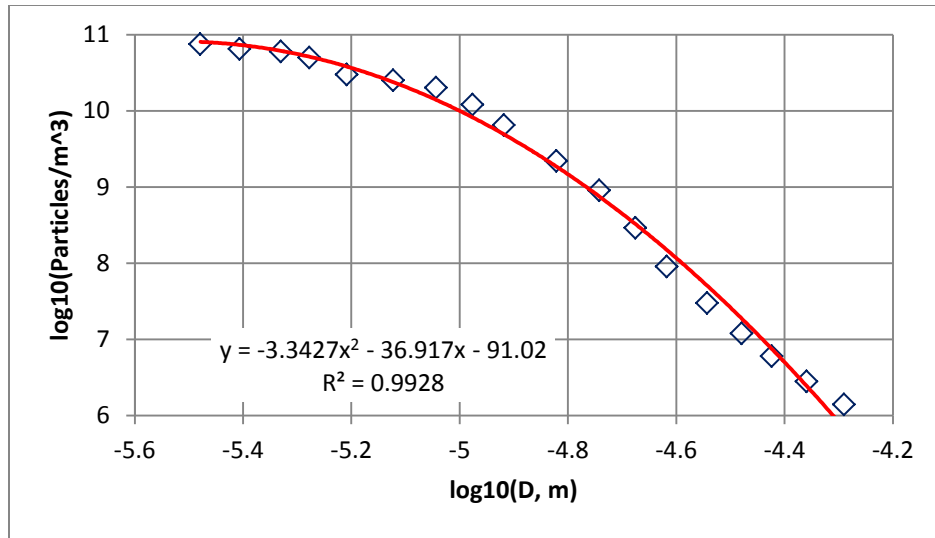
Figure 20 plots the predicted particle size distribution of *S. Dimorphus* determined by Reynolds' (2010) LISST results and Equation 3.54. The LISST results are used because they are the only set of results that span two orders of magnitude for particle size (from 1 μm to 200 μm for *D. Tertiolecta*). For particles greater than 50 μm in diameter (Figure 20(c)), the $N'(D)$ vs. D plot produces a linear correlation on a log-log plot. This means that Equation 3.50 is feasible, in which the slope of the line equals $-\gamma$. Data points for particles with a diameter of less than 3.3 μm (Figure 20(a)) and those whose diameters are between 3.3 and 50 μm (Figure 20(b)) fit a quadratic correlation on the log-log plot. These data can be summarized using the equations:

$$\begin{aligned} \log_{10}[N'(D)] &= -7.8816[\log_{10}(D)]^2 - 95.344\log_{10}(D) - 274.99 && \text{for } D \leq 3.3 \mu\text{m} \\ \log_{10}[N'(D)] &= -3.3427[\log_{10}(D)]^2 - 36.917\log_{10}(D) - 91.02 && \text{for } 3.3 \mu\text{m} < D \leq 50 \mu\text{m} \\ \log_{10}[N'(D)] &= -3.8181\log_{10}(D) - 10.099 && \text{for } D > 50 \mu\text{m} \end{aligned} \quad (3.54)$$

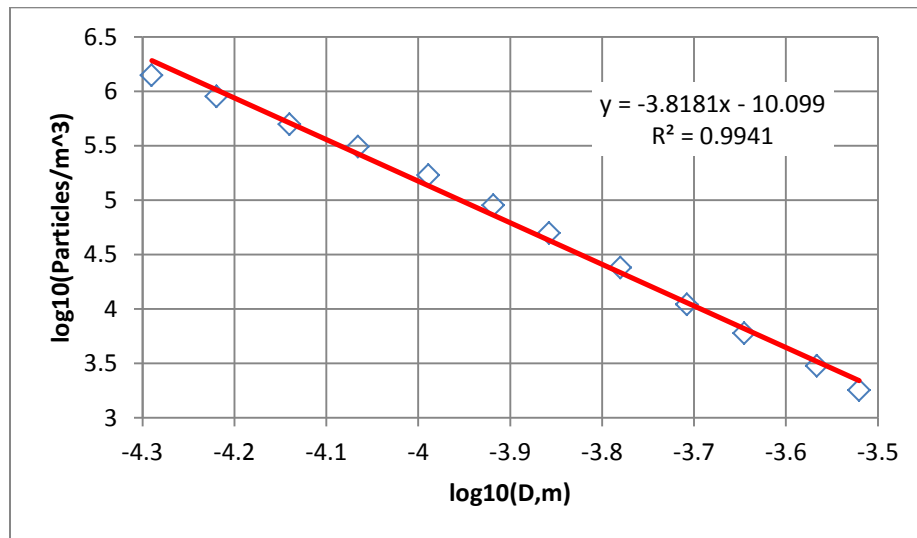
in which $N'(D)$ is the number of particles of a given diameter per cubic meter of fluid and D is the diameter in meters. The correlation is very close ($R^2 > 0.99$) to a linear or quadratic equation.



(a) Particle diameter is less than 3.3 μm



(b) Particle diameter is between 3.3 and 50 μm



(d) Particle diameter is greater than 50 μm

Figure 20: Log-log plot of predicted particle size distribution for *S. Dimorphus*. The blue diamonds show each data point as adapted from Reynolds' (2010) measurements and the red line is a trend line.

3.4.3. Particle Mass Distribution

Equation 3.55 is used to determine the total mass per cubic meter of particles with a certain diameter, or the amount of algae that separates into particles of a given size after accounting for mass. The mass is simply the number of particles multiplied by particle volume and particle density:

$$m = N'(D) \frac{4}{3} \pi \left(\frac{D_p}{2} \right)^3 \rho_p \quad (3.55)$$

Figure 21 plots the total mass of particles with a given diameter against particle diameter in a log-log plot. It was expected the mass would be low at the lowest and highest diameters. Equation 3.56 shows that particle mass increases with the cube of the particle diameter. As the diameter decreases, the mass of the particle very rapidly decreases even as the amount of particles continues to rise. However, due to the shape of the particle size distribution, the total mass vs. diameter plot has two peaks, at about 1 μm and 6 μm . A local minimum is present around 3.3 μm . The mass-weighted particle size distribution follows Equation 3.47. All of the equations are based on mass vs. size correlation that considers Figure 16 and Equation 3.46. The R^2 value for each equation in Equation 3.56 is greater than 0.93.

$$\begin{aligned} \log_{10}[M(D)] &= -7.458[\log_{10}(D)]^2 - 87.06[\log_{10}(D)] - 256.5 && \text{for } D \leq 3.3 \mu\text{m} \\ \log_{10}[M(D)] &= 2.168[\log_{10}(D)]^3 + 28.48[\log_{10}(D)]^2 + 121.3[\log_{10}(D)] + 162.7 && \text{for } 3.3 \mu\text{m} < D \leq 50 \mu\text{m} \\ \log_{10}[M(D)] &= -1.291[\log_{10}(D)]^3 - 10.89[\log_{10}(D)] - 27.46 && \text{for } D > 50 \mu\text{m} \end{aligned} \quad (3.56)$$

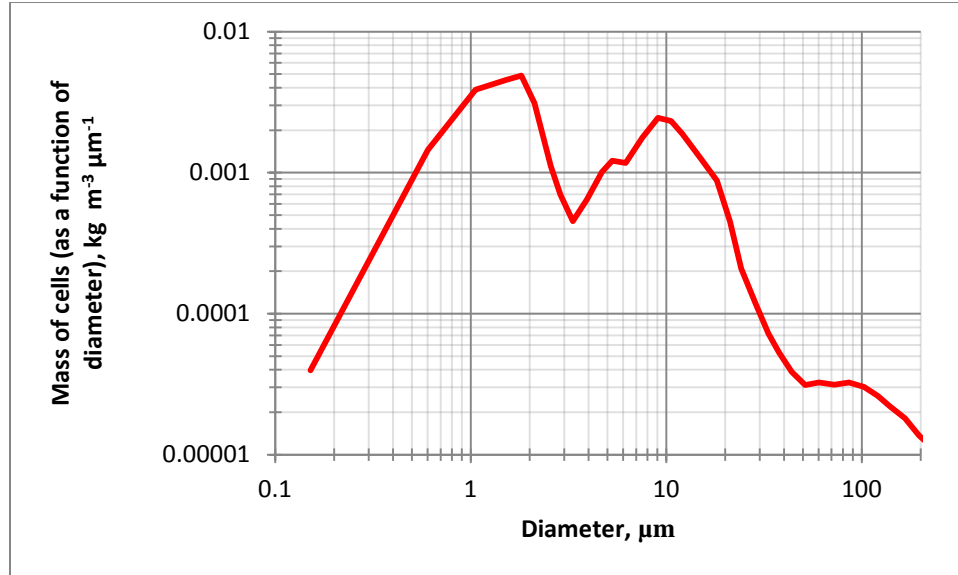


Figure 21: Log-log plot of mass-weighted particle size distribution for *S. Dimorphus*. Data for particles 1.8 μm or larger are adapted from Reynolds' (2010) particle size distribution data. Data for particles smaller than 1.8 μm are extrapolated from Reynolds' data.

In order to simulate the flow of particles through the gravity settler, particles of 319 different size ranges are considered. Each size range spans a distance of between 0.1 and 2 μm, depending on the mass of cells in that size range, as plotted in Figure 21. Most of the algae exist in particles with diameters less than 30 μm, so smaller size intervals are examined in this range. The total particle mass of all the particles in a size range is calculated from Equation 3.57, the definite integral of the mass vs. diameter plot:

$$\int_{LL}^{UL} M(D)dD \tag{3.57}$$

In which LL and UL are the lower and upper limits of a given particle size range, M (D) is mass as a function of diameter which can be calculated based on the data in Figure 21.

:

$$\begin{aligned}
\log_{10}[M(D)] &= -7.8816[\log_{10}(D)]^2 - 92.344[\log_{10}(D)] && \text{for } D \leq 3.3 \mu\text{m} \\
&\quad - 272.78 \\
\log_{10}[M(D)] &= 2.2842[\log_{10}(D)]^3 + 30.119[\log_{10}(D)]^2 && \text{for } 3.3 \mu\text{m} < D \leq 50 \mu\text{m} \\
&\quad + 128.94[\log_{10}(D)] + 174.53 && \text{(3.58)} \\
\log_{10}[M(D)] &= -1.2906[\log_{10}(D)]^2 - 10.884[\log_{10}(D)] \\
&\quad - 0.9873 && \text{for } D > 50 \mu\text{m}
\end{aligned}$$

Mass distribution can be solved for directly by taking the exponential of Equation 3.58:

$$\begin{aligned}
M(D) &= 10^{-7.8816[\log_{10}(D)]^2 - 92.344[\log_{10}(D)] - 272.78} && \text{for } D \leq 3.3 \mu\text{m} \\
M(D) & && \text{for } 3.3 \mu\text{m} < D \leq 50 \mu\text{m} \\
&= 10^{2.2842[\log_{10}(D)]^3 + 30.119[\log_{10}(D)]^2 + 128.94[\log_{10}(D)] + 174.53} && \text{(3.59)} \\
M(D) &= 10^{-1.2906[\log_{10}(D)]^2 - 10.884[\log_{10}(D)] - 0.9873} && \text{for } D > 50 \mu\text{m}
\end{aligned}$$

Table III in the Appendix lists each particle size range, the total mass of particles of that size range per cubic meter of fluid, the percentage of the total particle mass that each particle size range takes up, the average particle mass, the mass-weighted average particle diameter, its settling velocity, and settling time.

3.5. Flow Distribution

Fluid and algae particles enter the gravity settler through inlet ports on the top. Upon entering the settler, the fluid and particles will travel in the negative z-direction, toward the bottom of the settler. As the fluid and particles approach the bottom of the settler, they will flow in the positive x-direction toward the outlets of the settler. This

change in direction is the result of the force of pumps removing fluid from the outlet region.

Figure 22 shows a streamline plot of the fluid flow entering the settler. The streamlines show that the fluid quickly shifts from going downward to traveling downward to traveling toward the outlets. Figure 21 shows that the fluid velocity profile takes approximately 3 cm to fully develop. This is also illustrated in Figure 7(b). As the flow is fully developing, fluid velocity exists in the y- and z-directions, but these fluid velocities will become zero once the flow is fully developed. Figure 6(b) can be used to estimate the flow distribution for a 3D model.

Figure 22 also indicates the presence of eddies in the region behind the inlet to the settler. Eddies are movements in the fluid that differ from the rest of the velocity profile and can result in circular currents or whirlpools (Sell 2002). Figure 22 shows that most of the fluid travels toward the outlet while only a small percentage of the fluid moves toward the inlet region. Therefore the presence of eddies can be assumed to have a negligible effect on the flow distribution of the particles and fluid and can be ignored.

Algae particles are assumed to be distributed uniformly within the fluid at the inlet. Therefore, a higher amount of particles exists in the center of the inlet than near the edges, as shown by the streamlines being closer to each other at the center of the inlet on Figure 22. This translates to a higher amount of particles settling from near the center of the gravity settler, rather than near the top and bottom of the settler. For example, Figure 22 shows that half of the fluid (10 of the 20 streamlines) exists at a height of between 0.36 cm and 0.68 cm, which is roughly the middle 30% of the settler.

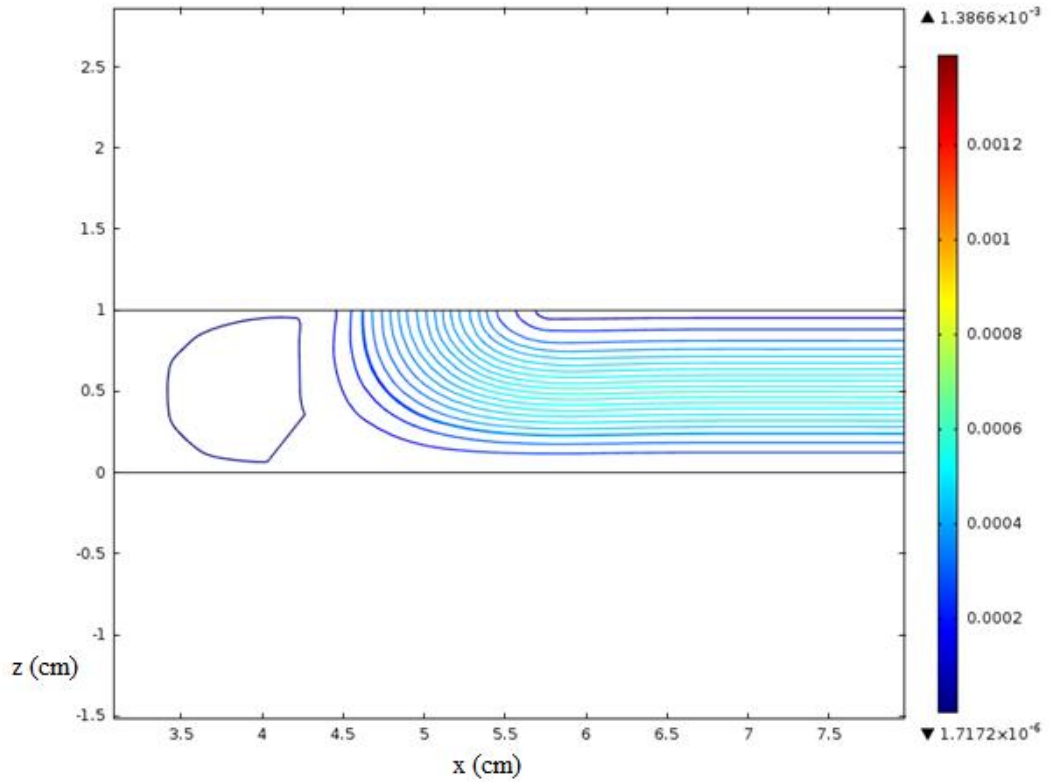


Figure 22. Flow distribution and fluid velocity profile near the inlet of a 2D gravity settler model.

The flow distribution is necessary to determine the effectiveness of the gravity settler. When the velocity profile becomes fully developed, particles of all sizes may exist at any height within the settler. Particles near the bottom of the settler will not have to travel as far in order to reach the concentrated underflow outlet, while particles near the top of the settler will have to travel a much greater distance in order to reach the concentrated underflow.

3.6. Simulation Algorithm

A MATLAB[®] interface was formulated to calculate the trajectories of particles of all sizes in the gravity settler simultaneously. The code to this interface is shown in Section 8.3 of the Appendix. Algae particle size distribution from Reynolds' (2010) data is recorded in the program. The user is prompted to enter the angle of inclination from the horizontal plane, the inlet flow rate of the algae/water mix (which is converted into velocity), the percentage of water that exits the settler through each outlet, and the length of the settler.

The MATLAB[®] interface uses this information and equations derived by Kondrat'ev (2003) and Cheng (2009). The equations used in the interface estimated the settling velocity of algae particles as a function of their diameter and density, as well as fluid density and viscosity, and the velocity profile of the fluid. The equations used were Equations 3.10, 3.23, 3.26, and 3.33-37, which are found in Section 3.1, to calculate the settling velocity of each size of particle. The x- and z-components of fluid velocity were analyzed, and the interface returned whether particles of each size are removed from the settler via the overflow or the underflow outlet, based on the distance the particle travels in the z-direction throughout the settler. The program also calculates the percent of algae that exits through the overflow and underflow outlets, the concentrations of the two outlet streams (as a ratio of outlet concentration to inlet concentration), and the smallest size particle that sinks far enough in order to exit the settler via the underflow.

This interface was first tested against the simulations in COMSOL[™] to determine if the results are consistent. The trajectories of select particle sizes for a base case (45 degree angle of inclination, 20 mL/min inlet flow rate, 80% of water exiting through the

overflow, and 59 cm settler length) are measured using both the MATLAB® interface and COMSOLTM simulations. Ten particle sizes were compared, ranging in diameter from 0.5 to 200 μm . Particle distribution in the case is based on the 20 streamlines in Figure 21. Five percent of particles of a given size were assumed to travel along each streamline at the inlet. The particle trajectories calculated by the MATLAB® program matched the paths generated by the COMSOLTM simulation within 1% (based on distance traveled in the z-direction) for all cases except the case of extremely large particles (diameter greater than 50 μm), in which the difference was still within 5%.

Next, the percentage of fluid exiting via the overflow outlet was optimized. A low percentage would result in a less concentrated underflow outlet stream and a high percentage a more concentrated underflow stream. However, as more fluid exits the settler through the overflow outlet, more algae will also exit through the overflow, resulting in a smaller percentage of the algae fed to the system that is recovered in the underflow outlet and can be cultivated into biofuel. The percent of fluid leaving the settler via the overflow outlet is critical because a 50-100-fold increase in algae concentration is needed for the algae to be cultivated into biofuel (Smith 2013). Increasing the algae concentration 50-fold would require over 98% of the fluid to be removed; however doing so would also remove a significant amount of small algae particles, which could not be used later in this process.

Next, the inlet flow rate was varied using the split of the water determined above, and the base-case angle of inclination and settler length. A lower flow rate allows for a greater residence time, meaning that the particles have more time to settle to the bottom of the settler, and the underflow would have a higher concentration of algae. However, at

low flow rates, the drag force from the fluid on the particles is lower, and there is a greater chance of the particles sticking to the bottom of the settler and not flowing toward the outlet. Another disadvantage associated with a low flow rate is increased operating costs. The settler would have to be in use for a longer amount of time to dewater the same amount of algae.

After determining the optimal flow rate, the angle of inclination was analyzed. As the angle of inclination from the horizontal plane increases, the component of gravity in the direction of flow increases, while the component of gravity in the direction perpendicular to flow (the direction in which the particles settle) decreases. This would result in fewer algae settling and a less concentrated underflow stream. Lower angles of inclination increase the residence time and allow for more algae to settle. However, at low angles of inclination, there is very little force of gravity in the direction of flow, making it more likely for the algae particles to stick on the bottom of the settler and not flow toward the outlet.

The particles must travel at a minimum velocity to avoid sticking to the settler. This velocity is referred to as “scouring velocity.” Scouring is a process in which a surface is cleaned either by rubbing or washing (Meriam-Webster 2013). In this case, the bottom of the settler is scoured by the movement of the fluid and particles near the bottom of the settler. The scouring velocity necessary to prevent algae particles from settling on the bottom of the settler is dependent on several factors, such as the particle size and density, fluid density and viscosity, and the material that the bottom of the settler is made with.

Last, the length of the settler was examined. The advantage of using a longer

settler is that the residence time would be increased and more algae particles would settle to the bottom. The disadvantage of using a longer settler is the higher cost of the materials to build the settler. A longer settler may be considered if it results in a significant increase in concentration. Otherwise, it would result in additional costs with little additional production.

The program makes use of the particle size distribution determined in Section 3.3, flow distribution determined in Section 3.4, and many of the equations from Sections 3.1 and 3.3 to simulate the flow of fluid and particles through the settling region of the gravity settler. The program calculates the percent of algae by mass that exits the settler via the overflow and underflow. An “enrichment factor” can be calculated from these values. For the purposes of this project, the enrichment factor is defined as the ratio of algae concentration (in terms of mass per volume) in the underflow outlet to the algae concentration in the inlet. The program also determines the ratio of overflow concentration to inlet concentration. Finally, the program calculates the diameter of the smallest particle that is able to settle far enough to exit the settler through the underflow. Particles smaller than this diameter do not settle far enough and would exit through the overflow with most of the water.

The objective of this experiment is to find the conditions in which the highest concentrations of algae can be generated, while also recovering the highest possible percentage of the inlet algae as possible. Algae particles leaving through the upper outlet stream are the smallest of the algae particles. It would be difficult to recycle these particles since they do not settle quickly. It is unlikely that any algae that do leave through the low-concentration upper outlet could be dewatered without using expensive

methods, such as centrifugation. If the algae concentration is high enough in the underflow outlet stream, the algae may proceed to the next step in the generation process for biodiesel.

CHAPTER IV

RESULTS AND DISCUSSION

4.1. Base Case

A base case is considered on the gravity settler. The inlet flow rate is 20 mL/min, the angle of inclination is 45 degrees above the horizontal plane, the outlet flow rate ratio such that 90% of the water leaves the settler through the overflow outlet and 10% of the water leaves through the underflow outlet, and the length of the settler is 59 cm. This base case is simulated using both COMSOL MultiphysicsTM and the MATLAB[®] interface explained in Section 2.3. This base case only considers particles entering at the top of the settler, as the purpose is to compare the settling velocity calculations of the MATLAB[®] interface and the COMSOLTM simulations. Figure 23 shows the results of both simulations.

According to Figure 23, both the MATLAB[®] program and the COMSOLTM simulation show that particles greater than 12.9 μm will leave the settler through the underflow outlet. Based on the particle size distribution developed using the research of Reynolds (2010), Hall (1998), and Wang (2013), 38.2% of the algae settle and exit via

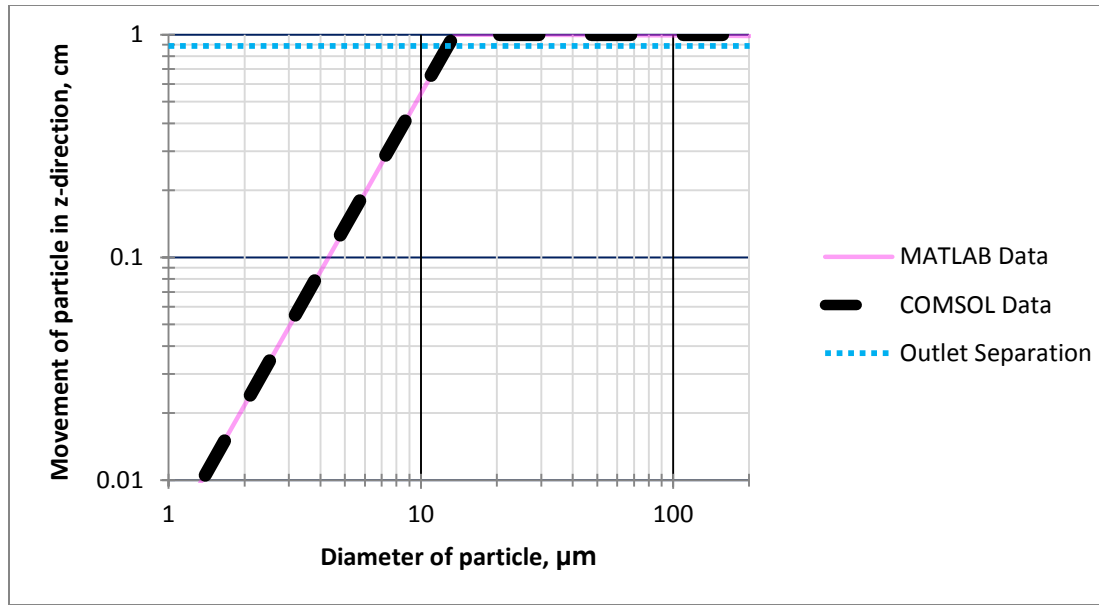


Figure 23: Movement of particles as a function of particle diameter for the case of 20 mL/min inlet flow rate, 45° angle of inclination, 90% of fluid exiting via overflow outlet, and 59 cm settler length. Particles that travel more than 0.84cm (the dotted line) will exit through the underflow. This value is determined by taking the integral of the velocity profile from Figure 11.

the underflow. This creates a concentration increase, as the concentration of the underflow outlet is 3.82 times that of the inlet. While this is a large increase, using one settler at these conditions is far from enough to increase algae concentration to a high enough level to allow for the cultivation of algae for the production of biodiesel. Algae cells must be concentrated 50-100 times their normal level in order to be used in biofuel production (Smith 2013).

The next several sections will examine the settler from as one of the variables is manipulated and the others remain constant at the same value of this base case. The objective is to find the conditions of the settler that allow for a 50-fold increase in algae concentration while recovering as much algae as possible and maintaining a flow that is fast enough to not allow the algae to stick to the bottom of the settler and form clumps. As explained in Section 3.6, scouring velocity must be considered.

4.2. Residence Time vs. Settling Time

A particle's residence time is the amount of time it takes for the particle to travel from the inlet of the settler to its outlet. The residence time is a function of the fluid inlet flow rate and the length, width, and height of the gravity settler. Residence time is calculated by dividing the length of the settler by the particle velocity in the x-direction, as described in Equation 3.39. A particle with a greater residence time is more likely to settle, simply because it has a longer opportunity to do so.

A particle's settling time is the amount of time it takes for the particle to move to the bottom of the gravity settler. As shown in Equation 3.40, the settling time is the height of the settler divided by the z-component of the particle velocity. Furthermore, the time it takes a particle to settle a certain percentage of the settler can also be calculated, by simply inserting the percentage into the equation:

$$t_{s,p,Pct} = \frac{Pct * H - z_0}{u_{p,z}} \quad (4.1)$$

in which $t_{s,p,Pct}$ is the time it takes a particle to settle a given percent of the settler height, H is the settler height, z_0 is the initial position of the particle on the z-axis, and Pct is the percent of the height. This settling time is more useful than the settling time for the entire height of the gravity settler because a particle only needs to settle a specified percent of the settler's height in order to settle and leave the settler through the concentrated underflow outlet and because not all particles are at the top point of the flow distribution.

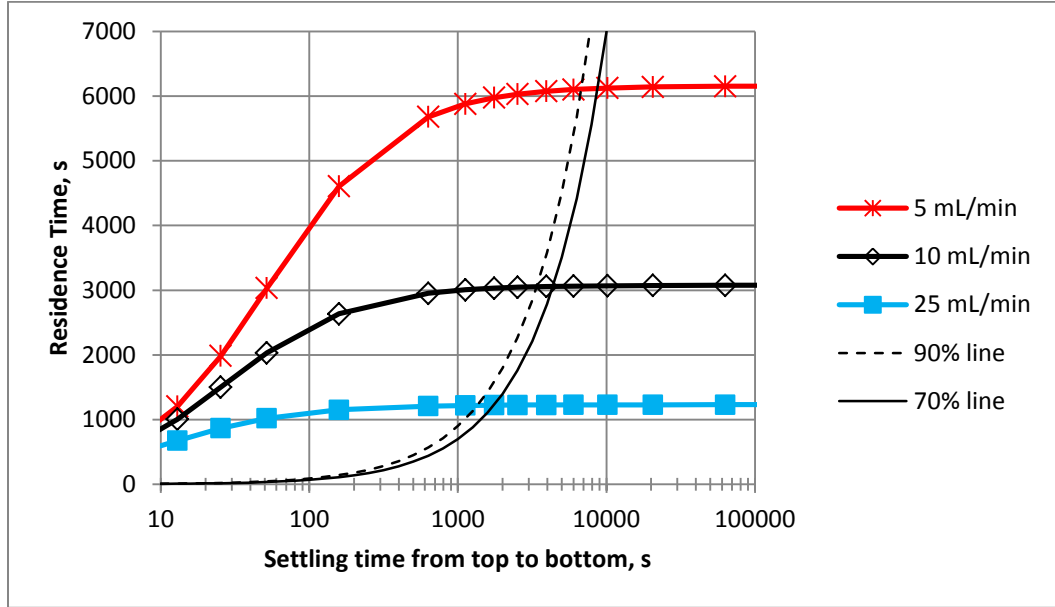
Figures 24 and 25 compare residence time to settling time at varying angles of inclination and inlet flow rates. From Equation 3.12, the particle's drag force is directly proportional to its diameter. A small particle therefore receives less influence from the

drag force exerted by the fluid and will move more slowly throughout the fluid (Kondrat'ev 2003). There is, however, a minimum flow rate and therefore a maximum settling and residence time. This is because of the force of gravity on the particle. The gravitational acceleration is not dependent on a particle's mass. Particles of all masses fall at the same rate (Wolfs 2008). The maximum residence time is seen on Figures 24 and 25.

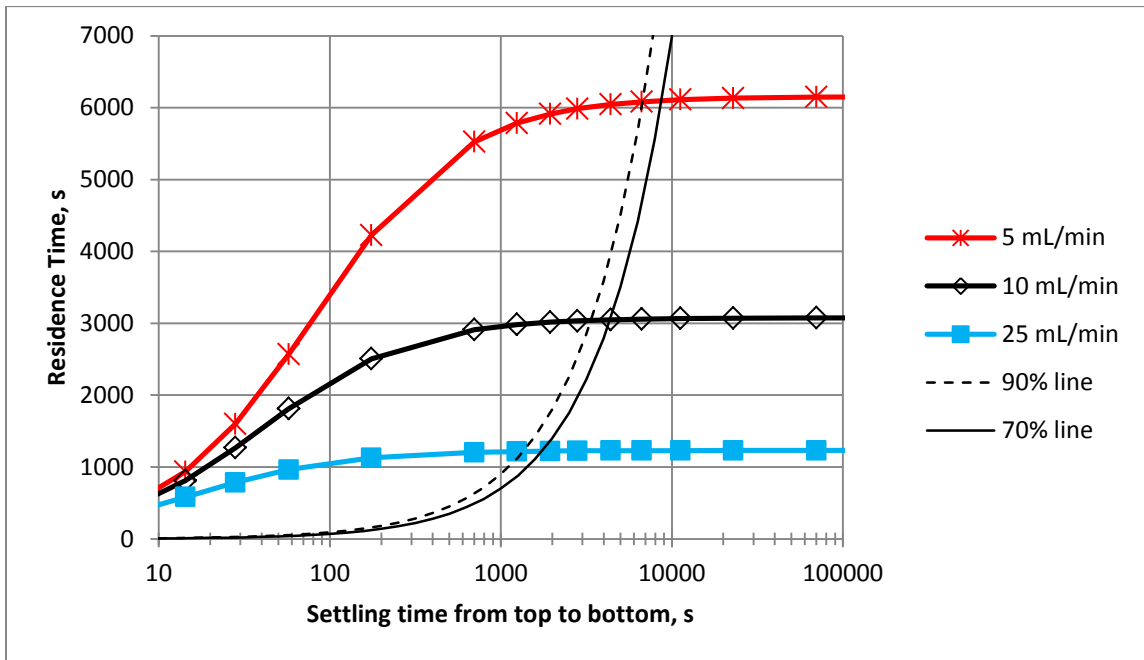
Figure 24 shows that as the velocity of the fluid decreases, its residence time increases. This increase is inversely proportional for the smallest particles, but weaker as the particle size increases. At high settling times (greater than 3,000 s), the residence time reaches a maximum. This is because the drag force on the particle is effectively zero and the only particle movement is the result of the constant gravitational acceleration. Figure 25 shows a slight increase in residence time as the angle of inclination decreases. This is because at a shallower angle of inclination, the component of gravity in the direction of flow (the x-direction) is smaller, while the component of gravity in the settling direction (the z-direction) is larger. This change in angle would therefore decrease the settling time while increasing the residence time for a particle of a given size.

The "90% line" and "70% line" shown on Figures 24 and 25 correspond to the line on the chart in which the particle's residence time is equal to 90% or 70% of its settling time. This is significant because these lines can quickly make it clear whether particles with a given residence time and/or settling time will be able to settle quickly enough to reach the underflow outlet in a situation where 90% or 70% of the fluid exits

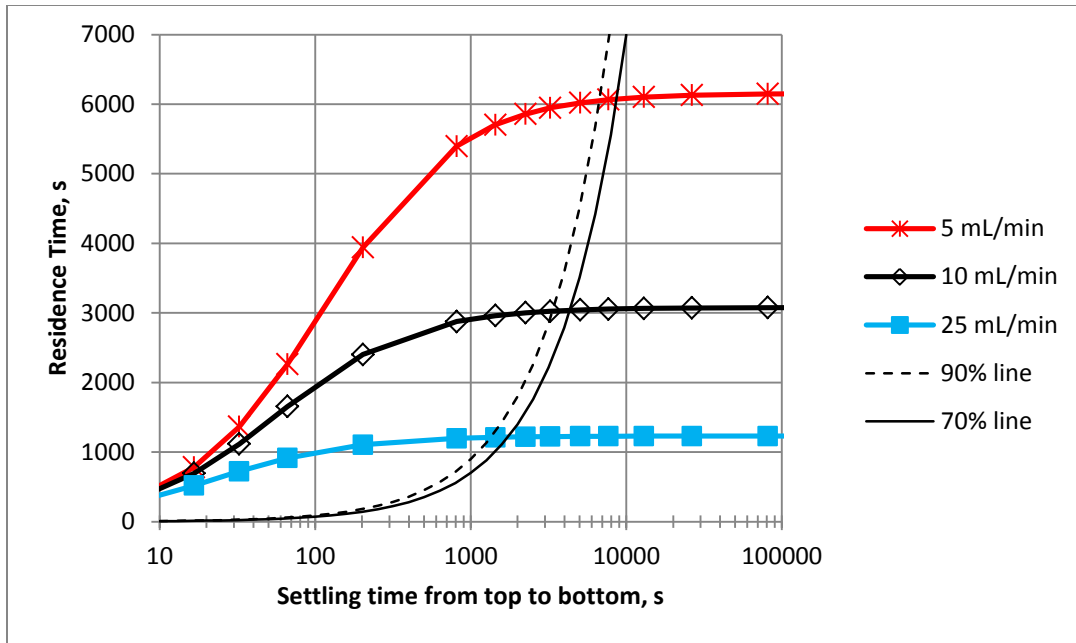
through the underflow outlet. In order for the particle to settle into the underflow region, its residence time must be greater than its settling time multiplied by the percent of water



(a) 25 degree angle of inclination



(b) 35 degree angle of inclination



(c) 45 degree angle of inclination

Figure 24: Residence time as a function of settling time and inlet flow rate at a settler length of 59 cm and an angle of inclination of (a) 25 degrees, (b) 35 degrees, and (c) 45 degrees.

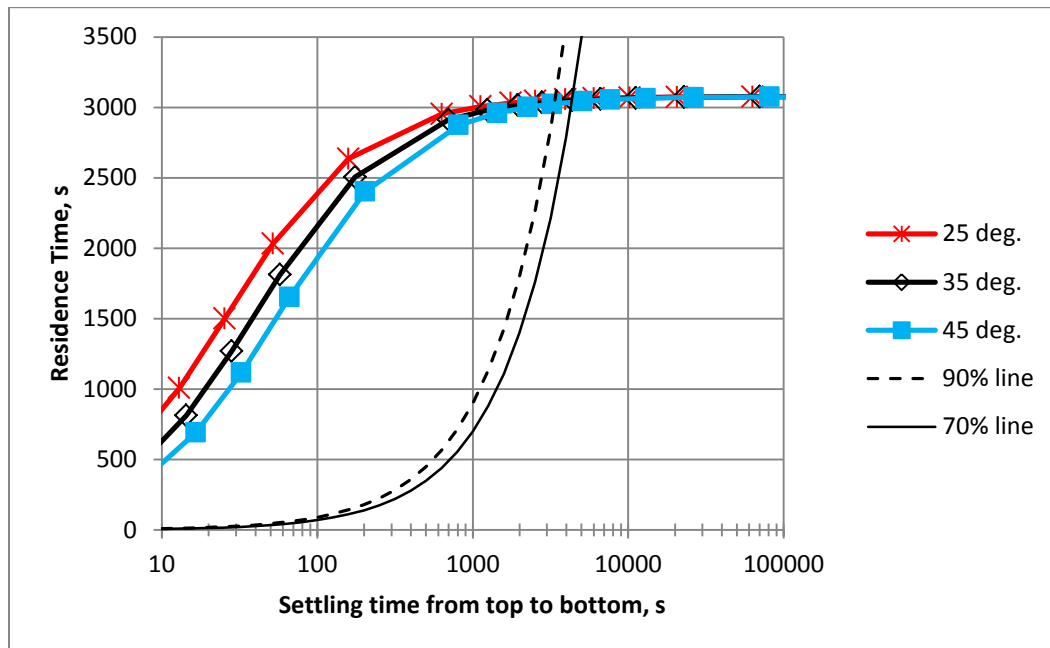


Figure 25: Residence time as a function of settling time and angle of inclination at a settler length of 59 cm and an inlet flow rate of 10 mL/min

that exits the settler through the overflow, as shown on Inequality 4.2:

$$\tau_p > t_{s,p} * Pct. \quad (4.2)$$

in which Pct is the percent of water that exits the settler through the overflow region. For graphical purposes, the portions of Figures 24 and 25 above the 90% line and 70% line signify the particles that will exit the settler through the concentrated underflow outlet.

Figure 26 corresponds to Figures 24 and 25 by plotting the residence time and settling time against the particle diameter. Figure 26 confirms that the larger particles have lower residence and settling times than smaller particles. This figure can be used to determine whether a particle of a given size will settle into concentrated underflow outlet or be forced out the dilute overflow outlet by comparing the residence time to the settling time and using Inequality 4.2. Figure 26 shows that for an angle of inclination of 35 degrees, particles greater than 7 μ m in diameter for a slow 5 mL/min flow rate and 15 μ m for a fast 25 mL/min flow rate will exit through the underflow outlet.

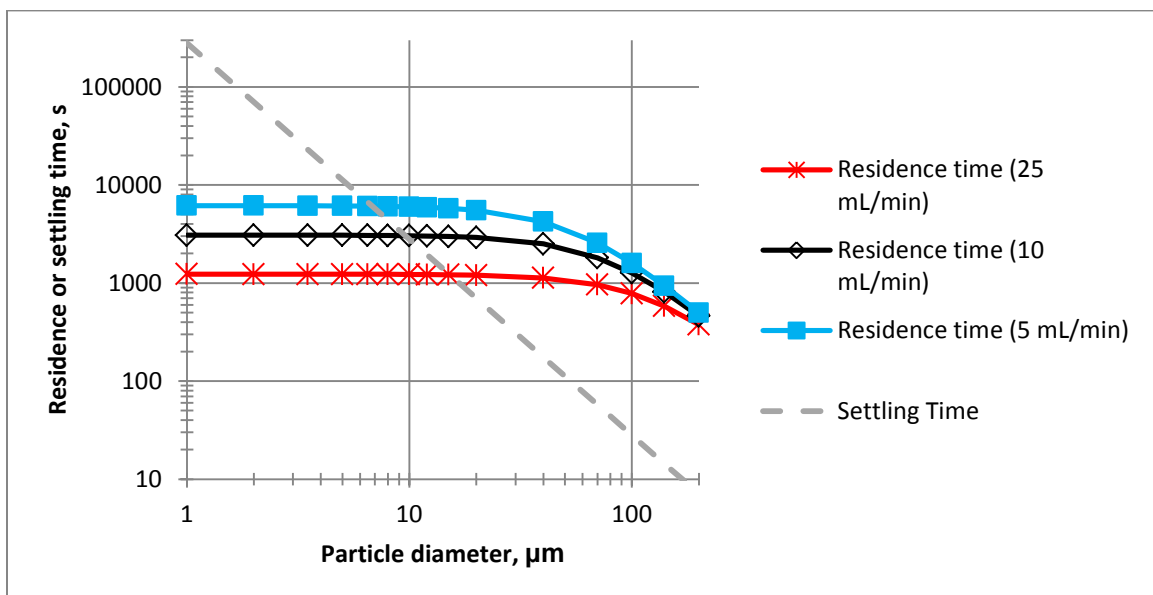


Figure 26: Residence time and settling time as a function of particle diameter and inlet flow rate at a 35° angle of inclination and a 59 cm settler length.

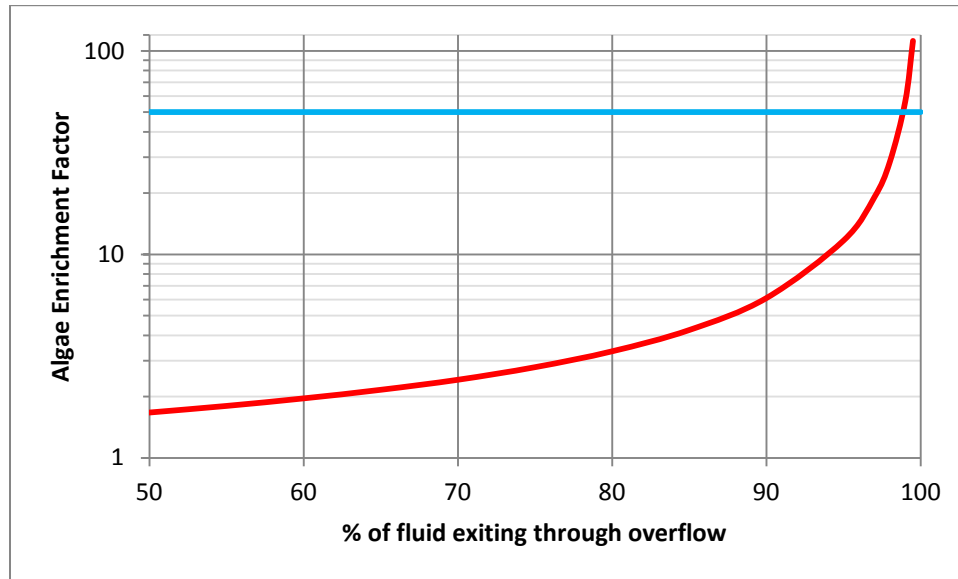
4.3. Effect of the Outlet Flow Rate Ratio on Settler Performance

Using a constant 45 degree angle of inclination, 20 mL/min inlet flow rate and 59 cm settler length, the ratio of outlet flow rates was manipulated. Outlet splits ranging from 50% to just under 100% of the fluid exiting via the overflow outlet were considered. Having more than 50% of the water leave the settler through the underflow would result in very low, if any, concentration increase because a majority of the water is still present with the algae in the underflow. Having less than 5% of the water leave through the underflow may result in a higher amount of algae particles leave through the overflow.

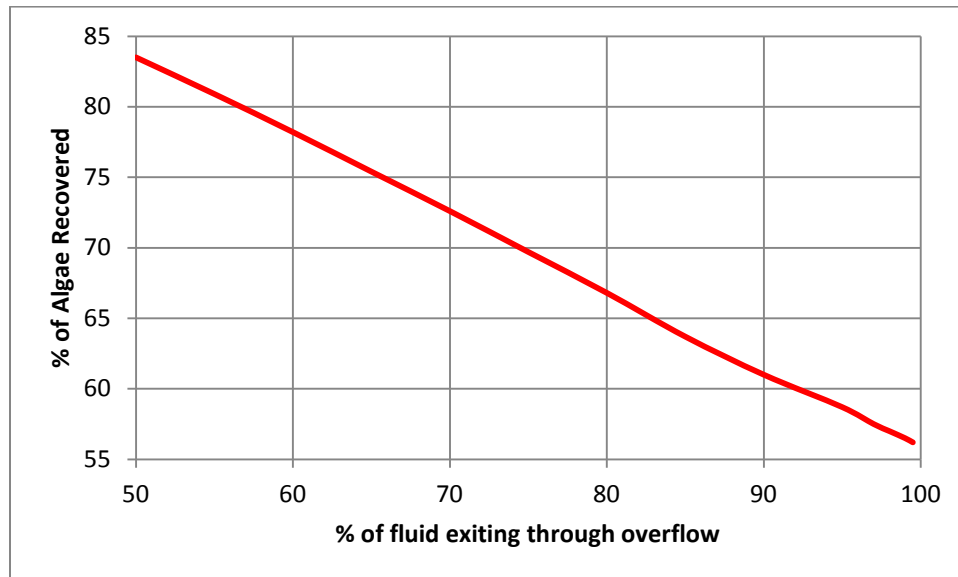
Figure 27 plots (a) the algae enrichment factor, which can be defined as the ratio of algae concentration in the underflow outlet to the concentration of the inlet, and (b) the percent of algae recovered as a function of the percent of water that exits the settler through the overflow outlet. The figure shows that as a higher percent of water exits through the overflow outlet, the enrichment factor increases, particularly when this percentage is greater than 90. However, as more water leaves through the overflow, more algae also leave through the overflow, and cannot be used for cultivation into biofuel. Figure 27(b) shows that the algae recovery rate decreases linearly as the concentration increases

The blue line on Figure 27(a) shows that in order to increase the algae concentration 50-fold, as is required for cultivation into biodiesel (Smith 2013), almost 99% of the fluid would have to be removed. Removing 99% of the fluid would also result in a higher amount of algae being removed from the system. In addition, the removal of this much fluid would result in a very slow fluid velocity in the outlet region, which makes it more likely that particles would stick to the walls. As explained earlier, a

certain “scouring velocity” of the fluid must be achieved in order to prevent the particles from sticking to the walls of the settler.



(a) Enrichment factor vs. percent of fluid exiting through overflow



(b) Algae recovery rate vs. percent of fluid exiting through overflow

Figure 27: Algae enrichment factor and recovery rate as a function of percent of water exiting through the overflow, at a 45° angle of inclination, 20 mL/min inlet flow rate, and 59 cm settler length

4.4. Multi-Stage Operation

A two- or three-stage settler would allow these high concentrations to be reached while recovering more algae, because the settler is not removing very high amounts of water and algae in a single step. The results of the previous section show that a 90/10 split of water between the overflow and underflow outlets generates a 6.10-fold concentration increase of algae. Adding a second stage with a 90/10 split of water would increase the enrichment factor by a factor greater than 6.10. This is because most of the small algae particles that would leave through the overflow of the second settler have already left the system through the overflow of the first settler. An example of a two-stage system is shown in Figure 28.

The settler length, height, angle of inclination, and outlet flow rate ratio are kept constant throughout the system. This is done in order to quickly increase the algae concentration and utilize a high percent of the algae that settles to the underflow outlet in the first settler. In the second settler, a particle would settle the same distance as it did in the first settler in order to leave the system through the underflow outlet. Since most of the small particles with low settling velocities have already left the system, a higher percent of particles that enters the second settler is expected to settle, as compared to the first settler. The overflow product of the second settler would be almost pure fluid at a flow rate of 90% of the inlet flow rate to the second settler. The underflow product would contain almost all of the algae and 10% of the fluid from the inlet

The second and subsequent stages would be designed so the fluid velocity is equal to that of the first settler. This is done by multiplying the width of the settler by the ratio of inlet flow rates of the second and first stage, as shown in Equations 4.3 and 4.4:

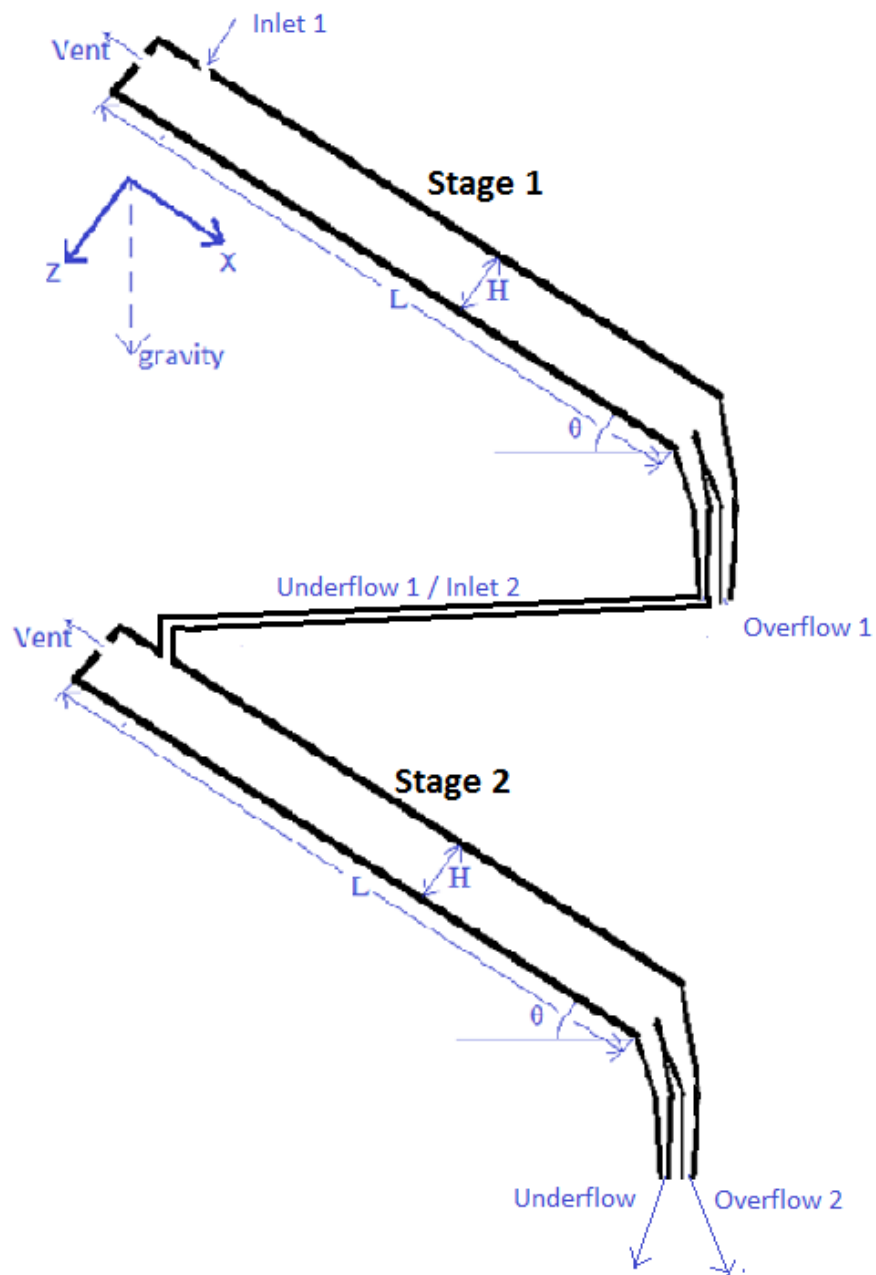


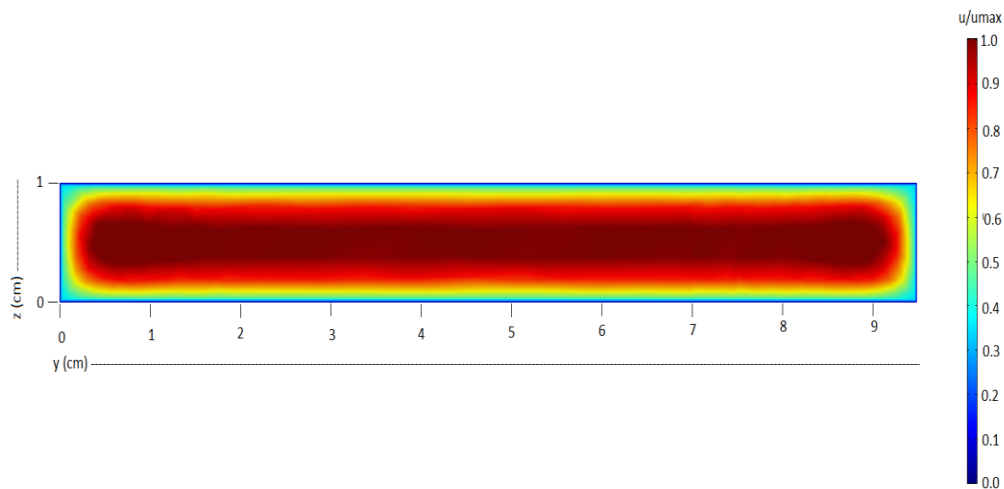
Figure 28: Schematic of a 2-stage gravity settler system

$$u_f = Q_{f,1}HW_1 = Q_{f,n}HW_n \quad (4.3)$$

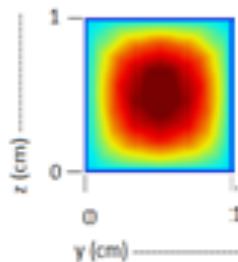
$$W_n = W_1 \frac{Q_{f,n}}{Q_{f,1}} \quad (4.4)$$

in which u_f is the constant fluid velocity, $Q_{f,1}$ and $Q_{f,n}$ are the fluid flow rates in the stage 1 and subsequent stage n , respectively, H is the height of the settler, and W_1 and W_n are the widths of stages 1 and n , respectively.

As the width of a settler is decreased, its edges become closer. This results in a velocity profile where a greater percent of the flow is affected by the edge. Figure 29 shows the velocity profile for 2 stages: A stage that is 9.6 cm wide, like the settler that is being examined and a stage that is 0.96 cm wide, or one tenth the width of the first settler.



(a) Velocity profile for settler 9.6 cm wide



(b) Velocity profile for settler 0.96 cm wide

Figure 29: Velocity profile for gravity settlers 9.6 cm and 0.96 cm in width

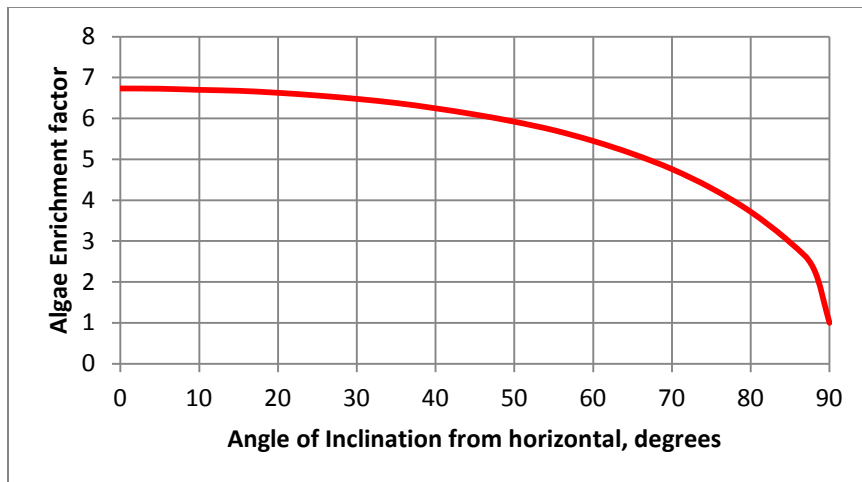
The velocity profile in the second settler has more end effects than the velocity profile in the first settler. This will result in a higher percentage of the particles traveling more slowly and a greater chance of particles sticking to the side walls of the settler. Scouring velocity must be taken into consideration when the second settler is modeled. The use of a narrow settler as shown in Figure 29(b) is likely limited to use at the laboratory scale. Gravity settlers at the industrial scale will be much wider, and the edge effects of the velocity profile would be negligible for a second and likely a third settler.

The case of a 45 degree angle of inclination, a 20 mL/min inlet flow rate, a 59 cm settler length, and 90% of the fluid exiting through the overflow outlet produces an enrichment factor of 6.10 for a single stage. The second stage is expected to have a higher enrichment factor than the first stage because the particle size distribution in the second stage favors larger particles that are more likely to settle. For example, with these conditions, the inlet to the second stage contains less than 25% of the small particles (particles whose diameters are less than 6 μm) that entered the first stage, while it contains over 90% of the large particles (particles whose diameters are greater than 12 μm) that entered the first stage.

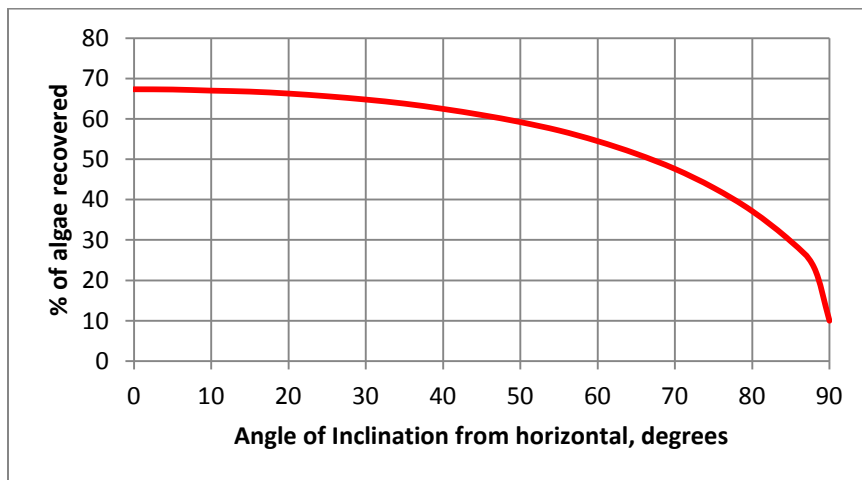
In order to increase the enrichment factor, the values of the angle of inclination, inlet flow rate, and settler length will be examined. A second MATLAB interface, very similar to the program explained in Section 2.3, was designed to measure the particle trajectories in a second or any subsequent gravity settler. This interface is shown in Section 8.4 of the Appendix.

4.5. Effect of the Angle of Inclination on Settler Performance

Next, the angle of inclination is examined. The outlet flow rate split ratio is held constant at 90% of the water leaving through the overflow, the inlet flow rate constant at 20 mL/min, and the length of the settler constant at 59 cm. The angle of inclination is varied from 0 to 90 degrees, representing all slopes between a horizontal settler and a vertical settler. Figure 30 shows (a) the enrichment factor and (b) the percent of algae recovered as a function of the angle of inclination.



(a) *Enrichment Factor vs. angle of inclination*



(b) *Algae recovery rate vs. percent of water exiting through overflow*

Figure 30: Algae enrichment factor and recovery rate as a function of percent of angle of inclination, with 90% of the water exiting via the overflow, a 20 mL/min inlet flow rate, and a 59 cm settler length

Figure 30 shows that both the enrichment factor and the recovery rate of algae decrease as the angle of inclination increases. The decreases in enrichment factor and recovery rate are small for angles of inclination below 60 degrees, but they become larger for steeper angles. Although lower angles of inclination generate a higher enrichment factor, particles at lower angles of inclination will be more likely to stick to the bottom and not move than if the angle of inclination were higher, because the component of gravity in the direction of flow decreases as the angle of inclination decreases.

A method to determine the optimal angle of inclination would be to compare the x-component of the velocity of particles near the bottom of the settler to the enrichment factor. At higher angles of inclination, the velocity of a 20 μm particle in the direction of flow is higher because the component of gravity in the x-direction is greater. The size of 20 μm is chosen because it is large enough that the particle would generally settle, but also a size that is relatively common in the system, as shown by Figure 21. Figure 31 plots the particle velocity in the x-direction at a distance of 0.02 cm from the bottom of the settler as a function of angle of inclination.

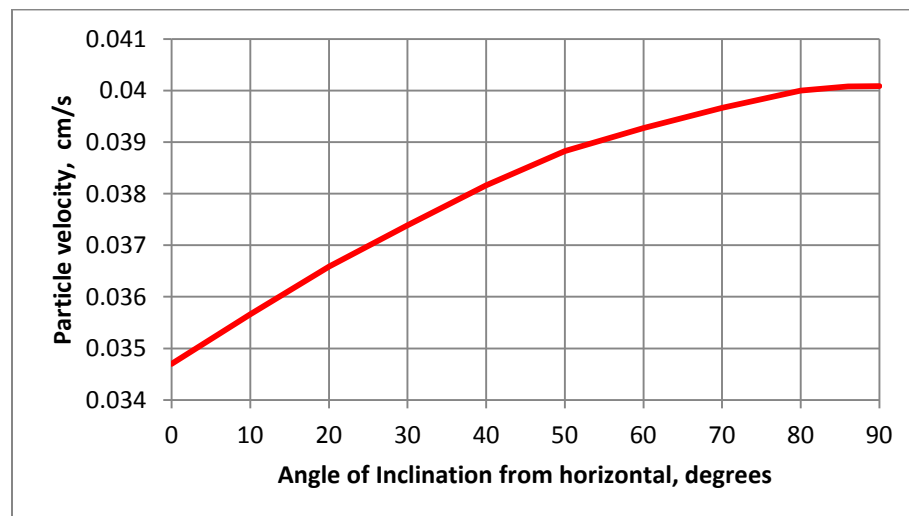


Figure 31: Velocity of a 20 μm particle at $z=0.02$ cm as a function of angle of inclination

Figure 31 shows that as angle of inclination increases, particle velocity also increases. In order to determine an optimal angle of inclination, the particle velocity is multiplied by the enrichment factor. These results are shown on Figure 32.

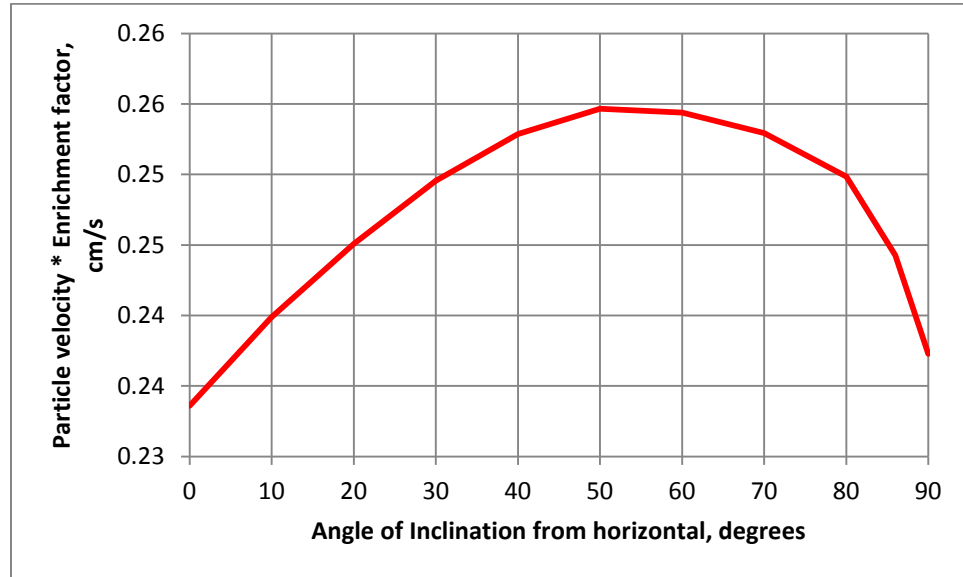
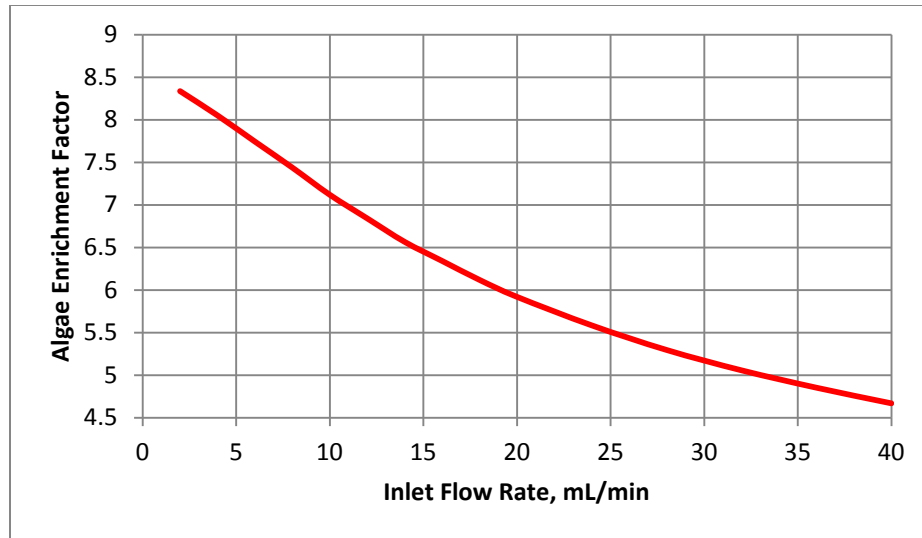


Figure 32: The product of particle velocity (from Figure 31) and enrichment factor (from Figure 30(a)) as a function of angle of inclination.

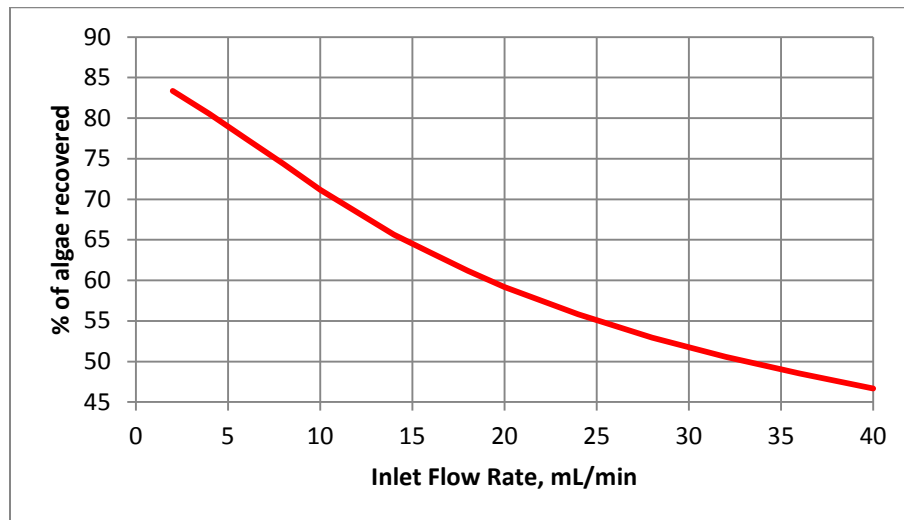
Figure 32 shows that the optimal angle of inclination is around 50 degrees. At this angle, the advantages of a high enrichment factor and a high particle velocity are combined. This system produces an enrichment factor of 5.919 in one stage. This angle will be used as the inlet flow rate and settler length are studied.

4.6. Effect of the Inlet Flow Rate on Settler Performance

Next, the inlet flow rate is examined. The outlet flow rate split ratio is held constant at 90% of the fluid leaving through the overflow, the angle of inclination constant at 50 degrees, and the length of the settler constant at 59 cm. Flow rates between 2 mL/min and 30 mL/min were simulated. Figure 33 plots (a) the enrichment factor and (b) the percent of algae recovered as a function of inlet flow rate.



(a) *Enrichment factor vs. inlet flow rate*



(b) *Recovery rate vs. inlet flow rate*

Figure 33: Algae enrichment factor and recovery rate as a function of inlet flow rate, with a 50 degree angle of inclination, 90% of the water exiting via the overflow, and a 59 cm settler length

The optimal inlet flow rate can be the highest flow rate that can generate a 50-fold concentration increase. Figure 33 shows that the concentration can not be increased 50-fold using a single stage. Figure 34 plots the enrichment factor of a two-stage system as a function of the inlet flow rate to the first stage. According to Figure 12, the highest flow rate that can produce a 50-fold concentration increase with two stages is 18 mL/min. There, 18 mL/min is considered the optimal flow rate for this settler.

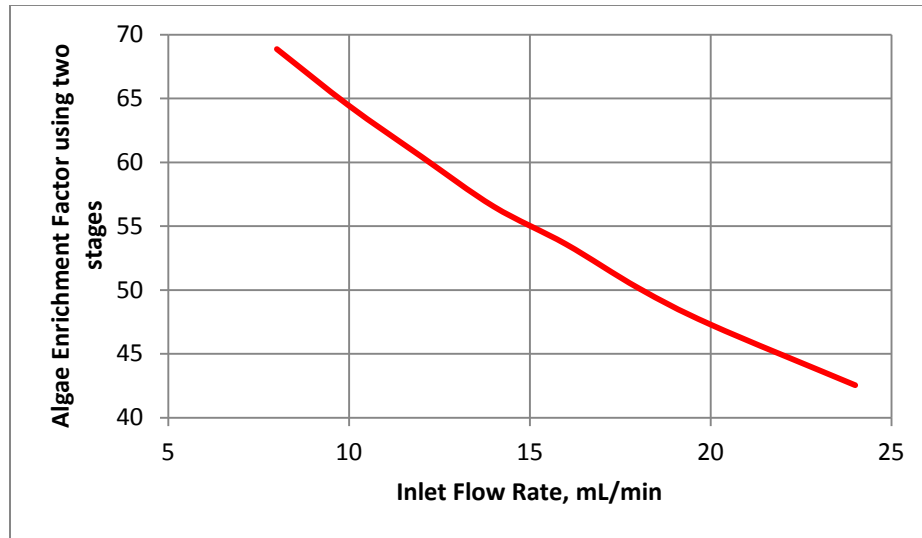


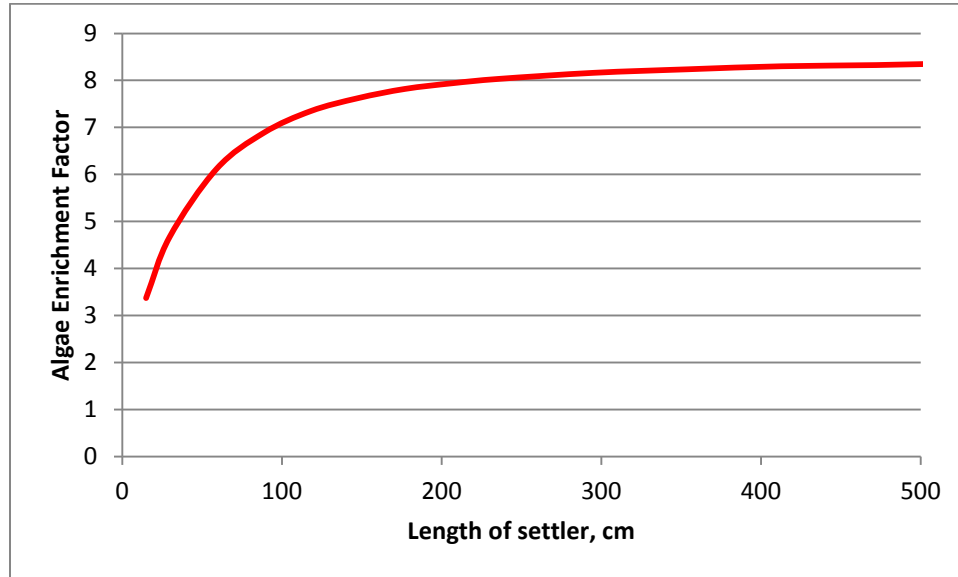
Figure 34: Enrichment factor vs. inlet flow rate for a two-stage system.

4.7. Effect of the Length of the Gravity Settler on its Performance

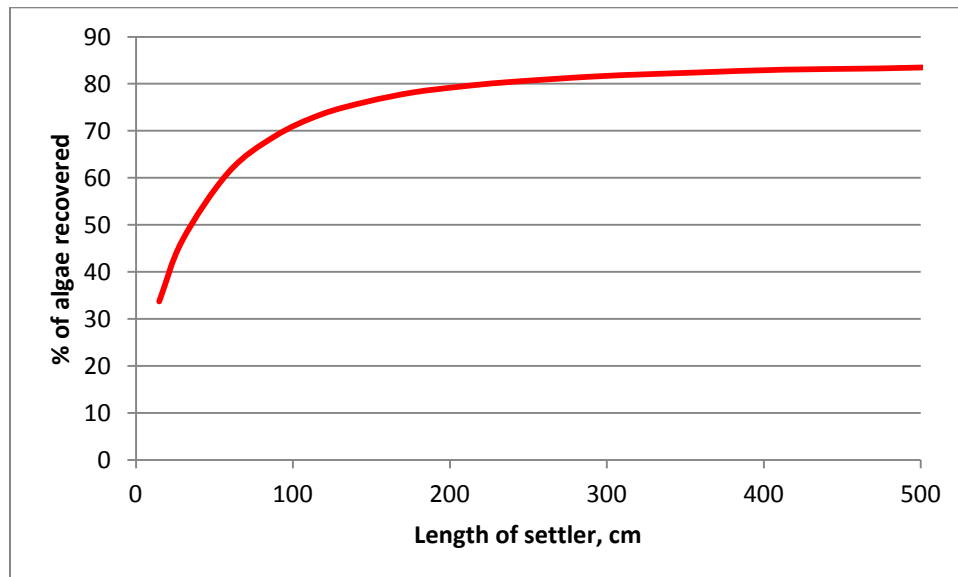
Using the optimal conditions previously determined, a 50-degree angle of inclination, 18 mL/min inlet flow rate, and 90% of the fluid exiting the settler through the overflow, the length of the settler is varied. Settler lengths ranging from 14.8 cm (one quarter of the given settler length) to 500 cm (approximately 8 times the given settler length) are considered. Figure 35 plots (a) the enrichment factor and (b) the percent of algae recovered as a function of settler length.

As Figure 35 shows, the enrichment factor and algae recovery rate increase sharply as length increase for lengths up to 200 cm. As the length continues to increase, the enrichment factor and recovery rate will increase asymptotically. An infinitely long settler in which algae particles of all sizes have the time to settle will have an enrichment factor of 10.0 and an algae recovery rate of 100%. It is theoretically impossible to increase the algae concentration 50-fold using a single stage because 10% of the fluid joins any recovered algae in the underflow. The optimal settler length varies as the inlet

flow rate varies. For an 18 mL/min flow rate, the optimal length is 59 cm. A higher flow rate would result in a longer optimal length, and a lower flow rate would result in a shorter optimal length.



(a) *Enrichment factor vs. length of settler*



(b) *Recovery rate vs. length of settler*

Figure 35: Algae enrichment factor and recovery rate as a function of the length of the gravity settler, with a 35 degree angle of inclination, 90% of the water exiting via the overflow, and an 18 mL/min inlet flow rate.

4.8. Number of Stages

A second MATLAB[®] interface, very similar to the program explained in Section 2.3, was designed to measure the particle trajectories in a second or any subsequent gravity settler. The results of this program, using the optimal conditions found in Sections 4.3 through 4.7, are shown on Table I. Table I shows that these conditions allow for a 50-fold concentration increase to take place in two stages. The table also shows that for a two-stage operation, the enrichment factor is 50.2 and 50.2% of the algae are recovered in the underflow of stage 2.

Adding a third settler would increase the concentration of algae to 400-500 times its original concentration. This may be useful for some applications, but it is unnecessary for the cultivation of algae to biofuel, since only a 50-fold increase is needed. Algae can still be cultivated with a 2-stage system, so adding a third stage would not do anything productive while increasing capital and operating costs.

Stage	Quantity	Inlet	Overflow	Underflow
1	Water flow rate (mL/min)	18.0	16.2	1.8
	Percent of Algae in:	100.0	38.8	61.2
	Enrichment Factor (based on inlet of stage 1)	1.00	0.431	6.12
	Fluid velocity (cm/s)	0.0317	0.0580	0.0064
	Settler Dimensions	L = 59 cm, W = 9.6 cm, H = 1 cm		
2	Water flow rate (mL/min)	1.80	1.62	0.18
	Percent of Algae in:	61.2	11.0	50.2
	Enrichment factor (based on inlet of stage 1)	6.12	1.22	50.2
	Water velocity (cm/s)	0.0317	0.0580	0.0064
	Settler Dimensions	L = 59 cm, W = 9.6 cm, H = 1 cm		

Table I: Summary of concentrations and flow rates for two-stage system with 50 degree angle of inclination, 18 mL/min inlet flow rate, 90% of water leaving settler through upper outlet, and 59 cm settler length.

4.9. Summary of Optimal Conditions

The optimal conditions are those conditions that produce the desired concentration increase at the lowest cost while recovering as many algae particles as possible. These conditions are an angle of inclination of 50 degrees above the horizontal plane, an 18 mL/min inlet flow rate, and 90% of the water exiting via the overflow outlet. These conditions allow for a high degree of separation between algae and water while still allowing for the algae particles to be influenced by the force of gravity and for the highest possible recovery rate of algae. The optimal results are displayed on Table II:

Angle of inclination	50 degrees
Percent of water in overflow	90%
Inlet Flow Rate	18 mL/min
Length of Settler	59 cm
Number of Settlers	2

Table II: Optimal Conditions for algae/water separation

CHAPTER V

COMPARISON OF RESULTS TO SIMILAR EXPERIMENTS

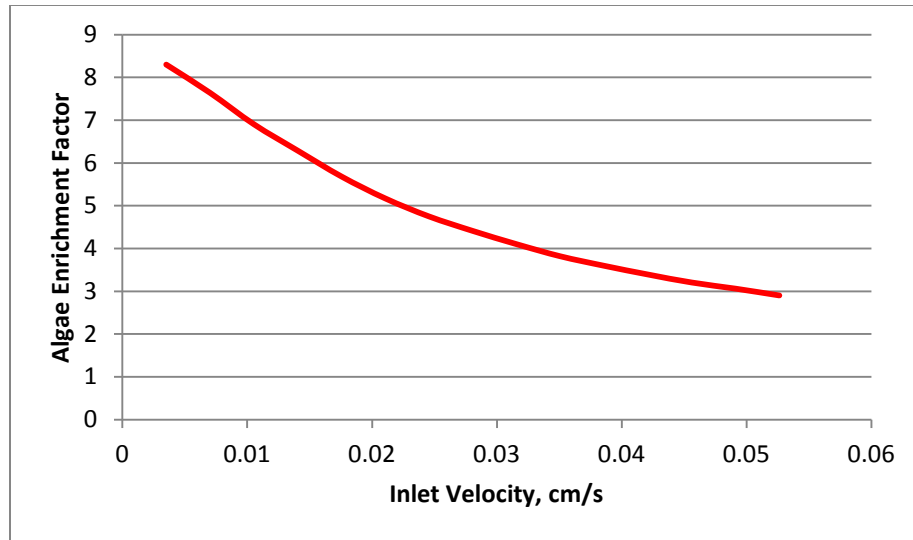
Similar experiments have been conducted in the past. The results from this experiment can be compared to the results of previous experiments for the purposes of verification. One of these similar experiments was the research of Smith and Davis (2013). Smith and Davis found the retention of algae, and therefore the concentration of algae in the underflow, to decrease as the feed velocity increases. Although this experiment compares the algae concentration to the inlet flow rate, flow velocity can easily be calculated to replace inlet flow rate. The feed velocities used by Smith and Davis are similar to those used in this experiment. Smith and Davis (2013) also found that a decrease in angle of inclination from the horizontal results in a more concentrated algae stream. Smith and Davis find that approximately 70% more algae enter the underflow outlet for an 8 degree angle of inclination as compared to a 55 degree angle of inclination.

The results of this experiment contain trends comparable to the results obtained by Nasr-El-Din, Masliyah, and Nandakumar (1990); Laskovski et al (2006); and Salem,

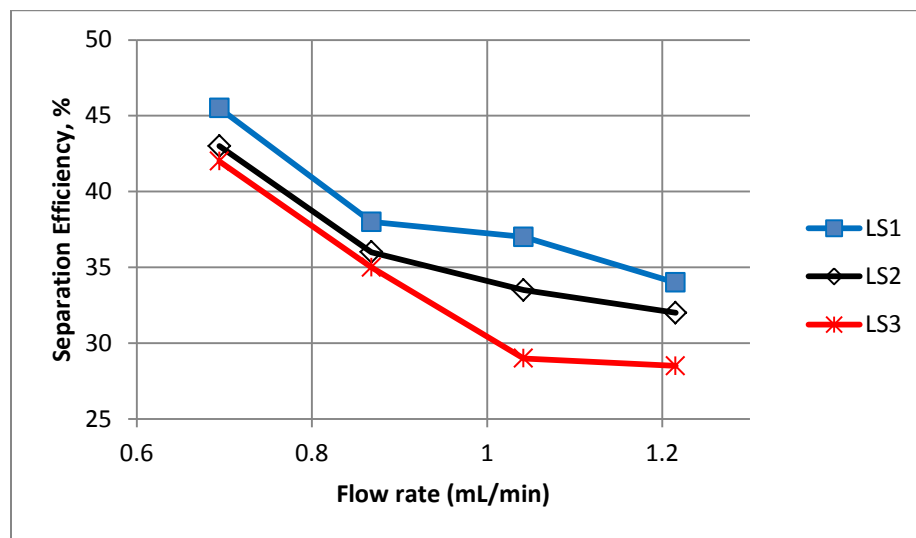
Okoth, and Thoming (2011). Nasr-El-Din, Masliyah, and Nandakumar (1990) explain that as the amount of fluid sent to the overflow increases, the amount of particles sent to the overflow also increases, but this increase is slower. This results in a much higher concentration in the underflow, particularly when almost all of the water is sent into the underflow. This is shown by the optimal conditions of this experiment that call for 90% of the water to leave the overflow. Laskovski et al (2006) confirm that the separation of particles between the top and bottom of a channel is based on factors including the size and density of the particle, the density of the fluid, the inclination angle used, and the particle Reynolds number, a function of velocity.

Salem, Okoth, and Thoming (2011) determined both numerically and experimentally that the separation efficiency is inversely proportional to the inlet flow rate. Figure 36 compares the results of this experiment to the results obtained by Salem. Although the actual numbers are different because Salem's research involved the settling of particles of a higher density than algae (Salem 2011) and a steeper angle of inclination (Salem 2011), the trends in the data are the same. Both this project (Figure 36(a)) and Salem's gravity settler experiment (Figure 36(b)) show a sharp decline in separation efficiency for increasing flow rate at low flow rates as the flow rate increases. At higher flow rates, this decrease in separation efficiency becomes less severe.

One of the most significant components of this experiment is the calculation of algal settling velocity. Therefore, the comparison of the settling velocity values to values for settling velocity measured in literature and found experimentally is important for the verification of results. Figure 37 compares the settling velocity from the equations in Section 3.1 to algal settling velocity found through experiments in literature.



(a) Algae enrichment factor vs. inlet velocity



(b) Separation Efficiency (directly proportional to enrichment factor) vs. flow rate for Salem's research. (Adapted from data acquired by Salem, Okoth, and Thoming (2011))

Figure 36: Comparison of trends in results from this project to trends from Salem's (2011) research. The difference in volumetric flow rates is because Salem's research was done using a solid material whose properties are different from those of algae.

Figure 37 shows that the calculated settling velocity data from this experiment are within the region of error when compared to measured data from three published experiments for the diameter ranges covered by those experiments. The experiments examined covered particles ranging in size from 5 μm to 200 μm . The most important range

of particle sizes are those between 5 and 30 μm . This is because in almost all cases, particles smaller than 5 μm in diameter will not settle and leave the settler through the dilute overflow. Particles greater than 30 μm are almost certain to settle and exit the settler through the concentrated underflow.

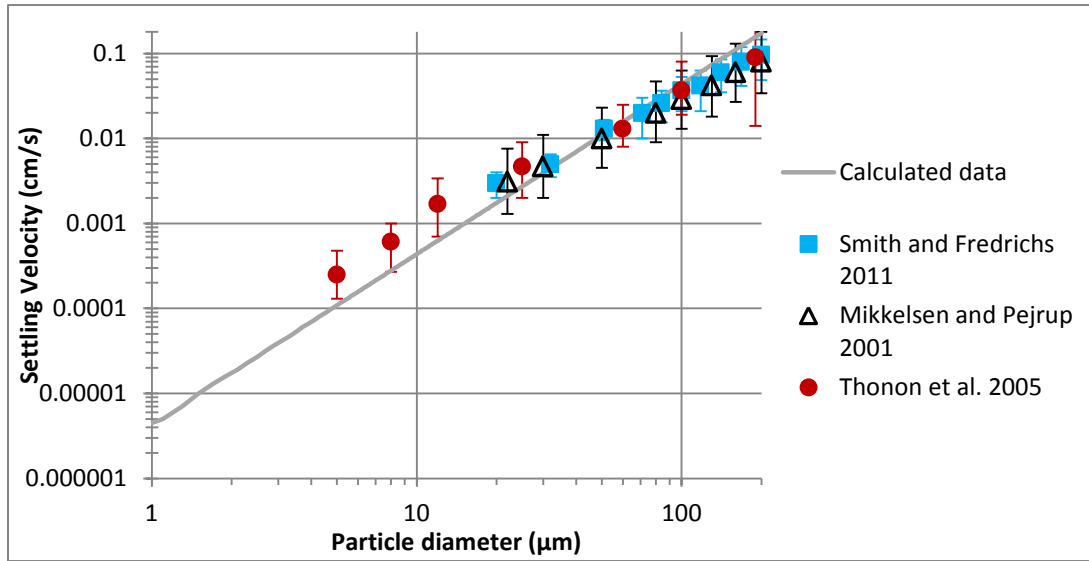


Figure 37: Comparison of calculated settling velocity data to algae and particle settling velocity data found in literature. Error values are included in each of the sources.

The biggest drawback to the comparisons in Figure 37 is the lack of measurements for particles smaller than 5 μm in diameter. However, the calculated settling velocity for these particles (or particles of any size) can be compared to other calculations made. Figure 38 compares the calculations of this experiment to calculations reported by Pitt and Clark (2007). Pitt and Clark's calculations are similar to the model used in this experiment, as their calculations are based on the settling relationships of Stokes and Newton. Data from these calculations are plotted for particles ranging from 2 μm in diameter to 10 cm, which is much greater than any particle examined in this experiment. Figure 38 shows that the values of settling velocity calculated in this experiment very closely match the values from literature.

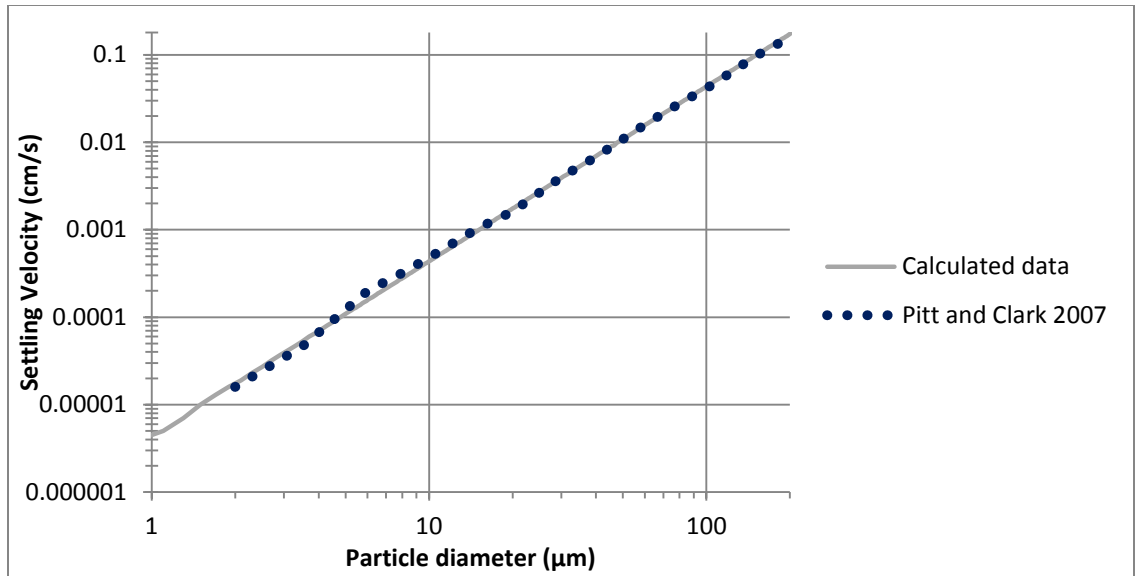
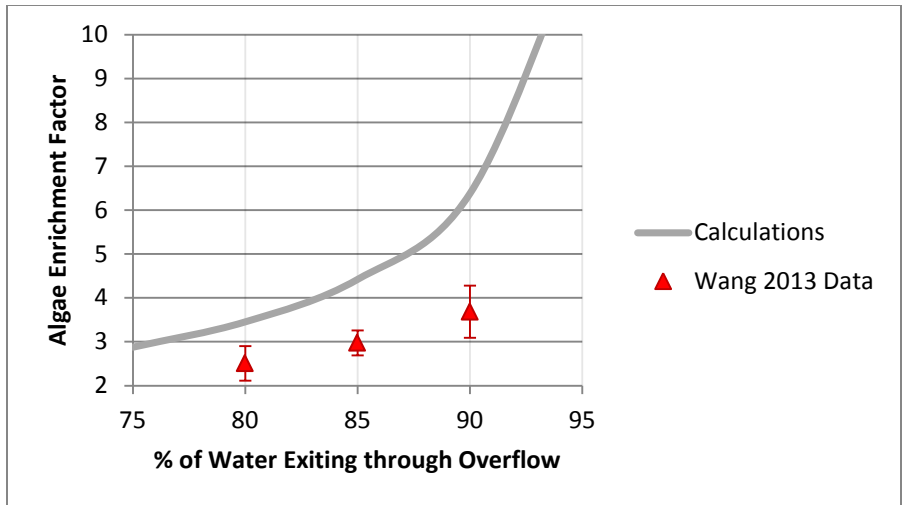


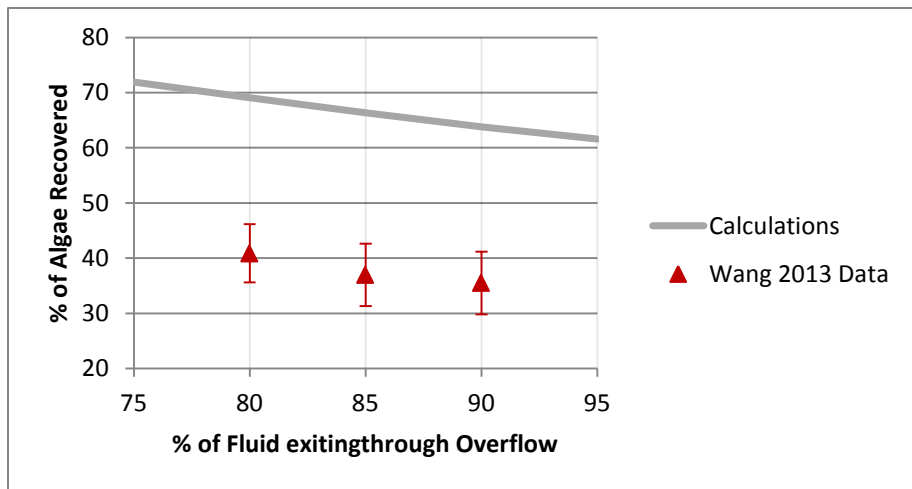
Figure 38: Comparison of calculated settling velocity data to settling velocity calculation reported by Pitt and Clark (2007)

The most comparable experiment was performed by Wang et al (2013). This experiment was performed at Cleveland State University and made use of the actual gravity settler described in Section 2.1. Rather than simulating the movement of the water and algae particles, Wang’s experiment examined the separation of water from two species of algae cells, including *S. Dimorphus* cells. Wang’s data were accumulated by measuring the amount of algae in both the overflow and underflow outlets of the settler for several days after the settling process begins. The average values were taken and the standard deviations were noted (Wang 2013). The results of this experiment are compared to the results of Wang et al. on Figures 39 and 40.

Figure 39 compares the plot of the enrichment factor and recovery rate against the outlet flow rate ratio (Figure 27) against Wang’s data. The data for both the enrichment factor and the recovery rate exceed the experimental data obtained by Wang et al. The calculated enrichment factor exceeds the experimental value between 40 and 75%, or 2-3



(a) Algae enrichment factor vs. percent of water exiting through overflow



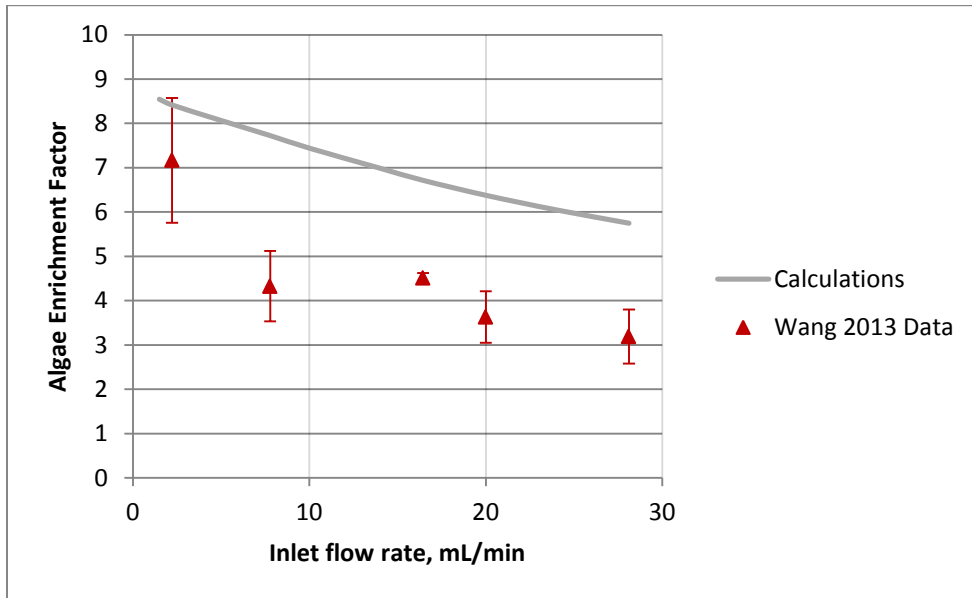
(b) Algae recovery rate vs. percent of water exiting through overflow

Figure 39: Algae concentration ratio and recovery rate as a function of percent of water exiting through the overflow, at a 35° angle of inclination, 20 mL/min inlet flow rate, and 59 cm settler length, for both this experiment and Wang's (2013) experiment

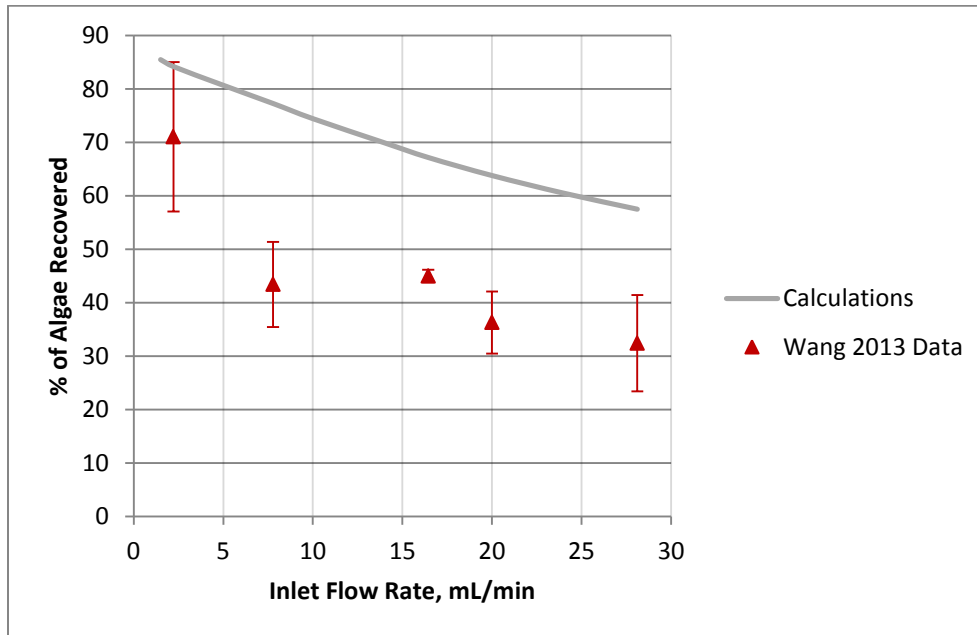
times the margin of error. Likewise, the recovery rate of algae is about 75% greater than the experimental values, or about 4 times the margin of error.

Figure 40 compares the plot of concentration ratio and recovery rate against the inlet flow rate (Figure 33) against Wang's data. Figure 40(a) shows that the calculated enrichment factors are 20-80% greater than the experimental values. Figure 40(b) shows that the calculated recovery rates are also about 20-80% greater than the experimental

values. In both cases, the calculations vary from the experimental values by about 1-3 times the size of the error bars.



(a) Enrichment factor vs. inlet flow rate



(b) Recovery rate vs. inlet flow rate

Figure 40: Algae concentration ratio and recovery rate as a function of inlet flow rate, with a 35 degree angle of inclination, 90% of the water exiting via the overflow, and a 59 cm settler length, for both this experiment and Wang's (2013) experiment.

There are several factors that can account for the difference between the experimental data and the calculations from the simulations. First, the simulations do not take into account particles sticking to the walls or bottom of the settler. The calculation assumes that any particle that sticks to the bottom of the settler will ultimately make it into the underflow region. In reality, this is not always the case. Second, the value of density of the algae particles used in these calculations was $1,080 \text{ kg/m}^3$. Values ranged in literature between $1,050$ and $1,080 \text{ kg/m}^3$, but $1,080$ was chosen because it was the most common value found in literature. A lower density value would have decreased the particle settling velocity, enrichment factor, and recovery rate, and using a lower density value would have also decreased the difference between this project and Wang's experiment. Last, there is the possibility of error from the particle size distribution. While *S. dimorphus* and *D. tertiolecta* have many similar properties, as explained in Section 3.4.2, the method of converting the size distribution for *D. tertiolecta* to size distribution for *S. dimorphus* was not exact.

While there is a difference in the data, Figures 39 and 40 show consistencies between the trends of algae concentration and recovery from COMSOL™ simulations and the MATLAB® program to those values found experimentally. The values predicted by these simulations and calculations can be used to interpolate and extrapolate Wang's data.

This experiment can quickly expand upon Wang's experiment and any other experiment that involves the separation of algae from water using this inclined settler design by adjusting the values of angle of inclination, inlet flow rate, outlet flow rate ratio, and settler length, width and height. Furthermore, this experiment can be

conducted to analyze the separation of any solid particle from any fluid by simply modifying the material properties on the COMSOL™ simulation or the MATLAB® program. The generation of nearly equivalent results to Wang's data indicates that data generated with this experiment are valid and may be used either to interpolate or extrapolate the data found by Wang, or for further research such as a scale-up experiment.

CHAPTER VI

CONCLUSIONS AND RECOMMENDATIONS

6.1 Concluding Remarks

The COMSOLTM simulations and MATLAB[®] calculations show that an inclined gravity settler can be an effective way to remove water from algae particles so the algae may be used in the production of biodiesel. Forcing more water to exit the settler through the overflow outlet increases the concentration of algae in the underflow outlet. Using a lower angle of inclination from the horizontal plane increases the concentration of algae in the underflow outlet. Using a lower inlet flow rate increases the concentration of algae in the underflow outlet.

The optimal conditions for dewatering are a 50-degree angle of inclination above the horizontal plane, an 18 mL/min inlet flow rate, and length of 59 cm. A system of two gravity settlers connected in series is necessary to generate the required 50-fold increase in algae concentration for biofuel production. Ninety percent of the water that enters the first settler will leave through the overflow. Ninety percent of the remaining water

becomes the overflow product of the second settler. At these conditions, 50.2% of the algae are still in the underflow stream, while just 1% of the water remains in the underflow. This results in a 50.2-fold concentration increase, which is sufficient for biodiesel production.

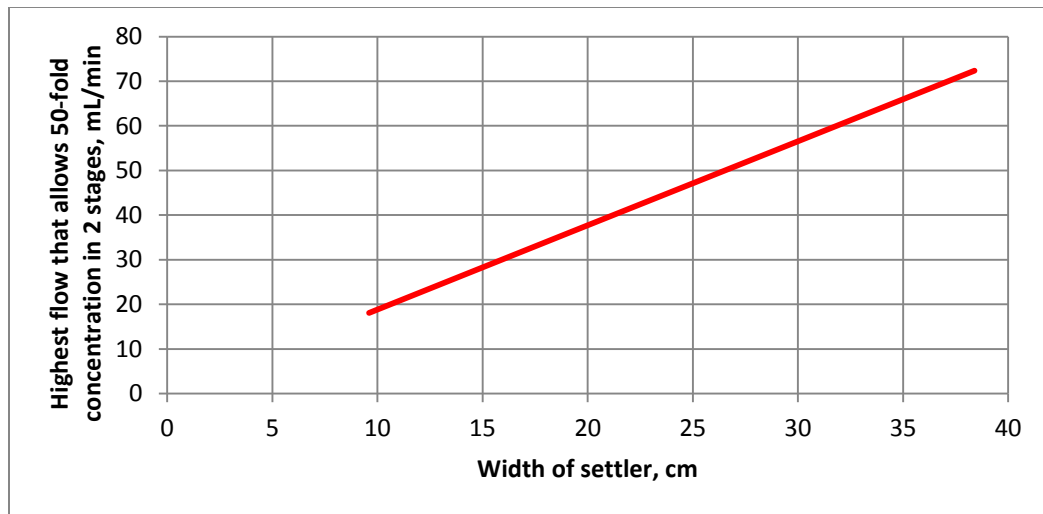
6.2 Recommendations and Further Research

The next logical step in the process would be to scale up the gravity settler for industrial use. This can be done by either adding multiple layers to increase the surface area, or by increasing the width or the length of the settler. Figure 41 shows that an increasing the length and width of the settler both have a proportional effect on the amount of fluid that can enter the settler. Both methods require adding the same amount of material to the settler to increase the inlet flow rate. I would recommend using the same length and a larger width in order to reduce the amount of fluid influenced by “end effects.”

The use of a settler with multiple layers has been tested by Laskovski et al. (2006); Salem, Okoth, and Thoming (2011), and Smith and Davis (2013). An increase in the number of layers in a given height will result in more particles settling toward the bottom and eventually leaving the settler through the underflow outlet (Smith 2013). It would result in more biofuel production for a given inlet flow rate than a gravity settler without layers can yield. The disadvantages associated with this method are a greater likelihood of algae cells becoming stuck in the settler, simply because of having less room to move and settle. Furthermore, studies of layered settlers only focus on those with an inlet on the bottom. Research would need to be conducted on layered settlers with an inlet at the top.



(a) Inlet flow rate vs. settler length at a constant width of 9.6 cm



(b) Inlet flow rate vs. settler width at a constant length of 59 cm

Figure 41: Comparison of highest flow rate possible to obtain an enrichment factor of 50 in two stages as a function of the (a) length and (b) width of the settler.

The MATLAB[®] interface shows that an increase in width of the settler will increase the algae that can be concentrated at a proportional rate. This is because an increase in width accompanied by a proportional increase in inlet flow rate will maintain a constant fluid velocity in the settler, as shown in Equation 4.1. Further research will

need to be conducted in order to determine which scale-up method will generate a higher amount of concentrated algae at a given inlet flow rate.

Also, I would recommend running tests on the actual gravity settler system for a second stage. Although the simulations show that the concentration is increased tenfold in a second stage without any risk of particles getting stuck, there is concern as to what would happen in the underflow outlet region of this stage. The high algae concentration increases the risk of particles becoming stuck in the outlet region. However, as this region is vertical, the force of gravity may be enough to maintain the motion of the concentrated algae. Additionally, the decrease in width for the second settler called for in Section 4.4 will maintain the same velocity that existed in the first settler. While the simulations indicate that the second stage should run normally, an actual experiment using the conditions of the second stage is needed to confirm this, as the decrease in width may have an effect on the velocity profile of the water in the settler. Velocity at the walls of the settler is zero, and the walls would be closer together. The region of the settler near the walls would account for a higher percentage of the settler.

REFERENCES

- Addison, Keith (2007). "Oil Yields and Characteristics." 04 October 2012.
<<http://journeytoforever.org/biodieselyield.html>>
- Anderson, Chris (2008). "Count on Canola for Your Biodeisel." *Biodeisel Magazine*.
10 October 2012.<<http://www.biodieselmagazine.com/articles/2063/count-on-canola-for-your-biodiesel/>>
- Balat, Mustafa and Havva Balat (2010). "Progress in Biodiesel Processing." *Applied Energy* 87; pp. 1815-1835.
- Becker, E.W (2007). "Micro-Algae as a Source of Protein." *Biotechnology Advances* 25(2); pp.207-210.
- Berman, Y. and A. Tamir (2003). "Kinetics of Droplets' Sedimentation in a Continuous Gravity Settler." *Chemical Engineering Science* 58(10); pp. 2089–2102.
- Bikiri, Zahir, Derradji Chebli, and Saci Nacef (2012). "Dynamic Modelling [*sic*] of the Secondary Settler of a Wastewater Treatment via Activated Sludge to Low-Load." *Energy Procedia* 18; pp. 1-9.
- Campbell, Matthew N (2008). "Biodeisel: Algae as a Renewable Source for Liquid Fuel." *Geulph. Engineering Journal* 1; pp. 2-7.
- Cerff, Martin et al (2012). "Harvesting Freshwater and Marine Algae by Magnetic Separation: Screening of Separation Parameters and High Gradient Magnetic Filtration." *Bioresource Technology* 118; pp. 289-295.
- Cheng, Nian-Sheng (2009). "Comparison of Formulas for Drag Coefficient and Settling Velocity of Spherical Particles." *Powder Technology* 189(3); pp. 395-398.
- Davis, R.H. and H. Gecol (1996). "Classification of Concentrated Suspensions using Inclined Settlers." *International Journal of Multiphase Flow* 22(3); pp. 563-574.

- Del Coz Díaz, J.J, P.J. García Nieto, D. Castro-Fresno, and P. Menéndez Rodríguez (2011). “Steady State Numerical Simulation of the Particle Collection Efficiency of a New Urban Sustainable Gravity Settler using Design of Experiments by FVM.” *Applied Mathematics and Computation* 217; pp. 8166-8178.
- Geankoplis, Christie John (2003). *Transport Process and Separation Process Principles*, 4th Ed. New York City: Prentice Hall.
- Hall, J.A. and L.A. Golding (1998). “Standard methods for whole effluent toxicity testing: development and application.” Report no. MFE80205. NIWA report for the Ministry for the Environment, Wellington, New Zealand. <<http://www.mfe.govt.nz/publications/water/whole-effluent-toxicity-nov98/whole-effluent-toxicity-appendix-1-nov98.pdf>>
- Hesketh, Robert P (2008). “Flow Between Parallel Plates.” Rowan University . department of Chemical Engineering. 16 July 2013. <<http://users.rowan.edu/~hesketh/0906-309/Lectures/Flow%20Between%20Parallel%20Plates%20-%20Comsol2008.pdf>>
- Jonasz, M., and G. R. Fournier (2007). *Light Scattering by Particles in Water, Theoretical and Experimental Foundations*, Elsevier, Amsterdam. p 704
- Kandale, Ajit et al (2011). “Marine Algae: An Introduction, Food Value, and Medicinal Uses.” *Journal of Pharmacy Research* 4(1); pp. 219-221.
- Kondrat’ev, A.S. and E.A. Naumova (2003). “Calculation of Free Settling of Solid Particles in a Newtonian Liquid.” *Theoretical Foundations of Chemical Engineering*, 37(6); pp 606-612.
- Kraipech, W., A. Nowakowski, T. Dyakowski, and A. Suksangpanomrung (2005). “An investigation of the effect of the particle–fluid and particle–particle interactions on the flow within a hydrocyclone.” *Chemical Engineering Journal* 111(2-3); pp. 189-197.
- Laskovski, D. et al (2006). “Segregation of Hydraulically Suspended Particles in Inclined Channels.” *Chemical Engineering Science* 61(22); pp. 7269–7278.
- Liu, Tao, et al (2006). “Boundary-Element Simulation of Hydrodynamic Interaction of Two Smooth Spheres Suspended in an Unbounded Couette Flow.” *Applied Energy* 83; pp. 975-988.
- Meriam-Webster (2013) “Scour.” Meriam-Webster.com. 13 July 2013 <<http://www.merriam-webster.com/dictionary/scour>>

- Mikkelsen, O. and M. Pejrup (2001). "The Use of a LISST-100 In-Situ Laser Particle Sizer for In-Situ Estimates of Floc Size, Density, and Settling Velocity." *Geo-Marine Letters* 20; pp. 187-195.
- Milledge, John, and Sonia Heaven (2012). "A Review of the Harvesting of Micro-Algae for Biofuel Production." *Reviews in Environmental Science and Biotechnology* pp. 1-14.
- Milton, Greame W. and John R. Willis (2007). "On Modifications of Newton's Second Law and Linear Continuum Elastodynamics." *Proceedings of the Royal Society* 463; 855-880.
- Molina Grima, E. et al (2003). "Recovery of Microalgal Biomass and Metabodies: Process Options and Economics." *Biotechnology Advances* 20; pp. 491-515.
- Mostoufi, N. and J. Chaouki (1999). "Prediction of Effective Drag Coefficient in Fluidized Beds." *Chemical Engineering Science* 54(7); pp. 851-858.
- Mutanda, T. et al (2011). "Bioprospecting for Hyper-Lipid Producing Microalgal Strains for Sustainable Biofuel Production." *Bioresource Technology* 102(1); pp. 57-70.
- Nasr-El-Din, H.A, J.H. Masliyah, and K. Nandakumar (1990). "Continuous Gravity Separation of Concentrated Bidisperse Suspensions in an Inclined Plane Settler." *International Journal of Multiphase Flow* 16(5); pp. 909-919.
- Nelson, D., J. Liu, and K.P. Galvin (1997). "Autogenous Dense Medium Separation Using an Inclined Counterflow Settler." *Minerals Engineering* 10(8); pp. 871-881.
- Nurdogan, Y., and J. Oswald (1996). "Tube settling of high-rate pond algae." *Water Science & Technology* 33(7); pp. 229-241.
- Park, J.B.K, R.J. Craggs, and A.N. Shilton (2011). "Recycling Algae to Improve Species Control and Harvest Efficiency from a High Rate Algal Pond." *Water Research* 45(20); pp. 6637-6649.
- Patankar, N.A., P.Y. Huang, T. Ko, and D.D. Joseph (2001). "Lift-off of a single particle in Newtonian and Viscoelastic Fluids by Direct Numerical Simulation." *Journal of Fluid Mechanics* 438; pp. 67-100.
- Pitt, R. and S. Clark (2007). "Module 4b: Characteristics and Monitoring of Stormwater Particulates." University of Alabama. 01 May 2013. <<http://rpitt.eng.ua.edu/Class/ExperimentalDesignFieldSampling/Module%204/Test2.htm>>
- Reynolds, R.A., D. Stramski, V.M. Wright, and S.B. Wozniak (2010). "Measurements and characterization of particle size distributions in coastal waters." *Journal of Geophysical Research* 115, C08024.

- Salem, A.I., G, Okoth, and J. Thoming (2011). “An Approach to Improve the Separation of Solid–Liquid Suspensions in Inclined Plate Settlers: CFD Simulation and Experimental Validation.” *Water Research* 45(11); pp. 3541–3549.
- Sarkar, S., D. Kamilya, and B.C. Mal. “Effect of Geometric and process Variables on the Performance of Inclined Plate Settlers in Treating Aquacultural Waste.” *Water Research* 41(5); pp. 993-1000.
- Schaffner, J., A.L. Pfefferman, H. Eckhardt, and J. Steinhardt (2011). “Inflow Based Investigations on the Efficiency of a Lamella Particle Separator for the Treatment of Stormwater Runoffs.” *Water Science & Technology* 64(1); pp. 271-278.
- Sell, Anne (2002). “Eddies – An Introduction: Impact on Marine Food Chains.” University of Hamburg. 10 July 2013 <http://www.uni-hamburg.de/ihf/eddies_e.pdf>
- Sharrer, Mark, et al (2010). “The Cost and Effectiveness of Solids Thickening Technologies for Treating Backwash and Recovering Nutrients from Intensive Aquaculture Systems.” *Bioresource. Technology* 101; pp. 6630-6641.
- Shen, Ying, Zhijian Pei, Wenqiao Yuan, and Enrong Mao (2009). “Effect of Nitrogen and Extraction Method on Algae Lipid Yield.” *International Journal of Agricultural and Biological Engineering* 2(1); pp. 51-57.
- Smith, Benjamin T. and Robert H. Davis (2012). “Sedimentation of Algae using Naturally Available Magnesium-Based Flocculants.” *Algal Research* 1; pp. 32-39.
- Smith, Benjamin T. and Robert H. Davis (2013). “Particle Concentration Using Inclined Sedimentation via Sludge Accumulation and Removal for Algae Harvesting.” *Chemical Engineering Science* 91; pp. 79-85.
- Smith, S. Jarrell, and Carl. T. Fredrichs (2011). “Size and Settling Velocities of Cohesive Floccs and Suspended Sediment Aggregates in a Trailing Suction Hopper Dredge Plume.” *Continental Shelf Research* 31; pp. S50-S63.
- Suali, Emma, and Rosalam Sarbatly (2012). “Conversion of Microalgae to Biofuel.” *Renewable and Sustainable Energy Reviews* 16; pp. 4316-4342.
- Subharda, Bobbran G. (2010). “Sustainability of Algal Biofuel Production using Integrated Renewable Energy Park (IREP) and Algal Biorefinery Approach.” *Energy Policy* 38(10); pp. 5892-5901.
- Tang, Haiying et al (2011). “Potential of Microalgae Oil from *Dunaliella Tertiolecta* as a Feedstock for Biodiesel.” *Applied Energy* 88; pp. 3324-3330.

- Terfous, A. Hazzab, and A. Ghenaim (2013). "Predicting the Drag Coefficient and Settling Velocity of Spherical Particles." *Powder Technology* 239; pp. 12-20.
- Thonon, I. et al (2005). "In-Situ measurements of Sediment Settling Characteristics in Floodplains using a LISST-ST." *Earth Surface Processes and Landforms* 30; pp. 1327-1343.
- United States Department of Energy (2008). "Algal Biofuels." 01 October 2012. <<http://www1.eere.energy.gov/biomass/pdfs/algalbiofuels.pdf>>
- University of Colorado. "Soft-Bodied Stream Algae of California: Scenedesmus Dimorphus." 10 July 2013 <http://dbmuseblade.colorado.edu/DiatomTwo/sbsac_site/species.php?g=Scenedesmus&s=dimorphus>
- Wang, Zhaowei, Jing Hou, Dustin Bowden, and Joanne M. Belovich (2013) "Evaluation of an Inclined Gravity Settler for Microalgae Harvesting." Cleveland State University Department of Chemical and Biomedical Engineering. 24 April 2013.
- Wolfs, Frank (2008). "Chapter 14: Gravity." Department of Physics and Astronomy, . University of Rochester. 28 May 2013. <<http://teacher.pas.rochester.edu/phy121/lecturenotes/Chapter14/Chapter14.html#Heading1>>
- Yang, Y. and K. Gao (2003) "Effects of CO₂ Concentrations on the Freshwater Microalgae, *Chlamydomonas reinhardtii*, *Chlorella pyrenoidosa* and *Scenedesmus obliquus*, (Chlorophyta)." *Journal of Applied Phycology* 00; pp. 1-11.
- Zhang, Jie (1998). "Chapter 2. Motion of Particles through Fluids." Chemical and Process Engineering, University of Newcastle upon Tyne <<http://lorien.ncl.ac.uk/ming/particle/cpe124p2.html>>

APPENDIX

Tables and Charts

Table III: Particle Sizes, Masses, and Settling Properties

	Min. Diam. μm	Max. Diam. μm	Ave. Diam. μm	Particle Mass (kg/m³)	Percent of total mass	Settling velocity Cm/s	Settling time¹ s
1	0.40	0.60	0.50	0.01333	1.130	0.0000 ²	917000
2	0.60	0.80	0.70	0.02781	2.357	0.0000 ²	468000
3	0.80	1.00	0.90	0.03578	3.032	0.0000 ²	283000
4	1.00	1.20	1.10	0.03646	3.090	0.0000 ²	189000
5	1.20	1.40	1.30	0.03272	2.773	0.0000 ²	135000
6	1.40	1.60	1.50	0.02728	2.312	0.0000 ²	101000
7	1.60	1.80	1.70	0.02176	1.844	0.0000 ²	79300
8	1.80	2.00	1.90	0.01687	1.430	0.0000 ²	63500
9	2.00	2.20	2.10	0.01287	1.091	0.0000 ²	52000
10	2.20	2.40	2.30	0.00971	0.823	0.0000 ²	43300
11	2.40	2.60	2.50	0.00729	0.618	0.0000 ²	36700
12	2.60	2.80	2.70	0.00545	0.462	0.0000 ²	31400
13	2.80	3.00	2.90	0.00408	0.346	0.0000 ²	27200
14	3.00	3.20	3.10	0.00306	0.259	0.0000 ²	23800
15	3.20	3.40	3.30	0.00229	0.194	0.0000 ²	21000
16	3.40	3.60	3.50	0.00142	0.120	0.0001	18700
17	3.60	3.80	3.70	0.00198	0.168	0.0001	16700
18	3.80	4.00	3.90	0.00267	0.226	0.0001	15000
19	4.00	4.20	4.10	0.00345	0.292	0.0001	13600
20	4.20	4.40	4.30	0.00432	0.366	0.0001	12400
21	4.40	4.60	4.50	0.00524	0.444	0.0001	11300
22	4.60	4.80	4.70	0.00620	0.525	0.0001	10300
23	4.80	5.00	4.90	0.00719	0.609	0.0001	9550
24	5.00	5.10	5.05	0.00395	0.335	0.0001	8990
25	5.10	5.20	5.15	0.00419	0.355	0.0001	8650
26	5.20	5.30	5.25	0.00444	0.376	0.0001	8320

27	5.30	5.40	5.35	0.00467	0.396	0.0001	8010
28	5.40	5.50	5.45	0.00490	0.415	0.0001	7720
29	5.50	5.60	5.55	0.00511	0.433	0.0001	7440
30	5.60	5.70	5.65	0.00533	0.452	0.0001	7180
31	5.70	5.80	5.75	0.00553	0.469	0.0001	6930
32	5.80	5.90	5.85	0.00573	0.486	0.0001	6700
33	5.90	6.00	5.95	0.00592	0.502	0.0002	6480
34	6.00	6.10	6.05	0.00610	0.517	0.0002	6260
35	6.10	6.20	6.15	0.00628	0.532	0.0002	6060
36	6.20	6.30	6.25	0.00643	0.545	0.0002	5870
37	6.30	6.40	6.35	0.00658	0.558	0.0002	5690
38	6.40	6.50	6.45	0.00673	0.570	0.0002	5510
39	6.50	6.60	6.55	0.00684	0.580	0.0002	5340
40	6.60	6.70	6.65	0.00696	0.590	0.0002	5180
41	6.70	6.80	6.75	0.00708	0.600	0.0002	5030
42	6.80	6.90	6.85	0.00717	0.608	0.0002	4880
43	6.90	7.00	6.95	0.00726	0.615	0.0002	4750
44	7.00	7.10	7.05	0.00734	0.622	0.0002	4610
45	7.10	7.20	7.15	0.00740	0.627	0.0002	4480
46	7.20	7.30	7.25	0.00746	0.632	0.0002	4360
47	7.30	7.40	7.35	0.00750	0.636	0.0002	4240
48	7.40	7.50	7.45	0.00755	0.640	0.0002	4130
49	7.50	7.60	7.55	0.00759	0.643	0.0002	4020
50	7.60	7.70	7.65	0.00760	0.644	0.0003	3920
51	7.70	7.80	7.75	0.00762	0.646	0.0003	3820
52	7.80	7.90	7.85	0.00762	0.646	0.0003	3720
53	7.90	8.00	7.95	0.00763	0.647	0.0003	3630
54	8.00	8.10	8.05	0.00762	0.646	0.0003	3540
55	8.10	8.20	8.15	0.00761	0.645	0.0003	3450
56	8.20	8.30	8.25	0.00759	0.643	0.0003	3370
57	8.30	8.40	8.35	0.00756	0.641	0.0003	3290
58	8.40	8.50	8.45	0.00754	0.639	0.0003	3210
59	8.50	8.60	8.55	0.00750	0.636	0.0003	3130
60	8.60	8.70	8.65	0.00746	0.632	0.0003	3060
61	8.70	8.80	8.75	0.00741	0.628	0.0003	2990
62	8.80	8.90	8.85	0.00736	0.624	0.0003	2920
63	8.90	9.00	8.95	0.00732	0.620	0.0003	2860
64	9.00	9.10	9.05	0.00726	0.615	0.0004	2800
65	9.10	9.20	9.15	0.00720	0.610	0.0004	2740
66	9.20	9.30	9.25	0.00714	0.605	0.0004	2680
67	9.30	9.40	9.35	0.00707	0.599	0.0004	2620
68	9.40	9.50	9.45	0.00700	0.593	0.0004	2560
69	9.50	9.60	9.55	0.00693	0.587	0.0004	2510
70	9.60	9.70	9.65	0.00686	0.581	0.0004	2460

71	9.70	9.80	9.75	0.00679	0.575	0.0004	2410
72	9.80	9.90	9.85	0.00670	0.568	0.0004	2360
73	9.90	10.00	9.95	0.00663	0.562	0.0004	2310
74	10.00	10.10	10.05	0.00655	0.555	0.0004	2270
75	10.10	10.20	10.15	0.00647	0.548	0.0004	2220
76	10.20	10.30	10.25	0.00638	0.541	0.0005	2180
77	10.30	10.40	10.35	0.00631	0.535	0.0005	2140
78	10.40	10.50	10.45	0.00623	0.528	0.0005	2100
79	10.50	10.60	10.55	0.00614	0.520	0.0005	2060
80	10.60	10.70	10.65	0.00605	0.513	0.0005	2020
81	10.70	10.80	10.75	0.00597	0.506	0.0005	1980
82	10.80	10.90	10.85	0.00589	0.499	0.0005	1940
83	10.90	11.00	10.95	0.00581	0.492	0.0005	1910
84	11.00	11.10	11.05	0.00571	0.484	0.0005	1870
85	11.10	11.20	11.15	0.00564	0.478	0.0005	1840
86	11.20	11.30	11.25	0.00556	0.471	0.0006	1810
87	11.30	11.40	11.35	0.00548	0.464	0.0006	1780
88	11.40	11.50	11.45	0.00539	0.457	0.0006	1750
89	11.50	11.60	11.55	0.00531	0.450	0.0006	1710
90	11.60	11.70	11.65	0.00523	0.443	0.0006	1690
91	11.70	11.80	11.75	0.00514	0.436	0.0006	1660
92	11.80	11.90	11.85	0.00506	0.429	0.0006	1630
93	11.90	12.00	11.95	0.00498	0.422	0.0006	1600
94	12.00	12.10	12.05	0.00490	0.415	0.0006	1580
95	12.10	12.20	12.15	0.00483	0.409	0.0006	1550
96	12.20	12.30	12.25	0.00474	0.402	0.0007	1520
97	12.30	12.40	12.35	0.00466	0.395	0.0007	1500
98	12.40	12.50	12.45	0.00459	0.389	0.0007	1480
99	12.50	12.60	12.55	0.00452	0.383	0.0007	1450
100	12.60	12.70	12.65	0.00444	0.376	0.0007	1430
101	12.70	12.80	12.75	0.00437	0.370	0.0007	1410
102	12.80	12.90	12.85	0.00430	0.364	0.0007	1380
103	12.90	13.00	12.95	0.00422	0.358	0.0007	1360
104	13.00	13.10	13.05	0.00415	0.352	0.0007	1340
105	13.10	13.20	13.15	0.00408	0.346	0.0008	1320
106	13.20	13.30	13.25	0.00401	0.340	0.0008	1300
107	13.30	13.40	13.35	0.00393	0.333	0.0008	1280
108	13.40	13.50	13.45	0.00388	0.329	0.0008	1260
109	13.50	13.60	13.55	0.00381	0.323	0.0008	1240
110	13.60	13.70	13.65	0.00375	0.318	0.0008	1230
111	13.70	13.80	13.75	0.00368	0.312	0.0008	1210
112	13.80	13.90	13.85	0.00362	0.307	0.0008	1190
113	13.90	14.00	13.95	0.00356	0.302	0.0008	1170
114	14.00	14.10	14.05	0.00349	0.296	0.0009	1160

115	14.10	14.20	14.15	0.00343	0.291	0.0009	1140
116	14.20	14.30	14.25	0.00337	0.286	0.0009	1120
117	14.30	14.40	14.35	0.00332	0.281	0.0009	1110
118	14.40	14.50	14.45	0.00327	0.277	0.0009	1090
119	14.50	14.60	14.55	0.00320	0.271	0.0009	1080
120	14.60	14.70	14.65	0.00315	0.267	0.0009	1060
121	14.70	14.80	14.75	0.00310	0.263	0.0009	1050
122	14.80	14.90	14.85	0.00304	0.258	0.0010	1040
123	14.90	15.00	14.95	0.00299	0.253	0.0010	1020
124	15.00	15.20	15.10	0.00583	0.494	0.0010	1000
125	15.20	15.40	15.30	0.00564	0.478	0.0010	980
126	15.40	15.60	15.50	0.00545	0.462	0.0010	955
127	15.60	15.80	15.70	0.00526	0.446	0.0011	931
128	15.80	16.00	15.90	0.00509	0.431	0.0011	908
129	16.00	16.20	16.10	0.00491	0.416	0.0011	885
130	16.20	16.40	16.30	0.00474	0.402	0.0012	864
131	16.40	16.60	16.50	0.00459	0.389	0.0012	843
132	16.60	16.80	16.70	0.00444	0.376	0.0012	823
133	16.80	17.00	16.90	0.00428	0.363	0.0012	803
134	17.00	17.20	17.10	0.00414	0.351	0.0013	785
135	17.20	17.40	17.30	0.00401	0.340	0.0013	767
136	17.40	17.60	17.50	0.00388	0.329	0.0013	749
137	17.60	17.80	17.70	0.00375	0.318	0.0014	732
138	17.80	18.00	17.90	0.00363	0.308	0.0014	716
139	18.00	18.20	18.10	0.00352	0.298	0.0014	700
140	18.20	18.40	18.30	0.00340	0.288	0.0015	685
141	18.40	18.60	18.50	0.00329	0.279	0.0015	670
142	18.60	18.80	18.70	0.00320	0.271	0.0015	656
143	18.80	19.00	18.90	0.00309	0.262	0.0016	642
144	19.00	19.20	19.10	0.00300	0.254	0.0016	629
145	19.20	19.40	19.30	0.00290	0.246	0.0016	616
146	19.40	19.60	19.50	0.00282	0.239	0.0017	603
147	19.60	19.80	19.70	0.00274	0.232	0.0017	591
148	19.80	20.00	19.90	0.00266	0.225	0.0017	579
149	20.00	20.20	20.10	0.00256	0.217	0.0018	568
150	20.20	20.40	20.30	0.00249	0.211	0.0018	557
151	20.40	20.60	20.50	0.00242	0.205	0.0018	546
152	20.60	20.80	20.70	0.00235	0.199	0.0019	536
153	20.80	21.00	20.90	0.00228	0.193	0.0019	525
154	21.00	21.20	21.10	0.00222	0.188	0.0019	515
155	21.20	21.40	21.30	0.00215	0.182	0.0020	506
156	21.40	21.60	21.50	0.00209	0.177	0.0020	496
157	21.60	21.80	21.70	0.00202	0.171	0.0021	487
158	21.80	22.00	21.90	0.00197	0.167	0.0021	478

159	22.00	22.20	22.10	0.00191	0.162	0.0021	470
160	22.20	22.40	22.30	0.00186	0.158	0.0022	461
161	22.40	22.60	22.50	0.00182	0.154	0.0022	453
162	22.60	22.80	22.70	0.00177	0.150	0.0022	445
163	22.80	23.00	22.90	0.00171	0.145	0.0023	438
164	23.00	23.20	23.10	0.00166	0.141	0.0023	430
165	23.20	23.40	23.30	0.00163	0.138	0.0024	423
166	23.40	23.60	23.50	0.00158	0.134	0.0024	416
167	23.60	23.80	23.70	0.00153	0.130	0.0024	409
168	23.80	24.00	23.90	0.00150	0.127	0.0025	402
169	24.00	24.20	24.10	0.00146	0.124	0.0025	395
170	24.20	24.40	24.30	0.00143	0.121	0.0026	389
171	24.40	24.60	24.50	0.00139	0.118	0.0026	382
172	24.60	24.80	24.70	0.00136	0.115	0.0027	376
173	24.80	25.00	24.90	0.00132	0.112	0.0027	370
174	25.00	25.20	25.10	0.00129	0.109	0.0027	364
175	25.20	25.40	25.30	0.00126	0.107	0.0028	359
176	25.40	25.60	25.50	0.00123	0.104	0.0028	353
177	25.60	25.80	25.70	0.00119	0.101	0.0029	347
178	25.80	26.00	25.90	0.00117	0.099	0.0029	342
179	26.00	26.20	26.10	0.00114	0.097	0.0030	337
180	26.20	26.40	26.30	0.00112	0.095	0.0030	332
181	26.40	26.60	26.50	0.00109	0.092	0.0031	327
182	26.60	26.80	26.70	0.00106	0.090	0.0031	322
183	26.80	27.00	26.90	0.00104	0.088	0.0032	317
184	27.00	27.20	27.10	0.00101	0.086	0.0032	312
185	27.20	27.40	27.30	0.00099	0.084	0.0032	308
186	27.40	27.60	27.50	0.00097	0.082	0.0033	303
187	27.60	27.80	27.70	0.00096	0.081	0.0033	299
188	27.80	28.00	27.90	0.00093	0.079	0.0034	295
189	28.00	28.20	28.10	0.00091	0.077	0.0034	291
190	28.20	28.40	28.30	0.00090	0.076	0.0035	287
191	28.40	28.60	28.50	0.00087	0.074	0.0035	283
192	28.60	28.80	28.70	0.00085	0.072	0.0036	279
193	28.80	29.00	28.90	0.00084	0.071	0.0036	275
194	29.00	29.20	29.10	0.00083	0.070	0.0037	271
195	29.20	29.40	29.30	0.00080	0.068	0.0037	267
196	29.40	29.60	29.50	0.00079	0.067	0.0038	264
197	29.60	29.80	29.70	0.00077	0.065	0.0038	260
198	29.80	30.00	29.90	0.00076	0.064	0.0039	257
199	30.00	31.00	30.50	0.00356	0.302	0.0041	247
200	31.00	32.00	31.50	0.00325	0.275	0.0043	231
201	32.00	33.00	32.50	0.00296	0.251	0.0046	217
202	33.00	34.00	33.50	0.00273	0.231	0.0049	205

203	34.00	35.00	34.50	0.00251	0.213	0.0058	193
204	35.00	36.00	35.50	0.00232	0.197	0.0061	182
205	36.00	37.00	36.50	0.00216	0.183	0.0065	172
206	37.00	38.00	37.50	0.00202	0.171	0.0068	163
207	38.00	39.00	38.50	0.00189	0.160	0.0071	155
208	39.00	40.00	39.50	0.00177	0.150	0.0075	147
209	40.00	41.00	40.50	0.00168	0.142	0.0079	140
210	41.00	42.00	41.50	0.00158	0.134	0.0082	133
211	42.00	43.00	42.50	0.00150	0.127	0.0086	127
212	43.00	44.00	43.50	0.00143	0.121	0.0090	121
213	44.00	45.00	44.50	0.00136	0.115	0.0094	116
214	45.00	46.00	45.50	0.00130	0.110	0.0098	111
215	46.00	47.00	46.50	0.00125	0.106	0.0103	106
216	47.00	48.00	47.50	0.00120	0.102	0.0107	102
217	48.00	49.00	48.50	0.00116	0.098	0.0111	97.5
218	49.00	50.00	49.50	0.00112	0.095	0.0116	93.6
219	50.00	51.00	50.50	0.00109	0.092	0.0120	90.0
220	51.00	52.00	51.50	0.00123	0.104	0.0125	86.5
221	52.00	53.00	52.50	0.00122	0.103	0.0129	83.3
222	53.00	54.00	53.50	0.00120	0.102	0.0134	80.2
223	54.00	55.00	54.50	0.00119	0.101	0.0139	77.3
224	55.00	56.00	55.50	0.00119	0.101	0.0144	74.5
225	56.00	57.00	56.50	0.00118	0.100	0.0149	71.9
226	57.00	58.00	57.50	0.00117	0.099	0.0154	69.4
227	58.00	59.00	58.50	0.00117	0.099	0.0160	67.1
228	59.00	60.00	59.50	0.00116	0.098	0.0165	64.8
229	60.00	61.00	60.50	0.00114	0.097	0.0170	62.7
230	61.00	62.00	61.50	0.00114	0.097	0.0176	60.7
231	62.00	63.00	62.50	0.00113	0.096	0.0181	58.7
232	63.00	64.00	63.50	0.00112	0.095	0.0187	56.9
233	64.00	65.00	64.50	0.00112	0.095	0.0193	55.2
234	65.00	66.00	65.50	0.00112	0.095	0.0199	53.5
235	66.00	67.00	66.50	0.00111	0.094	0.0204	51.9
236	67.00	68.00	67.50	0.00110	0.093	0.0210	50.4
237	68.00	69.00	68.50	0.00109	0.092	0.0217	48.9
238	69.00	70.00	69.50	0.00109	0.092	0.0223	47.5
239	70.00	71.00	70.50	0.00107	0.091	0.0229	46.2
240	71.00	72.00	71.50	0.00106	0.090	0.0235	44.9
241	72.00	73.00	72.50	0.00105	0.089	0.0242	43.7
242	73.00	74.00	73.50	0.00104	0.088	0.0248	42.5
243	74.00	75.00	74.50	0.00103	0.087	0.0255	41.4
244	75.00	76.00	75.50	0.00103	0.087	0.0262	40.3
245	76.00	77.00	76.50	0.00101	0.086	0.0268	39.2
246	77.00	78.00	77.50	0.00100	0.085	0.0275	38.2

247	78.00	79.00	78.50	0.00100	0.085	0.0282	37.2
248	79.00	80.00	79.50	0.00099	0.084	0.0289	36.3
249	80.00	81.00	80.50	0.00098	0.083	0.0297	35.4
250	81.00	82.00	81.50	0.00098	0.083	0.0304	34.6
251	82.00	83.00	82.50	0.00097	0.082	0.0311	33.7
252	83.00	84.00	83.50	0.00096	0.081	0.0318	32.9
253	84.00	85.00	84.50	0.00096	0.081	0.0326	32.1
254	85.00	86.00	85.50	0.00094	0.080	0.0334	31.4
255	86.00	87.00	86.50	0.00093	0.079	0.0341	30.7
256	87.00	88.00	87.50	0.00093	0.079	0.0349	30.0
257	88.00	89.00	88.50	0.00092	0.078	0.0357	29.3
258	89.00	90.00	89.50	0.00092	0.078	0.0365	28.7
259	90.00	91.00	90.50	0.00091	0.077	0.0373	28.0
260	91.00	92.00	91.50	0.00090	0.076	0.0381	27.4
261	92.00	93.00	92.50	0.00090	0.076	0.0389	26.8
262	93.00	94.00	93.50	0.00089	0.075	0.0397	26.3
263	94.00	95.00	94.50	0.00089	0.075	0.0406	25.7
264	95.00	96.00	95.50	0.00087	0.074	0.0414	25.2
265	96.00	97.00	96.50	0.00086	0.073	0.0423	24.7
266	97.00	98.00	97.50	0.00086	0.073	0.0431	24.2
267	98.00	99.00	98.50	0.00085	0.072	0.0444	23.7
268	99.00	100.0	99.50	0.00085	0.072	0.0462	23.2
269	100.0	102.0	101.0	0.00166	0.141	0.0480	22.5
270	102.0	104.0	103.0	0.00164	0.139	0.0499	21.6
271	104.0	106.0	105.0	0.00162	0.137	0.0517	20.8
272	106.0	108.0	107.0	0.00159	0.135	0.0536	20.1
273	108.0	110.0	109.0	0.00157	0.133	0.0556	19.3
274	110.0	112.0	111.0	0.00155	0.131	0.0576	18.6
275	112.0	114.0	113.0	0.00152	0.129	0.0596	18.0
276	114.0	116.0	115.0	0.00150	0.127	0.0616	17.4
277	116.0	118.0	117.0	0.00148	0.125	0.0637	16.8
278	118.0	120.0	119.0	0.00145	0.123	0.0659	16.2
279	120.0	122.0	121.0	0.00143	0.121	0.0680	15.7
280	122.0	124.0	123.0	0.00140	0.119	0.0702	15.2
281	124.0	126.0	125.0	0.00139	0.118	0.0724	14.7
282	126.0	128.0	127.0	0.00137	0.116	0.0747	14.2
283	128.0	130.0	129.0	0.00135	0.114	0.0770	13.8
284	130.0	132.0	131.0	0.00132	0.112	0.0792	13.4
285	132.0	134.0	133.0	0.00150	0.127	0.0817	13.0
286	134.0	136.0	135.0	0.00148	0.125	0.0840	12.6
287	136.0	138.0	137.0	0.00145	0.123	0.0865	12.2
288	138.0	140.0	139.0	0.00144	0.122	0.0889	11.9
289	140.0	142.0	141.0	0.00130	0.110	0.0914	11.6
290	142.0	144.0	143.0	0.00129	0.109	0.0940	11.2

291	144.0	146.0	145.0	0.00127	0.108	0.0965	10.9
292	146.0	148.0	147.0	0.00125	0.106	0.0991	10.6
293	148.0	150.0	149.0	0.00123	0.104	0.1018	10.4
294	150.0	152.0	151.0	0.00122	0.103	0.1044	10.1
295	152.0	154.0	153.0	0.00120	0.102	0.1071	9.8
296	154.0	156.0	155.0	0.00118	0.100	0.1099	9.6
297	156.0	158.0	157.0	0.00117	0.099	0.1126	9.3
298	158.0	160.0	159.0	0.00114	0.097	0.1154	9.1
299	160.0	162.0	161.0	0.00113	0.096	0.1183	8.9
300	162.0	164.0	163.0	0.00112	0.095	0.1211	8.7
301	164.0	166.0	165.0	0.00110	0.093	0.1240	8.5
302	166.0	168.0	167.0	0.00109	0.092	0.1270	8.3
303	168.0	170.0	169.0	0.00107	0.091	0.1300	8.1
304	170.0	172.0	171.0	0.00105	0.089	0.1330	7.9
305	172.0	174.0	173.0	0.00099	0.084	0.1360	7.7
306	174.0	176.0	175.0	0.00097	0.082	0.1391	7.5
307	176.0	178.0	177.0	0.00096	0.081	0.1422	7.4
308	178.0	180.0	179.0	0.00094	0.080	0.1453	7.2
309	180.0	182.0	181.0	0.00093	0.079	0.1485	7.0
310	182.0	184.0	183.0	0.00092	0.078	0.1517	6.9
311	184.0	186.0	185.0	0.00091	0.077	0.1549	6.7
312	186.0	188.0	187.0	0.00090	0.076	0.1582	6.6
313	188.0	190.0	189.0	0.00089	0.075	0.1615	6.5
314	190.0	192.0	191.0	0.00087	0.074	0.1648	6.3
315	192.0	194.0	193.0	0.00086	0.073	0.1682	6.2
316	194.0	196.0	195.0	0.00085	0.072	0.1716	6.1
317	196.0	198.0	197.0	0.00084	0.071	0.1751	5.9
318	198.0	200.0	199.0	0.00083	0.070	0.1788	5.8
319	134.0	136.0	135.0	0.00081	0.069	0.1823	5.7

¹ *Settling time refers to the amount of time required for a particle to settle from the top of the settler to the bottom, a distance of 1 cm*

² *The settling velocity is not zero, but it is less than 0.00005 cm/s.*

Table IV: Comparing Outlet Flow Rate Ratio

Inlet mL/min	Upper mL/min	Lower mL/min	% water in upper outlet	Enrichment Factor	% Algae Recovery
20	10	10	50	1.67	83.5
20	11	9	55	1.80	80.9
20	12	8	60	1.96	78.2
20	13	7	65	2.16	75.4
20	14	6	70	2.42	72.6
20	15	5	75	2.79	69.7
20	16	4	80	3.34	66.8
20	17	3	85	4.25	63.7
20	18	2	90	6.10	61.0
20	19	1	95	11.7	58.7
20	19.4	0.6	97	19.1	57.5
20	19.6	0.4	98	28.5	57.0
20	19.8	0.2	99	56.5	56.5
20	19.9	0.1	99.5	112	56.2

For inlet flow rate of 20 mL/min, angle of inclination of 45° and 59 cm settler length

Table V: Comparing Angle of Inclination

Incl. Angle Degrees	Enrichment Factor	% Algae Recovery
0	6.732	67.32
5	6.726	67.26
10	6.698	66.98
15	6.675	66.75
20	6.626	66.26
25	6.559	65.59
30	6.477	64.77
35	6.377	63.77
40	6.246	62.46
45	6.095	60.95
50	5.919	59.19
55	5.711	57.11
60	5.448	54.48
65	5.134	51.34
70	4.760	47.60
75	4.293	42.93
80	3.715	37.15
85	2.966	29.66
88	2.323	23.23
90	1.000	10.00

For inlet flow rate of 20 mL/min, 90% of water leaves through overflow and 59 cm settler length

Table VI: Determining Optimal Angle of Inclination

Incl. Angle Degrees	Particle velocity near bottom cm/s	Enrichment factor * Particle velocity near bottom cm/s
0	0.0347	0.234
10	0.0357	0.240
20	0.0366	0.245
30	0.0374	0.250
40	0.0382	0.253
50	0.0388	0.255
60	0.0393	0.254
70	0.0397	0.253
80	0.0400	0.250
86	0.0401	0.244
90	0.0401	0.237

“Particle velocity near bottom” refers to the velocity of a particle 20 µm in diameter at a height of 0.02 cm above the bottom of the settler

Table VII: Comparing Inlet Flow Rate

Flow Rate mL/min	Enrichment factor	% Algae Recovery	Second Stage Enrichment Factor	Combined Enrichment Factor (1 st and 2 nd stage)
2	8.336	83.36	-	-
4	8.051	80.51	-	-
6	7.743	77.43	-	-
8	7.437	74.37	9.26	68.87
10	7.118	71.18	9.05	64.42
12	6.841	68.41	8.84	60.44
14	6.565	65.65	8.61	56.53
16	6.341	63.41	8.45	53.58
18	6.118	61.18	8.20	50.15
20	5.919	59.19	7.99	47.29
24	5.583	55.83	7.62	42.54
28	5.295	52.95	-	-
32	5.056	50.56	-	-
36	4.852	48.52	-	-
40	4.668	46.68	-	-

For a 50° angle of inclination , 90% of water leaves through overflow and 59 cm settler length

Table VIII: Comparing Settler Length

Length Ratio	Length (cm)	Enrichment Factor	Recovery Rate (%)
0.25	14.8	3.370	33.70
0.5	29.5	4.665	46.65
1.0	59.0	6.119	61.19
1.5	88.5	6.885	68.85
2.0	118.0	7.348	73.48
2.5	147.5	7.622	76.22
3.0	177.0	7.819	78.19
3.5	206.5	7.939	79.39
4.0	236.0	8.033	80.33
5.0	295.0	8.161	81.61
6.0	354.0	8.237	82.37
7.0	413.0	8.301	83.01
8.0	472.0	8.326	83.26
9.0	531.0	8.372	83.72

For inlet flow rate of 18 mL/min, angle of inclination of 50° and 90% of water exiting through overflow

Sample Calculation

Particle trajectory for a particle with a diameter of 5 μm, 50° angle of inclination, 18 mL/min inlet flow rate, and 90% of water exits the settler via the overflow outlet, length of settler = 59 cm

- Constants
 - Density of water: 1000 kg/m³
 - Dynamic viscosity of water: 0.001 kg/(m*s)
 - Kinematic viscosity of water: 10⁻⁶ m/s
- Velocity of Water (from Equation 4.1)

$$u_f = \frac{Q_{f-in}}{A_{CS}} = \frac{18 \text{ mL/min}}{9.6 \text{ cm}^2} * \frac{\text{cm}^3}{\text{mL}} * \frac{\text{min}}{60 \text{ s}} * \frac{\text{m}}{100 \text{ cm}} = 3.13 * 10^{-4} \text{ m/s}$$

- Particle Reynolds Number (from Equation 3.8)

$$Re = \frac{D_p u \rho_f}{\mu_f} = \frac{5 * 10^{-6} \text{ m} * 3.13 * 10^{-4} \frac{\text{m}}{\text{s}} * 1000 \frac{\text{kg}}{\text{m}^3}}{0.001 \frac{\text{kg}}{\text{m} * \text{s}}} = 1.57 * 10^{-3}$$

- Determine Critical Reynolds Number as defined by Patankar (2001). Determine Archamedes number from Equation 3.28:

$$Ar = \frac{\rho_f(\rho_p - \rho_f)gD_p^3}{\mu_f^2} = \frac{1000 \frac{kg}{m^3} \left(1080 \frac{kg}{m^3} - 1000 \frac{kg}{m^3}\right) * 9.81 \frac{m}{s^2} * (5 * 10^{-6} m)^3}{\left(0.001 \frac{kg}{m * s}\right)^2} = 9.81 * 10^{-5}$$

- Critical Reynolds Number interpolated from Patankar's (2001) data:

$$Re_{critical} = 3 * 10^{-2}$$

- This value is greater than the particle Reynolds Number, so the particle will not experience lift after settling toward the bottom of the settler.
- Using Equations 3.29 through 3.34, calculate settling velocity of particle in fluid
 - Assume $D_M = D_S = D_V = D = 5 * 10^{-6} m$

$$u_{s,0} = 10 \left(\frac{v_f}{D_m}\right) \left(\frac{2D_s + D_m}{D_m}\right) \left\{ \left[1 + \left(\frac{D_m}{2D_s + D_m}\right)^2 \frac{Ar}{30} \right]^{\frac{1}{2}} - 1 \right\}$$

$$= 10 \left(\frac{10^{-6} \frac{kg}{m * s}}{5 * 10^{-6} m}\right) (3) \left\{ \left[1 + \left(\frac{1}{3}\right)^2 \frac{9.81 * 10^{-5}}{30} \right]^{\frac{1}{2}} - 1 \right\} = 1.1 * 10^{-6} m/s$$

- Per Kondrat'ev (2003) the iterative steps described in Equations 3.29-3.34 are not needed because the particle Reynolds number is less than 1
- Calculate the x- and z- components of the settling velocity from Equations 3.35 and 3.36

$$u_{s,x} = u_s \sin(\theta) = 1.1 * 10^{-6} \frac{m}{s} * \sin(50) = 8.4 * 10^{-7} m/s$$

$$u_{s,z} = u_s \cos(\theta) = 1.1 * 10^{-6} \frac{m}{s} * \cos(50) = 7.1 * 10^{-7} m/s$$

- Calculate the x- and z-components of the particle velocity from Equations 3.37 and 3.38

$$u_{p,x} = u_{s,x} + u_{d,x} = 8.4 * 10^{-7} \frac{m}{s} + 3.13 * 10^{-4} \frac{m}{s} = 3.14 * 10^{-4} m/s$$

$$u_{p,z} = u_{s,z} + u_{f,z} = 7.1 * 10^{-7} \frac{m}{s} + 0 \frac{m}{s} = 7.1 * 10^{-7} m/s$$

- Calculate residence time by dividing the settler length by the particle velocity in the x direction (Equation 3.39)

$$\tau = \frac{L}{u_{p,x}} = \frac{0.59 m}{3.14 * 10^{-4} \frac{m}{s}} = 1879 s$$

- Particles of this size have a residence time of 745 seconds, or about 46 minutes

- Calculate the distance a particle travels in the z-direction during this time (Equation 3.41)

$$dz = u_{p,z} * \tau = 7.1 * 10^{-7} \frac{m}{s} * 1878 s = 0.0014 m$$

- Calculate the percent of the settler height that this size particle travels

$$\frac{dz}{H} = \frac{0.0014 m}{0.01 m} = 14\%$$

- Calculate the percent of the settler height that a particle must travel in order to reach the underflow outlet (Equation 3.39)

$$\int_0^{dz} u_{f,x}(z) dz = \frac{PCTW_{overflow}}{100}$$

- In which $PCTW_{overflow}$ is the percent of water that enters the overflow. In this case, it would be 90%. Calculating this integral, the water would have to travel 0.0084 m, or 84% of the height of the settler. Therefore, a particle must settle to a height of $z \leq 0.0016 m$ in order to exit through the underflow.
- Because a particle can start at any z-value ranging from $z=0$ to $z=100$ based on the inlet flow distribution explained using Figure 22, the percent of particles of this size that settler toward the underflow outlet will be estimated using Figure 22.
- Particles must start at a height at or below 0.0016 m (the point in which particles have settled far enough to enter the underflow) + 0.0014 m (the value of “dz,” or the distance a particle settles in the z-direction, so particles must be at $z \leq 0.0030 m$ once the flow is fully developed.
- According to Figure 22, approximately 20% of the particles will be at $z \leq 0.0030 m$ once the flow is fully developed.
- Therefore, 20% of particles with 5 μm diameters will settle to the underflow in these conditions, and 80% of these particles will remain in the overflow.

MATLAB® Script for First Settler

```
% This program uses the equations of settling velocity along with other
% given information to determine the trajectories of particles within a
% gravity settler
%
% This program also determines the amount of particles that exit the
% gravity settler via the upper (high water) region, and the lower
% (low-water) region of the settler, as well as concentrations of both
% streams (relative to the inlet stream)
% -----
%
% The positive x-direction is the direction of flow. The z-direction is
% positioned in such a way that gravity occurs at a specified angle between
% positive x and negative z.
% -----

clear; clc;
% -----
% %%%%%%%%%%          GIVEN DATA AND INPUT SETTLER PARAMETERS          %%%%%%%%%%
% -----
% Input angle of inclination
thetad = input('Enter angle of inclination (degrees above horizontal): ');
theta = thetad*3.1416/180; % radians

% Input initial flow rate
Qinml = input('\nEnter inlet flow rate (mL/min): ');
Qin = Qinml/1000000; % m^3/min

% Input percentage of fluid to leave upper outlet
split=101;
while split > 100 || split < 0
    fprintf('\nEnter percentage of fluid leaving the settler via the');
    split=input('\nupper outlet (non-algae outlet): ');

    % Verify that this percent is between 0 and 100
    if split > 100 || split < 0
        fprintf('\nError: Invalid Percentage');
    end
end

% Percentages of fluid in upper and lower outlets
Pctfup = split;
Pctflow = 100 - split;

% Dimentions of settler
% The settler being analyzed is 59 cm long and 1 cm in height
% However, allow user to input length of the settler

% length = 0.59; % m
lengthcm = input('\nEnter length of settler (cm): ');
length2 = lengthcm - 5; % cm, this is because the inlet is 5 cm past the
% back wall of the seettler
length = length2/100;

height = 0.01; % m
width = 0.095; % m
Acs = height*width; % m^2, cross sectional area

% Convert flow rate to velocity. v = Q/A

vin = Qin/Acs; % m/min
vin = vin/60; % m/s
```

```

% vin is the average fluid velocity. Per Figure 11, the average velocity
% is 0.65 times the maximum velocity.

vin_max = vin/0.65; % m/s

% Fluid Residence time = Length/Inlet Velocity
% Residence time only includes the time that the fluid is in the settling
% region of the settler, it does not include the time that the fluid is
% inside either of the outlet regions
tauf = length/vin; % s

% Constants
rhof = 1000; % kg/m^3, density of fluid
rhop = 1080; % kg/m^3, density of particle
muf = 0.00100; % kg/(m*s), dynamic viscosity of fluid
nuf = 10^-6; % m^2/s, kinematic viscosity of fluid

% -----
% %%%%%%%%%% GENERATE PARTICLE SIZE DISTRIBUTION %%%%%%%%%%
% -----

% Particle diameters
% This program considers particle diameters ranging from 0.50 um to 200 um
D2 = zeros(320,1); % particle diameter, m
D = zeros(319,1); % average particle diameter (for accurate plotting), m

% For example, the range of 0.5 um and 1.5 um would have an average
% diameter of 1.0 um. The arithmetic mean can be considered accurate due
% to the very small ranges of particle size being considered.
% D(1) will be the average value of D2(1) and D2(2).

i = 1; j = 1;

while i <= 24 % 0.4 to 5 um
    D2(i) = 0.2 + 0.2*i; % um
    D2(i) = D2(i)/1000000; % m
    if i ~= 1
        D(i-1) = (D2(i) + D2(i-1))/2;
    end
    i = i+1;
end

while i <= 124 % 5 to 15 um
    D2(i) = D2(i-1)*1000000 + 0.1; % um
    D2(i) = D2(i)/1000000; % m
    D(i-1) = (D2(i) + D2(i-1))/2;
    i = i+1;
end

while i <= 199 % 15 to 30 um
    D2(i) = D2(i-1)*1000000 + 0.2; % um
    D2(i) = D2(i)/1000000; % m
    D(i-1) = (D2(i) + D2(i-1))/2;
    i = i+1;
end

while i <= 269 % 30 to 100 um
    D2(i) = D2(i-1)*1000000 + 1; % um
    D2(i) = D2(i)/1000000; % m
    D(i-1) = (D2(i) + D2(i-1))/2;
    i = i+1;
end
end

```

```

while i <= 320 % 100 to 202 um
    D2(i) = D2(i-1)*1000000 + 2; % um
    D2(i) = D2(i)/1000000; % m
    D(i-1) = (D2(i) + D2(i-1))/2;
    i = i+1;
end

% Particle reynolds number for each diameter (Equation 3.8)
% Reynolds number =
% (diameter of particle*fluid velocity*fluid density)/(fluid viscosity)
Re = zeros(319,1);
i=1;
while i<=319
    Re(i) = (D(i)*vin*rhof)/(muf);
    i = i+1;
end

% Particle size and mass distribution is summarized in the Section 3.4.
% The mass of all particles within each particle size range can be
% determined by taking the definite integral Equation
% between predetermined lower and upper limits (terms in the D2 matrix)
%
% For D < 3.3 um
% M(D) = 10^{-7.88[log10(D)]^2 - 273}
%
% For 3.3 um < D < 50 um
% M(D) = 10^{2.28[log10(D)]^3 + 30.1[log10(D)]^2 + 129[log10(D)] + 175}
%
% For D > 50 um
% M(D) = 10^{-1.29[log10(D)]^2 - 10.9[log10(D)] - 0.987}
%
% List the percent of algae (by mass) that exists in particles within each
% size range

Pct=zeros(319,1);

Pct(1) = 1.130; Pct(2) = 2.357; Pct(3) = 3.032; Pct(4) = 3.090;
Pct(5) = 2.773; Pct(6) = 2.312; Pct(7) = 1.844; Pct(8) = 1.430;
Pct(9) = 1.091; Pct(10) = .823; Pct(11) = .618; Pct(12) = .462;
Pct(13) = .346; Pct(14) = .259; Pct(15) = .194; Pct(16) = .120;
Pct(17) = .168; Pct(18) = .226; Pct(19) = .292; Pct(20) = .366;
Pct(21) = .444; Pct(22) = .525; Pct(23) = .609; Pct(24) = .335;
Pct(25) = .355; Pct(26) = .376; Pct(27) = .396; Pct(28) = .415;
Pct(29) = .433; Pct(30) = .452; Pct(31) = .469; Pct(32) = .486;
Pct(33) = .502; Pct(34) = .517; Pct(35) = .532; Pct(36) = .545;
Pct(37) = .558; Pct(38) = .570; Pct(39) = .580; Pct(40) = .590;
Pct(41) = .600; Pct(42) = .608; Pct(43) = .615; Pct(44) = .622;
Pct(45) = .627; Pct(46) = .632; Pct(47) = .636; Pct(48) = .640;
Pct(49) = .643; Pct(50) = .644; Pct(51) = .646; Pct(52) = .646;
Pct(53) = .647; Pct(54) = .646; Pct(55) = .645; Pct(56) = .643;
Pct(57) = .641; Pct(58) = .639; Pct(59) = .636; Pct(60) = .632;
Pct(61) = .628; Pct(62) = .624; Pct(63) = .620; Pct(64) = .615;
Pct(65) = .610; Pct(66) = .605; Pct(67) = .599; Pct(68) = .593;
Pct(69) = .587; Pct(70) = .581; Pct(71) = .575; Pct(72) = .568;
Pct(73) = .562; Pct(74) = .555; Pct(75) = .548; Pct(76) = .541;
Pct(77) = .535; Pct(78) = .528; Pct(79) = .520; Pct(80) = .513;
Pct(81) = .506; Pct(82) = .499; Pct(83) = .492; Pct(84) = .484;
Pct(85) = .478; Pct(86) = .471; Pct(87) = .464; Pct(88) = .457;
Pct(89) = .450; Pct(90) = .443; Pct(91) = .436; Pct(92) = .429;
Pct(93) = .422; Pct(94) = .415; Pct(95) = .409; Pct(96) = .402;
Pct(97) = .395; Pct(98) = .389; Pct(99) = .383; Pct(100) = .376;
Pct(101) = .370; Pct(102) = .364; Pct(103) = .358; Pct(104) = .352;

```

```

Pct (105)= .346; Pct (106)= .340; Pct (107)= .333; Pct (108)= .329;
Pct (109)= .323; Pct (110)= .318; Pct (111)= .312; Pct (112)= .307;
Pct (113)= .302; Pct (114)= .296; Pct (115)= .291; Pct (116)= .286;
Pct (117)= .281; Pct (118)= .277; Pct (119)= .271; Pct (120)= .267;
Pct (121)= .263; Pct (122)= .258; Pct (123)= .253; Pct (124)= .249;
Pct (125)= .478; Pct (126)= .462; Pct (127)= .446; Pct (128)= .431;
Pct (129)= .416; Pct (130)= .402; Pct (131)= .389; Pct (132)= .376;
Pct (133)= .363; Pct (134)= .351; Pct (135)= .340; Pct (136)= .329;
Pct (137)= .318; Pct (138)= .308; Pct (139)= .298; Pct (140)= .288;
Pct (141)= .279; Pct (142)= .271; Pct (143)= .262; Pct (144)= .254;
Pct (145)= .246; Pct (146)= .239; Pct (147)= .232; Pct (148)= .225;
Pct (149)= .217; Pct (150)= .211; Pct (151)= .205; Pct (152)= .199;
Pct (153)= .193; Pct (154)= .188; Pct (155)= .182; Pct (156)= .177;
Pct (157)= .171; Pct (158)= .167; Pct (159)= .162; Pct (160)= .158;
Pct (161)= .154; Pct (162)= .150; Pct (163)= .145; Pct (164)= .141;
Pct (165)= .138; Pct (166)= .134; Pct (167)= .130; Pct (168)= .127;
Pct (169)= .124; Pct (170)= .121; Pct (171)= .118; Pct (172)= .115;
Pct (173)= .112; Pct (174)= .109; Pct (175)= .107; Pct (176)= .104;
Pct (177)= .101; Pct (178)= .099; Pct (179)= .097; Pct (180)= .095;
Pct (181)= .092; Pct (182)= .090; Pct (183)= .088; Pct (184)= .086;
Pct (185)= .084; Pct (186)= .082; Pct (187)= .081; Pct (188)= .079;
Pct (189)= .077; Pct (190)= .076; Pct (191)= .074; Pct (192)= .072;
Pct (193)= .071; Pct (194)= .070; Pct (195)= .068; Pct (196)= .067;
Pct (197)= .065; Pct (198)= .064; Pct (199)= .062; Pct (200)= .061;
Pct (201)= .251; Pct (202)= .231; Pct (203)= .213; Pct (204)= .197;
Pct (205)= .183; Pct (206)= .171; Pct (207)= .160; Pct (208)= .150;
Pct (209)= .142; Pct (210)= .134; Pct (211)= .127; Pct (212)= .121;
Pct (213)= .115; Pct (214)= .110; Pct (215)= .106; Pct (216)= .102;
Pct (217)= .098; Pct (218)= .095; Pct (219)= .092; Pct (220)= .104;
Pct (221)= .103; Pct (222)= .102; Pct (223)= .101; Pct (224)= .101;
Pct (225)= .100; Pct (226)= .099; Pct (227)= .099; Pct (228)= .098;
Pct (229)= .097; Pct (230)= .097; Pct (231)= .096; Pct (232)= .095;
Pct (233)= .095; Pct (234)= .095; Pct (235)= .094; Pct (236)= .093;
Pct (237)= .092; Pct (238)= .092; Pct (239)= .091; Pct (240)= .090;
Pct (241)= .089; Pct (242)= .088; Pct (243)= .087; Pct (244)= .087;
Pct (245)= .086; Pct (246)= .085; Pct (247)= .085; Pct (248)= .084;
Pct (249)= .083; Pct (250)= .083; Pct (251)= .082; Pct (252)= .081;
Pct (253)= .081; Pct (254)= .080; Pct (255)= .079; Pct (256)= .079;
Pct (257)= .078; Pct (258)= .078; Pct (259)= .077; Pct (260)= .076;
Pct (261)= .076; Pct (262)= .075; Pct (263)= .075; Pct (264)= .074;
Pct (265)= .073; Pct (266)= .073; Pct (267)= .072; Pct (268)= .072;
Pct (269)= .141; Pct (270)= .139; Pct (271)= .137; Pct (272)= .135;
Pct (273)= .133; Pct (274)= .131; Pct (275)= .129; Pct (276)= .127;
Pct (277)= .125; Pct (278)= .123; Pct (279)= .121; Pct (280)= .119;
Pct (281)= .118; Pct (282)= .116; Pct (283)= .114; Pct (284)= .112;
Pct (285)= .127; Pct (286)= .125; Pct (287)= .123; Pct (288)= .122;
Pct (289)= .110; Pct (290)= .109; Pct (291)= .108; Pct (292)= .106;
Pct (293)= .104; Pct (294)= .103; Pct (295)= .102; Pct (296)= .100;
Pct (297)= .099; Pct (298)= .097; Pct (299)= .096; Pct (300)= .095;
Pct (301)= .093; Pct (302)= .092; Pct (303)= .091; Pct (304)= .089;
Pct (305)= .084; Pct (306)= .082; Pct (307)= .081; Pct (308)= .080;
Pct (309)= .079; Pct (310)= .078; Pct (311)= .077; Pct (312)= .076;
Pct (313)= .075; Pct (314)= .074; Pct (315)= .073; Pct (316)= .072;
Pct (317)= .071; Pct (318)= .070; Pct (319)= .069;

```

```

% For this project, assume all particles are spherical. Although most
% particles are oblong or not completely spherical, the particle size
% distribution can be considered a function of the volume of the particle,
% rather than its diameter.

```

```

% Archimedes Number Ar = (particle density - fluid density)*(fluid density)
% * (gravity) * (diameter)^3 / (fluid dynamic viscosity)^2
% As shown on Equation 3.24

```

```

% -----
% %%%%%%%%%%          DETERMINE SETTLING VELOCITY          %%%%%%%%%%
% -----

g = 9.8065; % m/s^2, acceleration due to gravity

Ar = zeros(319,1);
i=1;
while i <= 319
    Ar(i) = ((rhop - rhof)*rhop*g*(D(i))^3)/(muf*muf);
    i=i+1;
end

%Solve for settling velocity at each diameter
SV = zeros(319,1);
i=1;
while i<=319

    % Determine a settling velocity based on Equation 3.30
    SV(i) = 30*(muf/D(i))*((1+(1/9)*(Ar(i)/30))^0.5 - 1);

    % Per Kondrat'ev (2003) p. 608, the iterations shown in Eq. 3.31-3.34
    % are only needed for 1 < Re < 1000. The particle Reynolds numbers in
    % this experiment are < 1 for almost all sizes, so the iteration
    % described on p. 609 (Kondrat'ev 2003) is necessary only for the
    % highest diameters. At even the highest flow rates examined Re > 1
    % only when D > 300 um. Even at these diameters, the Reynolds numbers
    % are < 5, and any reduction of settling velocity would be by less than
    % 15% (Kondrat'ev p. 609).Even at these reduced settling velocities,
    % these large particles would still move to the bottom of the settler
    % rather quickly.
    if Re(i) > 1
        SV(i) = 0.85*SV(i);
    end

    i = i+1;
end % of while(i) loop

% x and z components of settling velocity
SVx = zeros(319,1); SVz = zeros(319,1);

i=1;
while i<=319
    SVx(i) = SV(i)*sin(theta); % m/s
    SVz(i) = -SV(i)*cos(theta); % m/s
    % note that SVz is negative because settling velocity is in the
    % direction of gravity, which is an angle between the positive x and
    % negative z directions. The positive x-direction is the direction of
    % fluid flow.

    i=i+1;
end

% -----
% %%%%%%%%%%          FLOW DISTRIBUTION          %%%%%%%%%%
% -----

% 20 particles of each size will be considered. Each particle's initial
% z-coordinate corresponds to one of the streamlines as shown in Figure
% 3.14 when the fluid flow is fully developed. To simplify the
% calculation, it is assumed that before the velocity profile is fully
% developed, the particle trajectory is identical to the fluid motion.

```

```

% Define starting points (zstart)
zstart = zeros(20,1);
zstart(1) = .00911; % m
zstart(2) = .00834;
zstart(3) = .00782;
zstart(4) = .00735;
zstart(5) = .00693;
zstart(6) = .00653;
zstart(7) = .00619;
zstart(8) = .00580;
zstart(9) = .00545;
zstart(10) = .00509;
zstart(11) = .00476;
zstart(12) = .00444;
zstart(13) = .00411;
zstart(14) = .00374;
zstart(15) = .00337;
zstart(16) = .00299;
zstart(17) = .00265;
zstart(18) = .00208;
zstart(19) = .00152;
zstart(20) = .00079;

% "Pct2" is a modified version of "Pct." Pct2 considers both the particle
% size distribution and the flow distribution. Assume a particle has an
% equal chance of going on any stramline in Figure 21.

Pct2 = zeros(319,20);
i=1; k=1;
while i<=319
    while k <= 20
        Pct2(i,k) = Pct(i)/20;
        k=k+1;
    end % of "whlie k" loop
    k = 1;
    i = i+1;
end % of "while i" loop

% Particle velocity and residence time
% Per Equations 3.37 and 3.38, particle velocity is equal to the settling
% velocity plus the drag velocity. Drag velocity is assumed to equal the
% fluid velocity.

% There is no drag velocity in the z-direction, so particle velocity is
% equal to settling velocity.
PVz = zeros(319,1);
i=1;
while i <= 319
    PVz(i) = SVz(i);
    i=i+1;
end

% Particle velocity in the x-direction is dependent assumed equal to the
% settling velocity in the x-direction plus the drag velocity in the x-
% direction.

% Drag velocity in the x-direction is a function of z. The fluid velocity
% for each "starting point" on the z axis is calculated as the average of
% the fluid velocity in the range from z=0 to the starting point.
DVx = zeros(20,1);

% Based on velocity profile shown in Figure 11
DVx(1) = .7014*vin_max; DVx(2) = .7196*vin_max; DVx(3) = .7312*vin_max;

```

```

DVx(4) = .7326*vin_max; DVx(5) = .7298*vin_max; DVx(6) = .7169*vin_max;
DVx(7) = .7029*vin_max; DVx(8) = .6971*vin_max; DVx(9) = .6827*vin_max;
DVx(10)= .6648*vin_max; DVx(11)= .6544*vin_max; DVx(12)= .6330*vin_max;
DVx(13)= .6109*vin_max; DVx(14)= .5872*vin_max; DVx(15)= .5352*vin_max;
DVx(16)= .4654*vin_max; DVx(17)= .4447*vin_max; DVx(18)= .3542*vin_max;
DVx(19)= .2398*vin_max; DVx(20)= .1335*vin_max;

% Particle velocity = Settling velocity + drag velocity
PVx = zeros(319,20);
i=1; k=1;
while i <= 319
    while k <= 20
        PVx(i,k) = SVx(i) + DVx(k); % m/s
        k=k+1;
    end % of "while k" loop
    k=1;
    i=i+1;
end % of "while i" loop

% Particle Residence time. As defined by Equation 3.39, residence time is
% the amount of time it takes a particle to travel through the length of
% the settler

taup = zeros(319,20);
i=1; k=1;
while i <= 319
    while k <= 20
        taup(i,k) = length/PVx(i,k); % s, particle residence time
        k=k+1;
    end % of "while k" loop
    k=1;
    i=i+1;
end % of "while i" loop

% How far each particle travels in the z-direction (per Equation 3.41)
dz = zeros(319,20);
i=1; k=1;
while i<=319
    while k <= 20
        dz(i,k) = taup(i,k)*-SVz(i); % m, distance traveled by z particle

        % a particle can not travel below the bottom of the settler
        dz(i,k) = min(dz(i,k), zstart(k)); % m
        k=k+1;
    end % of "whlie k" loop
    k=1;
    i=i+1;
end % of "while i" loop

% Which particles leave which exit, based on the percentage of fluid that
% leaves each exit
% For example, if 90% of the fluid leaves the upper outlet, any of the
% particles in the top 90% of the fluid (any particle whose z position is
% between 0 cm and 0.90 cm) will go to the upper outlet, while any particle
% in the bottom 10% (whose z position is between 0.90 cm and 1 cm) will go
% to the lower outlet. Figure 13 on the report confirms this).

% zexit is the height of a particle inside the settler at the outlet.
zexit = zeros(319,20);
i=1; k=1;
while i<=319
    while k<=20
        zexit(i,k) = zstart(k) - dz(i,k); % m

```

```

        k=k+1;
    end % of "while k" loop
    k=1;
    i=i+1;
end % of "while i" loop

% zsplit is defined as the z value in which particles above this point will
% exit through the overflow and particles below that point will exit
% through the underflow.

% The value of z-split can be obtained and interpolated from Figure 22.
% The value of zsplit can be expressed as a function of the percent of
% fluid that exits the settler through the overflow outlet:
% zsplit = -7.6e-5*(Pct) + 0.0087

zsplit = -7.6e-5*split + 0.0087; % meters

% -----
% %%%%%%%%%%                OBTAINING AND DISPLAYING RESULTS                %%%%%%%%%%
% -----

% Determine enrichment factor and recovery rate for given conditions.

% The variable "outlet" measures whether a particle with a given diameter
% and starting point will leave the settler through the overflow or
% underflow.
% If outlet(i,k)=1, the particle of size range i and starting point k will
% leave through the overflow.
% If outlet(i,k)=2, the particle of size range i and starting point k will
% leave through the overflow.

% Display Header
fprintf('Diameter   Pct of   Pct to   Pct to   Residence \n');
fprintf('(um)       total    overfl  underfl  time (s)');
outlet=zeros(319,20);
recovery = 0; % Recovery rate (in terms of percent)
in_under = zeros(319,1); % percent of cells off each size in underflow;
i=1; k=1;
while i<=319
    while k<=20
        if zexit(i,k) < zsplit % if the particle is below the "split point"
            outlet(i,k)=2; % Particle exits through overflow
            recovery = recovery + Pct2(i,k);
            in_under(i)= in_under(i) + 5;
        else % if the particle is at or above the "split line"
            outlet(i,k) = 1;
            end % of "if zexit" statement
        k=k+1;
    end % of "while k" loop
    fprintf('\n %8.4f   %6.4f   %3.0f   %3.0f %8.4f', D(i)*1000000, Pct(i),
100-in_under(i), in_under(i), taup(i));
    k=1;
    i=i+1;
end % of "while i" loop

% Calculate enrichment factor from recovery rate
% Enrichment factor =
% (Algae concentration in underflow) / (Algae concentration in inlet)

enrich = (recovery/100)/(1-(split/100));

% Display enrichment factor and recovery rate
fprintf('\n\n Enrichment factor: %8.4f', enrich);

```



```
fprintf('\n Recovery rate: %8.4f percent', recovery);
```

```

% -----
%          %%%%%%%%%%          LIST OF VARIABLES          %%%%%%%%%%
% -----
% Variable | Description | Units
%          |            |
% Ain      | Area of inlet to settler | m^2
% Amtlow   | Amount of algae in lower outlet divided by algae | mL/min
%          | concentration |
% Amtup    | Amount of algae in upper outlet divided by algae | mL/min
%          | concentration |
% Ar       | Archimedes Number | unitless
% Conclow  | Ratio of concentration of algae in lower outlet to |
%          | concentration of algae in inlet | unitless
% Concup   | Ratio of concentration of algae in upper outlet to |
%          | concentration of algae in inlet | unitless
% D        | Average diameter in a given size range | m
% D2       | Lowest and highest diameters in a given size range | m
% DVx      | Drag velocity in x-direction | m/s
% DVz      | Drag velocity in z-direction | m/s
% dz       | Movement in the negative z-direction of particles | m
%          | of a given size range |
% enrich   | enrichment factor (underflow conc./inlet conc.) | unitless
% g        | Acceleration due to gravity | m/s^2
% height   | Height of the settling region of the settler | m
% i        | Counter used in "while" loops | unitless
% in_under | percent of cells off each size in underflow | percent
% j        | Power of 10 used to determine particle diameters | unitless
%          | used in this program |
% k        | Counter used in "while" loops | unitless
% length   | Length of the settling region of the settler | m
% lengthcm | Length of the settling region of the settler | cm
% muf      | Dynamic viscosity of the fluid | kg/(m*s)
% nuf      | Kinematic viscosity of the fluid | m^2/s
% outlet   | Determines whether particles of a given size range | unitless
%          | exit the settler via the upper or lower outlet |
% Pct      | Percent of the total amount of algae (by mass) that | unitless
%          | exists in each size range |
% Pctlow   | Percent of the total amount of algae (by mass) that | unitless
%          | Exits the settler via the lower outlet |
% Pctup    | Percent of the total amount of algae (by mass) that | unitless
%          | Exits the settler via the upper outlet |
% PVx      | Particle velocity in the x-direction | m/s
% PVz      | Particle velocity in the z-direction | m/s
% Qin      | Volumetric flow rate of fluid into the settler | m^3/min
% Qinml    | Volumetric flow rate of fluid into the settler | mL/min
% Re       | Reynolds number | unitless
% recovery | Recovery rate | percent
% rhof     | Density of the fluid | kg/m^3
% rhop     | Density of the particles | kg/m^3
% rin      | Radius of the fluid inlet regions | m
% split    | Percent of fluid from inlet that exits via the | unitless
%          | upper outlet |
% splitfrac | split (above), converted from percent to fraction | unitless
% SV       | Settling velocity of particle | m/s
% SVx      | Settling velocity of particle in x-direction | m/s
% SVz      | Settling velocity of particle in z-direction | m/s
% tauf     | Fluid residence time | s
% taup     | residence time of particles of a given size range | s
% theta    | angle of inclination | radians

```

```

% thetad   | angle of inclination                               | degrees
% vin      | inlet velocity of fluid                                 | m/s
% zsplit   | split (above), in terms of distance in z-direction        | m
% zstart   | Point on the z axis in which a particle "started"         | m
%          | its trajectory, its z-location once fluid flow was        |
%          | fully developed.                                          |
% -----
% End of program

```

MATLAB® Script for Second Settler

```

% This program uses the equations of settling velocity along with other
% given information to determine the trajectories of particles within a
% gravity settler
%
% This program also determines the amount of particles that exit the
% gravity settler via the upper (high water) region, and the lower
% (low-water) region of the settler, as well as concentrations of both
% streams (relative to the inlet stream)
% -----
%
% The positive x-direction is the direction of flow. The z-direction is
% positioned in such a way that gravity occurs at a specified angle between
% positive x and negative z.
% -----

clear; clc;
% -----
% %%%%%%%%%%          GIVEN DATA AND INPUT SETTLER PARAMETERS          %%%%%%%%%%
% -----
% Input angle of inclination
thetad = input('Enter angle of inclination (degrees above horizontal): ');
theta = thetad*3.1416/180; % radians

% Input initial flow rate
Qinml = input('\nEnter inlet flow rate for SECOND settler (mL/min): ');
Qin   = Qinml/1000000; % m^3/min

% Input percentage of fluid to leave upper outlet
split=101;
while split > 100 || split < 0
    fprintf('\nEnter percentage of fluid leaving the settler via the');
    split=input('\nupper outlet (non-algae outlet): ');

    % Verify that this percent is between 0 and 100
    if split > 100 || split < 0
        fprintf('\nError: Invalid Percentage');
    end
end

% Percentages of fluid in upper and lower outlets
Pctfup = split;
Pctflow = 100 - split;

% Dimentions of settler
% The settler being analyzed is 59 cm long and 1 cm in height
% However, allow user to input length of the settler

% length = 0.59; % m

```

```

lengthcm = input('\nEnter length of settler (cm): ');
length2  = lengthcm - 5; % cm, this is because the inlet is 5 cm past the
                        % back wall of the settler
length   = length2/100;

height = 0.01; % m
width  = 0.095; % m
% NOTE: this width is for the first stage, it must be adjusted accordingly
% (for example if only 10% of the fluid is present in the second stage, the
% width must be multiplied by 10%)

Acs    = height*width; % m^2, cross sectional area

% Convert flow rate to velocity. v = Q/A

vin    = Qin/Acs; % m/min
vin    = vin/60; % m/s

% vin is the average fluid velocity. Per Figure 11, the average velocity
% is 0.65 times the maximum velocity.

vin_max = vin/0.65; % m/s

% Fluid Residence time = Length/Inlet Velocity
% Residence time only includes the time that the fluid is in the settling
% region of the settler, it does not include the time that the fluid is
% inside either of the outlet regions
tauf    = length/vin; % s

% Constants
rhof    = 1000; % kg/m^3, density of fluid
rhop    = 1080; % kg/m^3, density of particle
muf     = 0.00100; % kg/(m*s), dynamic viscosity of fluid
nuf     = 10^-6; % m^2/s, kinematic viscosity of fluid

% -----
% %%%%%%%%%% GENERATE PARTICLE SIZE DISTRIBUTION %%%%%%%%%%
% -----

% Particle diameters
% This program considers particle diameters ranging from 0.50 um to 200 um
D2 = zeros(320,1); % particle diameter, m
D  = zeros(319,1); % average particle diameter (for accurate plotting), m

% For example, the range of 0.5 um and 1.5 um would have an average
% diameter of 1.0 um. The arithmetic mean can be considered accurate due
% to the very small ranges of particle size being considered.
% D(1) will be the average value of D2(1) and D2(2).

i = 1; j = 1;

while i <= 24 % 0.4 to 5 um
    D2(i) = 0.2 + 0.2*i; % um
    D2(i) = D2(i)/1000000; % m
    if i ~= 1
        D(i-1) = (D2(i) + D2(i-1))/2;
    end
    i = i+1;
end

while i <= 124 % 5 to 15 um
    D2(i) = D2(i-1)*1000000 + 0.1; % um
    D2(i) = D2(i)/1000000; % m

```

```

    D(i-1) = (D2(i) + D2(i-1))/2;
    i = i+1;
end

while i <= 199 % 15 to 30 um
    D2(i) = D2(i-1)*1000000 + 0.2; % um
    D2(i) = D2(i)/1000000; % m
    D(i-1) = (D2(i) + D2(i-1))/2;
    i = i+1;
end

while i <= 269 % 30 to 100 um
    D2(i) = D2(i-1)*1000000 + 1; % um
    D2(i) = D2(i)/1000000; % m
    D(i-1) = (D2(i) + D2(i-1))/2;
    i = i+1;
end

while i <= 320 % 100 to 202 um
    D2(i) = D2(i-1)*1000000 + 2; % um
    D2(i) = D2(i)/1000000; % m
    D(i-1) = (D2(i) + D2(i-1))/2;
    i = i+1;
end

% Particle reynolds number for each diameter (Equation 3.8)
% Reynolds number =
% (diameter of particle*fluid velocity*fluid density)/(fluid viscosity)
Re = zeros(319,1);
i=1;
while i<=319
    Re(i) = (D(i)*vin*rhof)/(muf);
    i = i+1;
end

% Particle size and mass distribution is summarized in the Section 3.4.
% The mass of all particles within each particle size range can be
% determined by taking the definite integral Equation
% between predetermined lower and upper limits (terms in the D2 matrix)
%
% For D < 3.3 um
% M(D) = 10^{-7.88[log10(D)]^2 - 273}
%
% For 3.3 um < D < 50 um
% M(D) = 10^{2.28[log10(D)]^3 + 30.1[log10(D)]^2 + 129[log10(D)] + 175}
%
% For D > 50 um
% M(D) = 10^{-1.29[log10(D)]^2 - 10.9[log10(D)] - 0.987}
%
% List the percent of algae (by mass) that exists in particles within each
% size range

Pct=zeros(319,1);

% Note: This is based on the particle size distribution for the first
% stage. In order to accurately model the second stage, change the 1.00
% multiplier on the right side of each Pct(i) to the fraction obtained from
% the underflow of the first stage (shown in the table at the outlet).
Pct(1) = 1.130*1.00; Pct(2) = 2.357*1.00;
Pct(3) = 3.032*1.00; Pct(4) = 3.090*1.00;
Pct(5) = 2.773*1.00; Pct(6) = 2.312*1.00;
Pct(7) = 1.844*1.00; Pct(8) = 1.430*1.00;
Pct(9) = 1.091*1.00; Pct(10) = .823*1.00;

```

Pct (11) = .618*1.00; Pct (12) = .462*1.00;
Pct (13) = .346*1.00; Pct (14) = .259*1.00;
Pct (15) = .194*1.00; Pct (16) = .120*1.00;
Pct (17) = .168*1.00; Pct (18) = .226*1.00;
Pct (19) = .292*1.00; Pct (20) = .366*1.00;
Pct (21) = .444*1.00; Pct (22) = .525*1.00;
Pct (23) = .609*1.00; Pct (24) = .335*1.00;
Pct (25) = .355*1.00; Pct (26) = .376*1.00;
Pct (27) = .396*1.00; Pct (28) = .415*1.00;
Pct (29) = .433*1.00; Pct (30) = .452*1.00;
Pct (31) = .469*1.00; Pct (32) = .486*1.00;
Pct (33) = .502*1.00; Pct (34) = .517*1.00;
Pct (35) = .532*1.00; Pct (36) = .545*1.00;
Pct (37) = .558*1.00; Pct (38) = .570*1.00;
Pct (39) = .580*1.00; Pct (40) = .590*1.00;
Pct (41) = .600*1.00; Pct (42) = .608*1.00;
Pct (43) = .615*1.00; Pct (44) = .622*1.00;
Pct (45) = .627*1.00; Pct (46) = .632*1.00;
Pct (47) = .636*1.00; Pct (48) = .640*1.00;
Pct (49) = .643*1.00; Pct (50) = .644*1.00;
Pct (51) = .646*1.00; Pct (52) = .646*1.00;
Pct (53) = .647*1.00; Pct (54) = .646*1.00;
Pct (55) = .645*1.00; Pct (56) = .643*1.00;
Pct (57) = .641*1.00; Pct (58) = .639*1.00;
Pct (59) = .636*1.00; Pct (60) = .632*1.00;
Pct (61) = .628*1.00; Pct (62) = .624*1.00;
Pct (63) = .620*1.00; Pct (64) = .615*1.00;
Pct (65) = .610*1.00; Pct (66) = .605*1.00;
Pct (67) = .599*1.00; Pct (68) = .593*1.00;
Pct (69) = .587*1.00; Pct (70) = .581*1.00;
Pct (71) = .575*1.00; Pct (72) = .568*1.00;
Pct (73) = .562*1.00; Pct (74) = .555*1.00;
Pct (75) = .548*1.00; Pct (76) = .541*1.00;
Pct (77) = .535*1.00; Pct (78) = .528*1.00;
Pct (79) = .520*1.00; Pct (80) = .513*1.00;
Pct (81) = .506*1.00; Pct (82) = .499*1.00;
Pct (83) = .492*1.00; Pct (84) = .484*1.00;
Pct (85) = .478*1.00; Pct (86) = .471*1.00;
Pct (87) = .464*1.00; Pct (88) = .457*1.00;
Pct (89) = .450*1.00; Pct (90) = .443*1.00;
Pct (91) = .436*1.00; Pct (92) = .429*1.00;
Pct (93) = .422*1.00; Pct (94) = .415*1.00;
Pct (95) = .409*1.00; Pct (96) = .402*1.00;
Pct (97) = .395*1.00; Pct (98) = .389*1.00;
Pct (99) = .383*1.00; Pct (100) = .376*1.00;
Pct (101) = .370*1.00; Pct (102) = .364*1.00;
Pct (103) = .358*1.00; Pct (104) = .352*1.00;
Pct (105) = .346*1.00; Pct (106) = .340*1.00;
Pct (107) = .333*1.00; Pct (108) = .329*1.00;
Pct (109) = .323*1.00; Pct (110) = .318*1.00;
Pct (111) = .312*1.00; Pct (112) = .307*1.00;
Pct (113) = .302*1.00; Pct (114) = .296*1.00;
Pct (115) = .291*1.00; Pct (116) = .286*1.00;
Pct (117) = .281*1.00; Pct (118) = .277*1.00;
Pct (119) = .271*1.00; Pct (120) = .267*1.00;
Pct (121) = .263*1.00; Pct (122) = .258*1.00;
Pct (123) = .253*1.00; Pct (124) = .249*1.00;
Pct (125) = .247*1.00; Pct (126) = .242*1.00;
Pct (127) = .244*1.00; Pct (128) = .231*1.00;
Pct (129) = .216*1.00; Pct (130) = .202*1.00;
Pct (131) = .389*1.00; Pct (132) = .376*1.00;
Pct (133) = .363*1.00; Pct (134) = .351*1.00;
Pct (135) = .340*1.00; Pct (136) = .329*1.00;

Pct (137)= .318*1.00; Pct (138)= .308*1.00;
Pct (139)= .298*1.00; Pct (140)= .288*1.00;
Pct (141)= .279*1.00; Pct (142)= .271*1.00;
Pct (143)= .262*1.00; Pct (144)= .254*1.00;
Pct (145)= .246*1.00; Pct (146)= .239*1.00;
Pct (147)= .232*1.00; Pct (148)= .225*1.00;
Pct (149)= .217*1.00; Pct (150)= .211*1.00;
Pct (151)= .205*1.00; Pct (152)= .199*1.00;
Pct (153)= .193*1.00; Pct (154)= .188*1.00;
Pct (155)= .182*1.00; Pct (156)= .177*1.00;
Pct (157)= .171*1.00; Pct (158)= .167*1.00;
Pct (159)= .162*1.00; Pct (160)= .158*1.00;
Pct (161)= .154*1.00; Pct (162)= .150*1.00;
Pct (163)= .145*1.00; Pct (164)= .141*1.00;
Pct (165)= .138*1.00; Pct (166)= .134*1.00;
Pct (167)= .130*1.00; Pct (168)= .127*1.00;
Pct (169)= .124*1.00; Pct (170)= .121*1.00;
Pct (171)= .118*1.00; Pct (172)= .115*1.00;
Pct (173)= .112*1.00; Pct (174)= .109*1.00;
Pct (175)= .107*1.00; Pct (176)= .104*1.00;
Pct (177)= .101*1.00; Pct (178)= .099*1.00;
Pct (179)= .097*1.00; Pct (180)= .095*1.00;
Pct (181)= .092*1.00; Pct (182)= .090*1.00;
Pct (183)= .088*1.00; Pct (184)= .086*1.00;
Pct (185)= .084*1.00; Pct (186)= .082*1.00;
Pct (187)= .081*1.00; Pct (188)= .079*1.00;
Pct (189)= .077*1.00; Pct (190)= .076*1.00;
Pct (191)= .074*1.00; Pct (192)= .072*1.00;
Pct (193)= .071*1.00; Pct (194)= .070*1.00;
Pct (195)= .068*1.00; Pct (196)= .067*1.00;
Pct (197)= .065*1.00; Pct (198)= .064*1.00;
Pct (199)= .302*1.00; Pct (200)= .275*1.00;
Pct (201)= .251*1.00; Pct (202)= .231*1.00;
Pct (203)= .213*1.00; Pct (204)= .197*1.00;
Pct (205)= .183*1.00; Pct (206)= .171*1.00;
Pct (207)= .160*1.00; Pct (208)= .150*1.00;
Pct (209)= .142*1.00; Pct (210)= .134*1.00;
Pct (211)= .127*1.00; Pct (212)= .121*1.00;
Pct (213)= .115*1.00; Pct (214)= .110*1.00;
Pct (215)= .106*1.00; Pct (216)= .102*1.00;
Pct (217)= .098*1.00; Pct (218)= .095*1.00;
Pct (219)= .092*1.00; Pct (220)= .104*1.00;
Pct (221)= .103*1.00; Pct (222)= .102*1.00;
Pct (223)= .101*1.00; Pct (224)= .101*1.00;
Pct (225)= .100*1.00; Pct (226)= .099*1.00;
Pct (227)= .099*1.00; Pct (228)= .098*1.00;
Pct (229)= .097*1.00; Pct (230)= .097*1.00;
Pct (231)= .096*1.00; Pct (232)= .095*1.00;
Pct (233)= .095*1.00; Pct (234)= .095*1.00;
Pct (235)= .094*1.00; Pct (236)= .093*1.00;
Pct (237)= .092*1.00; Pct (238)= .092*1.00;
Pct (239)= .091*1.00; Pct (240)= .090*1.00;
Pct (241)= .089*1.00; Pct (242)= .088*1.00;
Pct (243)= .087*1.00; Pct (244)= .087*1.00;
Pct (245)= .086*1.00; Pct (246)= .085*1.00;
Pct (247)= .085*1.00; Pct (248)= .084*1.00;
Pct (249)= .083*1.00; Pct (250)= .083*1.00;
Pct (251)= .082*1.00; Pct (252)= .081*1.00;
Pct (253)= .081*1.00; Pct (254)= .080*1.00;
Pct (255)= .079*1.00; Pct (256)= .079*1.00;
Pct (257)= .078*1.00; Pct (258)= .078*1.00;
Pct (259)= .077*1.00; Pct (260)= .076*1.00;
Pct (261)= .076*1.00; Pct (262)= .075*1.00;

```

Pct(263)= .075*1.00; Pct(264)= .074*1.00;
Pct(265)= .073*1.00; Pct(266)= .073*1.00;
Pct(267)= .072*1.00; Pct(268)= .072*1.00;
Pct(269)= .141*1.00; Pct(270)= .139*1.00;
Pct(271)= .137*1.00; Pct(272)= .135*1.00;
Pct(273)= .133*1.00; Pct(274)= .131*1.00;
Pct(275)= .129*1.00; Pct(276)= .127*1.00;
Pct(277)= .125*1.00; Pct(278)= .123*1.00;
Pct(279)= .121*1.00; Pct(280)= .119*1.00;
Pct(281)= .118*1.00; Pct(282)= .116*1.00;
Pct(283)= .114*1.00; Pct(284)= .112*1.00;
Pct(285)= .127*1.00; Pct(286)= .125*1.00;
Pct(287)= .123*1.00; Pct(288)= .122*1.00;
Pct(289)= .110*1.00; Pct(290)= .109*1.00;
Pct(291)= .108*1.00; Pct(292)= .106*1.00;
Pct(293)= .104*1.00; Pct(294)= .103*1.00;
Pct(295)= .102*1.00; Pct(296)= .100*1.00;
Pct(297)= .099*1.00; Pct(298)= .097*1.00;
Pct(299)= .096*1.00; Pct(300)= .095*1.00;
Pct(301)= .093*1.00; Pct(302)= .092*1.00;
Pct(303)= .091*1.00; Pct(304)= .089*1.00;
Pct(305)= .084*1.00; Pct(306)= .082*1.00;
Pct(307)= .081*1.00; Pct(308)= .080*1.00;
Pct(309)= .079*1.00; Pct(310)= .078*1.00;
Pct(311)= .077*1.00; Pct(312)= .076*1.00;
Pct(313)= .075*1.00; Pct(314)= .074*1.00;
Pct(315)= .073*1.00; Pct(316)= .072*1.00;
Pct(317)= .071*1.00; Pct(318)= .070*1.00;
Pct(319)= .069*1.00;

% Adjust percent
Pctadj = 100/sum(Pct);
i=1;
while i<=319
    Pct(i) = Pct(i)*Pctadj;
    i=i+1;
end

% For this project, assume all particles are spherical. Although most
% particles are oblong or not completely spherical, the particle size
% distribution can be considered a function of the volume of the particle,
% rather than its diameter.

% Archimedes Number Ar = (particle density - fluid density)*(fluid density)
% * (gravity) * (diameter)^3 / (fluid dynamic viscosity)^2
% As shown on Equation 3.24

% -----
% %%%%%%%%%% DETERMINE SETTLING VELOCITY %%%%%%%%%%
% -----

g = 9.8065; % m/s^2, acceleration due to gravity

Ar = zeros(319,1);
i=1;
while i <= 319
    Ar(i) = ((rhop - rhof)*rhof*g*(D(i))^3)/(muf*muf);
    i=i+1;
end

%Solve for settling velocity at each diameter
SV = zeros(319,1);
i=1;

```

```

while i<=319

    % Determine a settling velocity based on Equation 3.30
    SV(i) = 30*(nuf/D(i))*((1+(1/9)*(Ar(i)/30))^0.5 - 1);

    % Per Kondrat'ev (2003) p. 608, the iterations shown in Eq. 3.31-3.34
    % are only needed for 1 < Re < 1000. The particle Reynolds numbers in
    % this experiment are < 1 for almost all sizes, so the iteration
    % described on p. 609 (Kondrat'ev 2003) is necessary only for the
    % highest diameters. At even the highest flow rates examined Re > 1
    % only when D > 300 um. Even at these diameters, the Reynolds numbers
    % are < 5, and any reduction of settling velocity would be by less than
    % 15% (Kondrat'ev p. 609). Even at these reduced settling velocities,
    % these large particles would still move to the bottom of the settler
    % rather quickly.
    if Re(i) > 1
        SV(i) = 0.85*SV(i);
    end

    i = i+1;
end % of while(i) loop

% x and z components of settling velocity
SVx = zeros(319,1); SVz = zeros(319,1);

i=1;
while i<=319
    SVx(i) = SV(i)*sin(theta); % m/s
    SVz(i) = -SV(i)*cos(theta); % m/s
    % note that SVz is negative because settling velocity is in the
    % direction of gravity, which is an angle between the positive x and
    % negative z directions. The positive x-direction is the direction of
    % fluid flow.

    i=i+1;
end

% -----
% %%%%%%%%%%% FLOW DISTRIBUTION %%%%%%%%%%%
% -----
% 20 particles of each size will be considered. Each particle's initial
% z-coordinate corresponds to one of the streamlines as shown in Figure
% 3.14 when the fluid flow is fully developed. To simplify the
% calculation, it is assumed that before the velocity profile is fully
% developed, the particle trajectory is identical to the fluid motion.

% Define starting points (zstart)
zstart = zeros(20,1);
zstart(1) = .00911; % m
zstart(2) = .00834;
zstart(3) = .00782;
zstart(4) = .00735;
zstart(5) = .00693;
zstart(6) = .00653;
zstart(7) = .00619;
zstart(8) = .00580;
zstart(9) = .00545;
zstart(10) = .00509;
zstart(11) = .00476;
zstart(12) = .00444;
zstart(13) = .00411;
zstart(14) = .00374;
zstart(15) = .00337;

```



```

zstart(16) = .00299;
zstart(17) = .00265;
zstart(18) = .00208;
zstart(19) = .00152;
zstart(20) = .00079;

% "Pct2" is a modified version of "Pct." Pct2 considers both the particle
% size distribution and the flow distribution. Assume a particle has an
% equal chance of going on any stramline in Figure 21.

Pct2 = zeros(319,20);
i=1; k=1;
while i<=319
    while k <= 20
        Pct2(i,k) = Pct(i)/20;
        k=k+1;
    end % of "whlie k" loop
    k = 1;
    i = i+1;
end % of "while i" loop

% Particle velocity and residence time
% Per Equations 3.37 and 3.38, particle velocity is equal to the settling
% velocity plus the drag velocity. Drag velocity is assumed to equal the
% fluid velocity.

% There is no drag velocity in the z-direction, so particle velocity is
% equal to settling velocity.
PVz = zeros(319,1);
i=1;
while i <= 319
    PVz(i) = SVz(i);
    i=i+1;
end

% Particle velocity in the x-direction is dependent assumed equal to the
% settling velocity in the x-direction plus the drag velocity in the x-
% direction.

% Drag velocity in the x-direction is a function of z. The fluid velocity
% for each "starting point" on the z axis is calculated as the average of
% the fluid velocity in the range from z=0 to the starting point.
DVx = zeros(20,1);

% Based on velocity profile shown in Figure 11
DVx(1) = .7014*vin_max; DVx(2) = .7196*vin_max; DVx(3) = .7312*vin_max;
DVx(4) = .7326*vin_max; DVx(5) = .7298*vin_max; DVx(6) = .7169*vin_max;
DVx(7) = .7029*vin_max; DVx(8) = .6971*vin_max; DVx(9) = .6827*vin_max;
DVx(10)= .6648*vin_max; DVx(11)= .6544*vin_max; DVx(12)= .6330*vin_max;
DVx(13)= .6109*vin_max; DVx(14)= .5872*vin_max; DVx(15)= .5352*vin_max;
DVx(16)= .4654*vin_max; DVx(17)= .4447*vin_max; DVx(18)= .3542*vin_max;
DVx(19)= .2398*vin_max; DVx(20)= .1335*vin_max;

% Particle velocity = Settling velocity + drag velocity
PVx = zeros(319,20);
i=1; k=1;
while i <= 319
    while k <= 20
        PVx(i,k) = SVx(i) + DVx(k); % m/s
        k=k+1;
    end % of "while k" loop
    k=1;
    i=i+1;
end

```

```

end % of "while i" loop

% Particle Residence time. As defined by Equation 3.39, residence time is
% the amount of time it takes a particle to travel through the length of
% the settler

taup = zeros(319,20);
i=1; k=1;
while i <= 319
    while k <= 20
        taup(i,k) = length/PVx(i,k); % s, particle residence time
        k=k+1;
    end % of "while k" loop
    k=1;
    i=i+1;
end % of "while i" loop

% How far each particle travels in the z-direction (per Equation 3.41)
dz = zeros(319,20);
i=1; k=1;
while i<=319
    while k <= 20
        dz(i,k) = taup(i,k)*-SVz(i); % m, distance traveled by z particle

        % a particle can not travel below the bottom of the settler
        dz(i,k) = min(dz(i,k), zstart(k)); % m
        k=k+1;
    end % of "whlie k" loop
    k=1;
    i=i+1;
end % of "while i" loop

% Which particles leave which exit, based on the percentage of fluid that
% leaves each exit
% For example, if 90% of the fluid leaves the upper outlet, any of the
% particles in the top 90% of the fluid (any particle whose z position is
% between 0 cm and 0.90 cm) will go to the upper outlet, while any particle
% in the bottom 10% (whose z position is between 0.90 cm and 1 cm) will go
% to the lower outlet. Figure 13 on the report confirms this).

% zexit is the height of a particle inside the settler at the outlet.
zexit = zeros(319,20);
i=1; k=1;
while i<=319
    while k<=20
        zexit(i,k) = zstart(k) - dz(i,k); % m
        k=k+1;
    end % of "while k" loop
    k=1;
    i=i+1;
end % of "while i" loop

% zsplit is defined as the z value in which particles above this point will
% exit through the overflow and particles below that point will exit
% through the underflow.

% The value of z-split can be obtained and interpolated from Figure 22.
% The value of zsplit can be expressed as a function of the percent of
% fluid that exits the settler through the overflow outlet:
% zsplit = -7.6e-5*(Pct) + 0.0087

zsplit = -7.6e-5*zsplit + 0.0087; % meters

```

```

% -----
% %%%%%%%%%%          OBTAINING AND DISPLAYING RESULTS          %%%%%%%%%%
% -----

```

```

% Determine enrichment factor and recovery rate for given conditions.

% The variable "outlet" measures whether a particle with a given diameter
% and starting point will leave the settler through the overflow or
% underflow.
% If outlet(i,k)=1, the particle of size range i and starting point k will
% leave through the overflow.
% If outlet(i,k)=2, the particle of size range i and starting point k will
% leave through the overflow.

```

```

% Display Header
fprintf('Diameter   Pct of   Pct to   Pct to   Residence \n');
fprintf('(um)      total   overfl  underfl  time (s)');
outlet=zeros(319,20);
recovery = 0; % Recovery rate (in terms of percent)
in_under = zeros(319,1); % percent of cells off each size in underflow;
i=1; k=1;
while i<=319
    while k<=20
        if zexit(i,k) < zsplit % if the particle is below the "split point"
            outlet(i,k)=2; % Particle exits through overflow
            recovery = recovery + Pct2(i,k);
            in_under(i)= in_under(i) + 5;
        else % if the particle is at or above the "split line"
            outlet(i,k) = 1;
        end % of "if zexit" statement
        k=k+1;
    end % of "while k" loop
    fprintf('\n %8.4f   %6.4f   %3.0f   %3.0f %8.4f', D(i)*1000000, Pct(i),
100-in_under(i), in_under(i), taup(i));
    k=1;
    i=i+1;
end % of "while i" loop

```

```

% Calculate enrichment factor from recovery rate
% Enrichment factor =
% (Algae concentration in underflow) / (Algae concentration in inlet)

enrich = (recovery/100)/(1-(split/100));

```

```

% Display enrichment factor and recovery rate
fprintf('\n\n Enrichment factor: %8.4f', enrich);
fprintf('\n Recovery rate: %8.4f percent', recovery);

```

```

% -----
% %%%%%%%%%%          LIST OF VARIABLES          %%%%%%%%%%
% -----

```

Variable	Description	Units
Ain	Area of inlet to settler	m ²
Amtlow	Amount of algae in lower outlet divided by algae concentration	mL/min
Amtup	Amount of algae in upper outlet divided by algae concentration	mL/min
Ar	Archemedes Number	unitless
Conclow	Ratio of concentration of algae in lower outlet to concentration of algae in inlet	unitless

```

% Concup | Ratio of concentration of algae in upper outlet to |
% | concentration of algae in inlet | unitless
% D | Average diameter in a given size range | m
% D2 | Lowest and highest diameters in a given size range | m
% DVx | Drag velocity in x-direction | m/s
% DVz | Drag velocity in z-direction | m/s
% dz | Movement in the negative z-direction of particles | m
% | of a given size range |
% enrich | enrichment factor (underflow conc./inlet conc.) | unitless
% g | Acceleration due to gravity | m/s^2
% height | Height of the settling region of the settler | m
% i | Counter used in "while" loops | unitless
% in_under | percent of cells off each size in underflow | percent
% j | Power of 10 used to determine particle diameters | unitless
% | used in this program |
% k | Counter used in "while" loops | unitless
% length | Length of the settling region of the settler | m
% lengthcm | Length of the settling region of the settler | cm
% muf | Dynamic viscosity of the fluid | kg/(m*s)
% nuf | Kinematic viscosity of the fluid | m^2/s
% outlet | Determines whether particles of a given size range | unitless
% | exit the settler via the upper or lower outlet |
% Pct | Percent of the total amount of algae (by mass) that | unitless
% | exists in each size range |
% Pctlow | Percent of the total amount of algae (by mass) that | unitless
% | Exits the settler via the lower outlet |
% Pctup | Percent of the total amount of algae (by mass) that | unitless
% | Exits the settler via the upper outlet |
% PVx | Particle velocity in the x-direction | m/s
% PVz | Particle velocity in the z-direction | m/s
% Qin | Volumetric flow rate of fluid into the settler | m^3/min
% Qinml | Volumetric flow rate of fluid into the settler | mL/min
% Re | Reynolds number | unitless
% recovery | Recovery rate | percent
% rhof | Density of the fluid | kg/m^3
% rhop | Density of the particles | kg/m^3
% rin | Radius of the fluid inlet regions | m
% split | Percent of fluid from inlet that exits via the | unitless
% | upper outlet |
% splitfrac | split (above), converted from percent to fraction | unitless
% SV | Settling velocity of particle | m/s
% SVx | Settling velocity of particle in x-direction | m/s
% SVz | Settling velocity of particle in z-direction | m/s
% tauf | Fluid residence time | s
% taup | residence time of particles of a given size range | s
% theta | angle of inclination | radians
% thetad | angle of inclination | degrees
% vin | inlet velocity of fluid | m/s
% zsplit | split (above), in terms of distance in z-direction | m
% zstart | Point on the z axis in which a particle "started" | m
% | its trajectory, its z-location once fluid flow was |
% | fully developed. |
% -----
% End of program

```